ON THE DESIGN OF RESIDENTIAL CONDENSING GAS BOILERS

Mikael Näslund

Doctoral thesis
January 1997
Department of Heat and Power Engineering
Lund Institute of Technology
http://www.vok.lth.se

ISSN 0282–1990
ISRN LUTMDN/TMVK–1011–SE
Printed in Sweden
KFS AB
Lund 1997

To Lena

Summary

Two main topics are dealt with in this thesis. Firstly, the performance of condensing boilers with finned tube heat exchangers and premix burners is evaluated. Secondly, ways of avoiding condensate formation in the flue system are evaluated.

In the first investigation, a transient heat transfer approach is used to predict performance of different boiler configurations connected to different heating systems. The smallest efficiency difference between heat loads and heating systems is obtained when the heat exchanger gives a small temperature difference between flue gases and return water, the heat transfer coefficient is low and and the thermostat hysteresis is large. Taking into account heat exchanger size, the best boiler is one with higher heat transfer per unit area which only causes a small efficiency loss. The total heating cost at part load, including gas and electricity, has a maximum at the lowest simulated heat load. The heat supplied by the circulation heat pump is responsible for this.

The second investigation evaluates methods of drying the flue gases. Reheating the flue gases in different ways and water removal in an adsorbent bed are evaluated. Reheating is tested in two specially designed boilers. The necessary reheating is calculated to approximately 100–150°C if an uninsulated masonry chimney is used. The tested boilers show that it is possible to design a proper boiler. The losses, stand-by and convective/radiative, must be kept at a minimum in order to obtain a high efficiency.

Acknowledgements

It is a custom, like in the Academy awards ceremony, to thank people involved in the work. This is my contribution to this tradition.

Firstly, I would like to thank professor Lennart Thörnqvist, my supervisor, for help and support during the work. Professor Sven-Erik Ransmark should not be forgotten since he introduced me to the subject. During this work, laboratories have been designed and built. Without the help of Fredrik, John and Gunnar (all Johansson) pipes, valves, heat exchanger tubes e t c would have looked more like bad examples of art instead of nicely working laboratory equipment. I also thank the people at the Department for fruitful scientific discussions, social life and help with the administrative details of the projects.

I also mention Annika, Ebbe, Sven-Inge, Christer and Ulf, with whom I have worked with concerning pulse combustion in parallel with this work.

Financial support has been given by Värmeforsk, Swedish Gas Technology Center (SGC), The Swedish National Board for Technical and Industrial Development (NUTEK) and The National Board for Building Research (BFR).

And last, but not least, thanks to Lena and Greta (the cat). Greta has not done anything worse to the manuscript and files than shutting down the laptop when she walked across the keyboard.

Contents

List of Figures

List of Tables

Nomenclature

A	area, m^2
a	dimensionless length, –
b	fin thickness, m
b	dimensionless length, –
C_N	radiator element heat capacity, J/K
C	heat capacity, J/K
c	price, –
c	velocity, m/s
c_p	heat capacity, J/kg K
d	diameter, m
f	convective part of heating system output, –
g	gravity, 9.81 kg/m s^2
H	height, m
h	heat transfer coefficient, W/m^2K
I	relative load $(\dot{Q}_{rad}/\dot{Q}_b)$, –
I_0	zero degree Bessel function
I_1	first degree Bessel function
K	mass transfer coefficient, $kmol/m^2\,s$
K_0	zero degree Bessel function
K_0	first degree Bessel function
k	thermal conductivity, W/m K
l	length, m
M	molar weight, kg/kmol
m	mass, kg
$\dot{m}$	mass flow, kg/s
N	cycle frequency, 1/s
n	tube rows, –
n	cycles per hour, –
P	electrical input, W
p	pressure, N/m^2
Δp	logarithmic pressure difference, N/m^2
Q	heat energy, Ws
$\dot{Q}$	heat flow, W
q	specific heat flow, e.g. $\frac{\dot{Q}}{\dot{Q}_{input}}$, –
r	latent heat, J/kg
r	radius, m
s_1	longitudinal tube distance, m
s_1	transversal tube distance, m

T	temperature, K
t	time, s
U	overall heat transfer coefficient, W/K
W	electrical energy, Ws

Greek symbols

β	thermal expansion factor, –
η	efficiency, %
Θ	temperature difference, K
ϑ	temperature, K
λ	excess air ratio, –
ν	kinematic viscosity, m^2/s
ξ	friction factor, –
ρ	density, kg/m^3
τ	relative time, –
Φ	relative humidity, %
ω	humidity, kg_{H_2O}/kg

Dimensionless numbers

Bi	Biot number, –
j	Colburn factor, –
Nu	Nusselt number, –
Pr	Prandtl number, –
Ra	Rayleigh number, –
Re	Reynolds number, –
Sc	Schmidt number, –
St	Stanton number, –

Subscripts

a	fraction of burner input
ads	adsorbent
amb	ambient, outdoor
air	indoor air
$appl$	electric appliances
av	average
b	burner
b	fin base
b	building
cc	combustion chamber
chi	chimney
$cond$	condensation
$control$	control system
$conv$	convective
$cycle$	operating cycle
el	electricity
f	fin
fan	fan
fg	flue gas
$flow$	flow line, pipe
g	ground
H_2O	water
h	enthalpy
h	hydraulic
ign	ignition
in	inside

in	fluids entering
$in-line$	in-line tube arrangement
lf	loss through the flue
lh	loss from parts not containing water
lw	loss from water jackets
m	heat exchanger
$meas$	measured
nom	nominal
on	burner operating
off	burner stand by
out	output
out	outside
p	pre-purge
$pump$	circulation pump
r	roof
r	radius
rad	radiator, heating system
$return$	heating system return line
s	saturated state
sb	stand-by
$stag$	staggered tube arrangement
$store$	stored in heat exchanger
sun	solar radiation
tip	fin tip
$theo$	theoretical
$thermo$	thermostat
tot	total
$trans$	transmission
$vent$	ventilation
w	wall

Superscripts

n	radiator exponent

1

Introduction

A brief description of condensing boilers will be given in this chapter as well as the state of the art and the technology evolution for these boilers. It is assumed that the reader is familiar with the basic characteristics of condensing boilers regarding flue gas temperatures, boiler efficiency and material topics.

1.1 Energy Economics and Planning and Natural Gas

In the subject “Energy economics and planning”, efficient use of energy in various processes is studied. Primarily, centralized energy distribution systems on a municipal level are studied, e.g. electricity, district heating and natural gas. Examples of research topics in these areas are coincidence factors in electric heating and Demand Side Management (DSM), low return water temperature from consumer substations in district heating improving the operating conditions for a back pressure steam turbine and the overall heating efficiency of gas appliances.

In this section I present some advantages I think condensing gas boilers offer. Condensing boilers offer the possibility of a very high fuel utilization and thus of interest in “Energy economics and planning”. For a municipal utility, a maximized appliance efficiency is of interest since it minimises the transportation work. Of course, it will also reduce the gas sold to each customer. High efficiency can thus be an advantage for both the distribution company and the customer. A study of ways to improve the overall annual fuel utilization or efficiency will also provide a small contribution to the knowledge of load economizing and coincidence factors.

Natural gas is today used in all types of fuel consuming processes and one may easily point at both environmental and efficiency advantages in comparison with other fuels. In the sector of space heating, properties of both the fuel natural gas and the building can be noted for a potential of very efficient energy utilization. In this context are the properties divided into two categories, combustion and process.

Combustion of natural gas generates a larger amount of water compared to oil or coal combustion. Only when moist fuels, for example wood and peat, or hydrogen are used the flue gases will have a water content equivalent to that of natural gas combustion or higher. The high water content involves a high water dew point, approximately 50–60°C. The exact temperature is mainly dependent on the combustion air excess ratio. The negligible content of sulphur and heavy metals combined with the possibility to control the combustion in order to minimize the CO and NO_x emissions make natural gas an environmentally attractive fuel. It is worth mentioning catalytic combustion and surface combustion as attractive technical solutions especially well suited for gaseous fuels. The small emission levels should be taken into account as this thesis deals with gas appliances used in for example areas of single family houses, i.e. a great number of small emission sources at a low level above the ground in housing areas.

The process in which the fuel is used determine how far the flue gases can be cooled, i.e. the highest obtainable efficiency. The temperatures in space heating systems, more precisely the return temperature from the heating system, are often low enough to allow condensation of the water vapour in flue gases. Natural gas can thus be used to obtain very high efficiencies. Furthermore, the condensate from natural gas flue gases is less aggressive than the condensate from oil flue gases. Altogether this have lead to the development of condensing gas boilers at attractive prices for the consumer.

This thesis focusses on condensing gas boilers and energy economics and planning from a technical point of view. This means that the boiler design is studied and discussed in order to use the potential of high efficiency to a as high degree as possible, taking into account the wide range of operating conditions generated by different building characteristics as well as the climatic changes during the heating season. The approach is to look at the boiler, the heating system and the building as the necessary parameters in the system to be studied.

1.2 Evolution of Residential Condensing Gas Boilers

Condensation of water vapour in flue gases was reported in the 1930s but regarding condensate formation in the chimney. Until the 1970s research works only seem to deal with unwanted condensation and its effects on chimneys and gas appliance material according to a bibliography by Hindin [30]. The “energy crisis” and the increase of natural gas consumption, especially in Europe, during the 1970s draw the attention to higher efficiencies and condensing appliances.

1.2.1 Short History

Perhaps is the Canadian boiler Pulsamatic by Lucas-Rotax Ltd. the first condensing space heating appliance. It was developed in the late 1950s and used a pulse combustor. It is interesting to note that outdoor air was used as combustion air. Approximately 700 boilers were manufactured until 1966.

Kirk [38] writes 1974 that there is no widely used gas appliance that has an efficiency of 90% (based on the higher heating value) and utilizing the latent heat, i.e. condensation. He shortly mentions work at the American Gas Association on a condensing furnace with a stainless steel heat exchanger. The exhaust temperature was 49°C. A boiler equipped with a pulse combustor is also mentioned. In this boiler the latent heat was obviously recovered by transporting the flue gases through a water bath. Field [21] reports in 1974 on French experiences with condensing heat exchangers added to two 1.2 MW boilers for heating swimming pools. Operation began in 1971 following a prototype in 1970. In 1976 Rado [66] describes an evaluation made at Ruhrgas in Germany of an add-on condensing heat exchanger intended for use in space heating boilers. The unit tested was connected to a boiler of approximately 1 MW gas input. Measured efficiency at full load was 101.2%. The condensing heat exchanger was said to have been successfully used for swimming pool heating for several years.

In for example the Netherlands and in Great Britain the development of condensing appliances have been encouraged by research done at gas company research centres or equivalent, i.e. Gasunie Research and British Gas. In the Netherlands Gasunie Research 1979 presented a condensing boiler for the Dutch boiler manufacturers. The prototype had two heat exchangers and was rapidly developed. Basic data were transferred to licenced Dutch boiler manufacturers. In 1981 ten companies had developed boilers of different designs. VEG-Gasinstituut (now Gastec) later conducted a lot of work regarding corrosion and material topics. Gasunie has again developed a prototype condensing boiler described by Bootsma and Meijnen [9], this time with a modulating burner and hot tap water production in the same unit. This work is conducted in cooperation with Dutch boiler and burner manufacturers.

The work at British Gas can be studied in published reports, e.g. in the contributions to the International Gas Research Conference in 1986 and 1989. Searle and Allen [73] describe the development of a wall hung condensing boiler, Hargreaves and Patterson [27] describe an evaluation of burners and burner controls and Stevens and Morgan [79] present results from assessments of materials for condensing appliances. The contributions to the 1989 conference included work more related to the interaction between boiler and building; studies and calculations of flues by Etheridge et al. [20] and warm-air heating evaluation by Nevrala et al. [49].

Dedicated conferences have also shown the interest in and the need for research regarding condensing appliances. The conference "Condensing Heat Exchangers" (CHX) has been held twice, 1982 in Atlanta and in 1987 in Columbus, Ohio.

1.2.2 Boiler Design

Early condensing boilers often had two separate heat exchangers with condensation taking place in the second one. These boilers can be seen as non-condensing boilers with added condensing heat exchangers. Separate condensing heat exchangers were also available for domestic boilers and still are. New boilers often have a single heat exchanger. In Europe today, strictly condensing heat exchangers, either as a secondary heat exchangers or as added separate units, are mostly found in larger boiler installations for space heating. These basic designs are denoted the first and second generation condensing boilers by Jannemann [36]. In figure 1.1 they are schematically shown. These designs are later in this thesis called type I and type II.

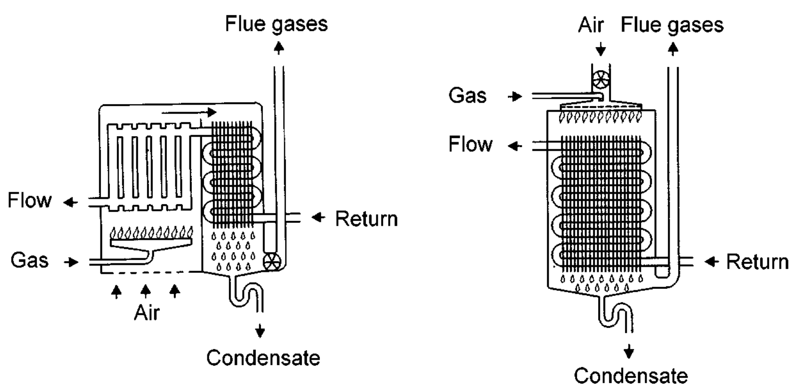

Figure 1.1: Basic condensing boiler designs according to Jannemann

The heating systems in North America are usually warm-air systems while hydronic systems dominate in Europe. These and other factors have lead to different paths in the boiler developments in the two continents. These differences are discussed in a paper by Searle et al. [74]. The topics discussed are condensate formation and amount, heat exchanger design and material, maintenance and possible fuel savings.

Today, the state of the art regarding European residential boilers is a low heat capacity boiler with an often finned tube heat exchanger and premixed combustion with either blue flames or a radiating glowing burner surface. Examples of this type are the Nefit Turbo (EcomLine), the EWFE Micromat and the Remeha Micron 2.

1.2.3 Boiler Performance

The efficiency of gas boilers has increased due to a number of improvements. Among them are increased heat insulation to reduce the convective heat loss and a lower flue gas temperature. The use of new burners often lower the flue loss due to lower excess air ratios. They also permit a reduced air flow through the boiler during the burner stand-by period, thus reducing the stand-by loss. A burner that is well suited for condensing appliances is a pulse combustor in which the pressure generated fits the higher pressure drop in condensing heat exchangers. Examples are the American furnace Lennox Pulse and the Hydrotherm Hydro Pulse boiler. Due to the higher pressure drop in condensing boilers a combustion air fan is necessary. A higher electricity consumption follows compared to traditional non-condensing boilers. The electricity consumption for space heating boilers and the interaction with other parts of the installation are discussed later in this thesis.

The gas consumption for space heating has been further reduced by control systems which better adapt the boiler operation to the heat demand. These improvements could lead to non-condensing boilers of good design with a low flue gas temperature and with an efficiency of the same order as the early condensing boilers. The boiler price is lower than for a condensing boiler. Today, non-condensing boilers can reach an annual efficiency of slightly above 90% (based on the lower heating value) which is an efficiency level comparable to those of early single family house condensing boilers. However, boilers of that kind may introduce new problems such as unwanted condensation in the boiler and corrosion problems in chimney liners.

Energy savings of 15–20% are often claimed when condensing boilers are compared to non-condensing boilers. This may be true when an old non-condensing boiler is retrofitted by a condensing boiler.

1.2.4 Economics and Regulations

The economic gain of condensing boilers can be smaller in the future due to a smaller efficiency difference between condensing and non-condensing boilers and a reduced heat demand in new buildings. Another competitor may be electrical heating if the total cost for the heating device and the heat distribution system is considered in low-energy houses with an annual net heat demand less than 10 000 kWh.

The use of condensing boilers in a particular country is depending not only on thermodynamic performance but also on regulations, political measures and taxation. One example is the possibility to locate the boiler in the attic as in the Netherlands, thus reducing the cost for a corrosion resistant chimney lining. The government may also encourage the use of certain technologies through subsidizes as in the Netherlands where approximately 10% of the boiler cost has been subsidized in order to increase the market share for condensing boilers. Fuel taxation can also control the use of the technology chosen. One example is the CO_2 tax in force in Sweden. Since Sweden does not have own fossil fuel sources, domestic fuels such as biomass can benefit from this.

1.3 Boiler Efficiency and the Building

The interaction between the building and the boiler involves a large number of topics. In-depth studies of the energy use in buildings to get thermal comfort often include air tightness aspects, indoor air flow calculations (using CFD codes) and consideration of solar radiation gain. The boiler has often been considered as a simple heat source. The building has been of greater importance in these studies. In studies where the interest is focussed on the boiler the opposite situation is often to be found. The boiler has been described in detail while the building and heating system are described together as a simple heat sink. These are the two main approaches taken in the literature. A general discussion on integrating these approaches is done by Hensen [29]. In the dissertations by Hensen [28] and Tang [80] both authors present models of the building and the different parts of the heating and ventilation system, e.g. the boiler, the heat distribution system, valves and the control system.

In 1972 Dittrich [18] presented a model for the calculation of the part-load operation of residential boilers. Many models have followed and these models are discussed in chapter 3. These models often consider the building as a simple static heat load. Some studies have dealt with the overall heating system. Four of them are here cronologically reviewed.

The oldest model of these is implemented in the American computer program HFLAME by Bonne et al. [7, 8] which has been used for evaluation of the entire system, consisting of a furnace, building and heating system. The model simulates the furnace or boiler dynamically and the heat load statically. Performance and efficiency are calculated from heat losses to the flue system during the burner on-period and off-period respectively. Calibration is made from one steady-state flue gas temperature and one temperature profile at part-load during a whole burner cycle. Electricity consumption for the heat distribution system is also included. The losses considered are the flue loss during burner operating time, the heat loss during the burner stand-by time and the air infiltration. Heat from the flue system to the heated space is also accounted for.

The model has not been used to point out an optimum furnace design. Common topics for evaluation have been various operating conditions, control systems, and heating system designs. For a natural gas fired warm-air furnace the influence of oversizing, reduced excess air ratio, intermittent ignition instead of a pilot flame, cycling frequency, different ways of combustion air supply and warm air flow and circulation air fan operation were evaluated.

Pickup and Miles [61] made in 1979 a British study of the overall system consisting of boiler, heating system and building. It included both space heating and hot tap water production. The authors strongly recommend low heat capacity boilers to obtain as high annual efficiency as possible. The investigations were directed towards the use of gas boilers in new low energy houses, approximately 4 kW heat demand at -1°C outdoor temperature. Commercially available boilers were tested in the laboratory and in field installations. It seems like night setback was assumed which may explain high heat losses for high heat capacity boilers. One may also suspect that these boilers were of an older design and not so well insulated as the new low heat capacity boilers. The authors provide recommendations for boiler sizing, heating system and control system. Some recommendations are perhaps closely linked to British building practice and thus not generally valid.

A similar and more recent study with the same aim as the British study is described by Nielsen and Spiegelhauer [51]. The aim was to develop a gas fired heating system for the year 2000. For this, three parts were identified: evaluation of the expected characteristics of future new Danish single family houses, assessment of the most suitable heat distribution system and finally development of burners and boilers. In the first part, the heat demand in new buildings was estimated. Together with the heat demand for additional heating following night setback and heat required for hot tap water production the necessary burner heat input was determined. The authors conclude that a gas input of approximately twice the heat demand at the design outdoor temperature is sufficient. For the anticipated new Danish single-family houses this involves a burner input of 10–15 kW. The best heat distribution system is according to the authors the commonly used hydronic system.

Two types of boiler designs were then considered, a high heat capacity boiler with no or only a small burner turn-down ratio or a low heat capacity boiler with a highly modulating burner. The turn-down ratio is mentioned as a main limitation in the latter design. The burner must also be environmentally friendly, i.e. the use of a low NO_x burner is required. Fibre burners are considered as suitable for the task and offer the possibility of obtaining a large turn-down ratio.

Further studies were suggested on the design of a high heat capacity and a low heat capacity boiler, development of air and fuel mixing systems for premix burners and finally design tools for small and medium sized boilers with premix burners. It was evaluated that a compact non-condensing cast iron boiler with an annual efficiency of 88–90% could be developed.

The recommendations regarding high heat capacity boilers are obviously contradictory in the British and in the Danish studies. The basic assumptions may be different, but differences in technical standards are probably also of importance for the standpoint on boiler design choice. In the Danish work, an extremely small heat loss from the boiler body is assumed, 50–100 W at 65°C boiler temperature. The equivalent heat loss of the heavy boilers in the British investigation were probably up to ten times this value, which may be a major explanation. The high heat capacity boiler with a one-step burner was in the Danish work considered to adapt better to different heating systems and therefore currently of greater interest than a low heat capacity boiler with a similar burner. Since the study was conducted in cooperation with Danish boiler companies the results are directed towards new products.

Jakob et al. [34, 35] have evaluated 21 design options from US Department of Energy for improved appliance efficiency. Options which increase the efficiency were economically assessed. A combination of literature data, experiments and furnace simulations were used for the evaluation. The total life-cycle costs were predicted and compared. Building characteristics were summarised as future heat loads.

The conclusion, from an economical point of view, is that the lowest life-cycle cost is obtained for furnaces having the lowest allowable efficiency. The baseline furnace selected had an input of approximately 22 kW and an annual efficiency of 85%. Design heat demand was approximately 9 kW. Among the design options studied, only a small efficiency improvement of 1–2% could be economically justified. Appliances with higher efficiencies suffered from higher costs either from the flue system or the from furnace itself. It should be remembered that the conclusion is made for the US price situation. Higher energy prices will for example increase the number of economically justifiable options.

These four studies are based either on measured data from individual furnace installations or a general discussion based on known characteristics. None of the models are general in the sense that the system performance can be calculated from an assumed system design.

1.4 Aims, Delimitations and Basic Considerations

In this thesis a central space heating system for single family houses consisting of a natural gas fired condensing boiler and a hydronic heating system is studied. The thesis consists of two main studies:

- A study of boiler performance changes for different boiler designs and heat loads.

- A study of different boiler designs to avoid the need for moisture resistant chimney liners when condensing boilers are used.

These studies also defines two aims. A third aim is the development of detailed models for prediction of boiler operation and its interaction with the building. The first study is limited to the boiler performance in a strictly technical manner, i.e. calculations of the local temperatures and heat flows in boilers and the resulting efficiency. The second study deals with the goal to technically evaluate boiler designs which make the use of chimney liners unnecessary. It can also be said to also deal with the issue that a reduced efficiency can be economically justified due to reduced installation costs.

The system study is based on an engineering approach. This means that the different parts of the heating system are quite well described and put together in a single model. It is not the intention to perform basic research in areas such as transient heat transfer, building modelling, fluid mechanics and so on.

The condensing boiler has a heat exchanger with no mixing of the fluids. The flue gas pressure is kept at the atmospheric level and only the combustion air humidity is added to the combustion process.

The heating system is a two-string hydronic system with a constant water flow and an outdoor temperature controlled flow temperature. Energy for space heating is only supplied by the heating system. Neither convective/radiative loss from the boiler nor heat from the chimney walls are considered useful in this approach. Excessive heat from electric appliances is not included in the heat supplied for space heating. The house is suitable for a single family; annual heat demands considered in the thesis are less than 30 000 kWh. It does not have a mechanical ventilation and thus no energy recovery from the indoor air leaving the house. The chimney assumed in this work is an uninsulated masonry chimney.

A number of investigations were required to fulfil the mentioned aims. The work may be cronologically divided into the following steps. The order of items also shows the development from laboratory tests to simulations of the entire heating system.

1. An experimental investigation of flue gas reheating in a commercially available boiler.
2. Development of a calculation model for the heat and mass transfer in chimneys.
3. Tests of specially designed condensing boilers with flue gas reheating.
4. Detailed modelling of heat and mass transfer in a well defined boiler and the dynamic characteristics of heating systems and buildings.

The economical consequenses of the suggested boiler designs are not discussed in this thesis. Furthermore, the discussion only deals with a boiler used for space heating, not hot tap water production as well. It is however possible in future work to include the sanitary hot water production in the model and methology developed.

1.4.1 Thesis Structure

The thesis is arranged as follows. Chapter **1, 2** and **3** form a background while chapter **4, 5** and **6** constitute the actual investigations. In **chapter 2** a "picture" of the boiler and its environment is presented. This is followed in **chapter 3** by a survey of methods of calculating boiler performance. Models are divided into models for prediction of part-load efficiency of existing boilers and models used as design tools. Comments are made on the different methods. Also, a discussion about electricity consumption is carried out. The purpose of this chapter is to point at the parameters important for the boiler performance and which also are needed for a detailed analysis of boilers.

A calculation model of boiler performance is presented in **chapter 4**. The boiler in the model consists of a burner firing down towards a cross flow heat exchanger. Thorough calculations in order to evaluate some design parameters are made.

In **chapter 5** and **6** flue gas drying by means of flue gas reheating or adsorption drying is studied. The content of these chapters is divided between calculations of the necessary flue gas temperature and humidity and experiments in boilers with and without flue gas reheating. Conclusions about boiler designs are drawn.

Chapter 7 contains a discussion and conclusions are drawn from the two studies.

1.5 Definitions

Throughout the thesis a number of terms are used. They can have slightly different meaning depending on the source. In this thesis they have the following meaning.

Boiler Heat generator intended for water based space heating systems, hydronic systems.

Control system The boiler or furnace monitoring system consisting of one or more of the following devices or functions: boiler thermostat, room thermostat, radiator valves, outdoor temperature control and night setback.

Convective/Radiative loss This is heat transferred from the boiler casing and water jackets to the surrounding boiler room.

Cycling frequency This is the frequency of the intermittent operation of a one-step burner. The cycling frequency is not fixed for a particular boiler and heat load.

Furnace Heat generator intended for warm-air space heating systems.

Heat capacity If a boiler has a high or low heat capacity is dependent on the burner input. No exact value is given to separate high and low heat capacity boilers. It is instead a general description of the boiler design. Remeha 1HR is an older, first generation, condensing boiler with two heat exchangers, one cast iron heat exchanger and one condensing heat exchanger consisting of a finned tube bundle in an aluminium alloy. The total weight is 134 kg and if 105 kg is assumed to be included in the heat exchanger this gives a heat capacity, related to the burner input, of approximately 3 000 J/kW K and 5 500 J/kW K including the 11 litre water content. The EWFE Micromat MZ22 has a total weight of 65 kg and if 40 kg is assumed to be an aluminium heat exchanger, a 18 kW gas input yields a heat capacity of 2 000 J/kW K and 2 500 J/kW K including an assumed 2 litre water content.

Heat demand The heat required to keep the indoor temperature constant at a certain level. It is only determined by the heat transfer characteristics of the building. Thus, no user behaviour is taken into account.

Heat output This is the boiler output at the water jackets at full load operation.

Heating system The heating system assumed in this study is a central two-string hydronic system.

Natural gas, heating value The lower heating value is used throughout the thesis unless other stated. This means that the efficiencies are approximately 10% higher than if the higher heating value is considered as long as the the fuel is natural gas H. The gas composition used is 91.1% CH_4, 4.7% C_2H_6, 1.7% C_3H_8, 1.4% C_4H_{10}, 0.5% CO_2 and 0.6% N_2. The lower heating value is 39.0 MJ/m^3.

Operating cycle This is the time between two burner starts, i.e. including pre-purge time, burner operation and stand-by.

Part-load operation This occurs when the heat load is less than the boiler heat output. The part-load efficiency is the relation between useful heat at the water jackets and the gas input at part-load operation.

Pre-purge loss This loss occurs during the pre-purge time and is the energy used for heating the combustion air until the flame ignites. In condensing boilers water is also evaporated.

Pre-purge time The time from the start of the combustion air fan to the flame ignition.

Relative time This is a dimensionless burner operating time. The relative time, τ, denotes the share of time the burner operates between two starts.

Stand-by loss An air flow through the boiler to the flue that cools the heat exchanger determines this loss. It is the heat transferred to the air flow and further to the flue system. It occurs from the time the burner has stopped until the combustion air fan starts.

Start/stop effect The start/stop effect is the difference in heat output when only the cycling frequency is changed. Water temperatures are constant. Both positive and negative values are possible indicating gains and losses respectively.

2

Space Heating Boiler Characteristics

In this chapter, heat flows in boilers as well as overall boiler characteristics are described. The aim is to show the parameters necessary for an accurate simulation of the boiler performance in a building. The building is in this chapter represented by a simple steady-state heat load.

2.1 Boiler Heat Flows

Modelling boiler characteristics and using the results for boiler design require a detailed picture of the heat flows to and from the boiler as well as inside the boiler. It is suitable to express the different heat flows as a function of time since the intermittent (on/off) operation of many burners gives a transient heat transfer in normal operation. This is also the case in boilers equipped with modulating boilers at low heat loads. A general expression for the heat transferred to the heating system $\dot{Q}_{rad}$ assuming no heat loss in the distribution system then yields

$$\dot{Q}_{rad}(t) = \dot{Q}_b(t) - \dot{Q}_{lh}(t) - \dot{Q}_{store}(t) - \dot{Q}_{lw}(t) - \dot{Q}_{lf}(t) \tag{2.1}$$

where $\dot{Q}_b$ is the burner input, $\dot{Q}_{lh}$ is the heat loss from not water cooled hot spots, $\dot{Q}_{store}$ is the heat stored in the the heat exchanger, pipes and water, $\dot{Q}_{lw}$ is the heat loss from water cooled parts, $\dot{Q}_{lf}$ is the loss to the flue system and t is a time parameter. The different heat flows may of course also be dependent on parameters like temperatures and heat loads. The parameter $\dot{Q}_{store}$ denotes heat stored in the heat exchanger material during the burner operation and released to the heating system during the burner stand-by period as a result of the cyclic operation.

Among the time dependent parameters, only the heat delivered to the heating system $\dot{Q}_{rad}$ and the flue loss $\dot{Q}_{lw}$ during burner operation would in practice be possible to measure directly. The remaining losses, i.e. the heat loss to the surrounding room and the stand-by loss, are given as the remainder when a heat balance is set up around the system. The accuracy in this way of determining these losses is likely to be bad due to their small part of the the total heat flow.

However, in practice will a boiler meet heat loads in a limited number of operating conditions. For a boiler with a one-step burner these are full load and stand by. A two-step burner either operates in full load and low load or in low load and stand by. Finally, the modulating burner either operates within the turn-down ratio or in lowest fuel input and stand by. The part-load performance for a particular heat load may therefore be expressed as a combination of two operating conditions. Often are these approximated as steady-state conditions. The following discussion will deal with a boiler with a one-step burner. The approach is easily adapted to the other burners mentioned. The two steady-state operating conditions are shown in figure 2.1.

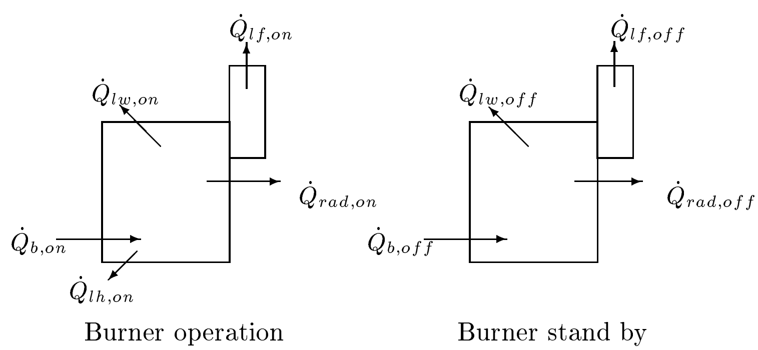

Figure 2.1: Energy flows in a boiler during burner operation and burner stand by

During the burner operating time, the gas input to the main burner is $\dot{Q}_{b,on}$ while it is $\dot{Q}_{b,off}$ during the main burner stand-by period in case of a pilot burner. From the boiler, the useful heat $\dot{Q}_{rad,on}$ and $\dot{Q}_{rad,off}$ are taken during the burner operating and stand-by times respectively. An accurate heat balance must also include the energy supplied to the water circulation pump which gives a small contribution to the heating of the water.

The different heat losses are transferred either to the flue or to the surrounding room. During the main burner operating time the flue loss is determined by the flue gas temperature at the boiler outlet, the excess air ratio for the combustion, and in case of condensation, the water content in the flue gases. The flue loss when the main burner is not operating, $\dot{Q}_{lf,off}$, is determined by a possible flow of cooling air through the boiler.

The heat loss to the surrounding room, $\dot{Q}_{lw,on} + \dot{Q}_{lh,on}$, during the main burner operation and the corresponding values during burner stand by is also named convective and/or radiative loss. $\dot{Q}_{lh,on}$ denotes the heat loss from hot surfaces on the burner and flame radiation from an atmospheric burner if used, and $\dot{Q}_{lw}$ the heat loss from the boiler surface including the water jackets. The heat balances in steady-state conditions thus become

$$\dot{Q}_{b,on} = \dot{Q}_{rad,on} + \dot{Q}_{lf,on} + \dot{Q}_{lw,on} + \dot{Q}_{lh,on} \tag{2.2}$$

during burner operation and

$$a\,\dot{Q}_{b,on} = \dot{Q}_{rad,off} + \dot{Q}_{lf,off} + \dot{Q}_{lw,off} + \dot{Q}_{lh,off} \tag{2.3}$$

during burner stand by. The pilot burner input $\dot{Q}_{b,off}$ has been replaced by the expression $a\,\dot{Q}_{b,on}$, i.e. a fraction of the main burner input.

In this discussion of heat balances, complete combustion has been assumed. In a well adjusted gas burner this can be anticipated, but during the first seconds of burner operation higher amounts of unburnt hydrocarbons and carbon monoxide are emitted. Long operating times reduce this loss to a negligible part of the heat input. However, extremely short operating times can be obtained at low heat loads in boilers with low heat capacities, and in bad installations.

Rawe and Schultz [68] studied the heat losses from residential boilers in order to determine the size of the convective/radiative and stand-by losses. Their test set up allowed a separation of the losses.

8 different boilers, manufactured between 1971 and 1988, equipped with both atmospheric and fan assisted burners were tested. In figure 2.2 some of the presented results are shown. The three graphs show the heat loss to the surrounding room, the stand-by loss and in the third graph both the heat loss and the stand-by loss for two boilers. The losses, expressed as a percentage of the burner input, are functions of the difference between the average boiler temperature and the boiler room temperature, $\Delta\vartheta$.

The heat loss to the boiler room, q_{St}, is expressed as radiation loss and shows the same behaviour for all tested boilers, only the value differs. Stand-by loss for one of the boilers is shown in the lower left graph. The two upper curves show the stand-by loss with gas or electrical boiler heating. In the latter case, the water cirquit contains an electric heater outside the boiler unlike the first case where the burner is used. The difference in stand-by loss may be explained by different heat exchanger temperatures when either the burner or the electric heating is used to maintain the boiler temperature. The air flowing through the boiler is likely to be affected by these different surface temperatures. In the French test (French standard NF D30001), the boiler temperature is kept constant using external heating of the water

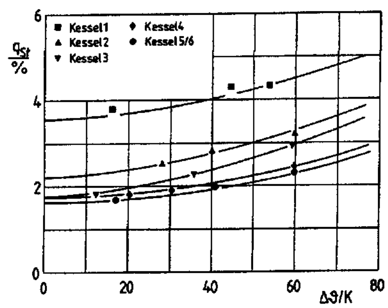

Lower left graph

– Interior losses, electric heating

△ External losses, electric heating

◇ Total losses, electric heating

□ Losses, gas firing

Lower right graph

◇ Stand-by losses

◆ Radiation losses

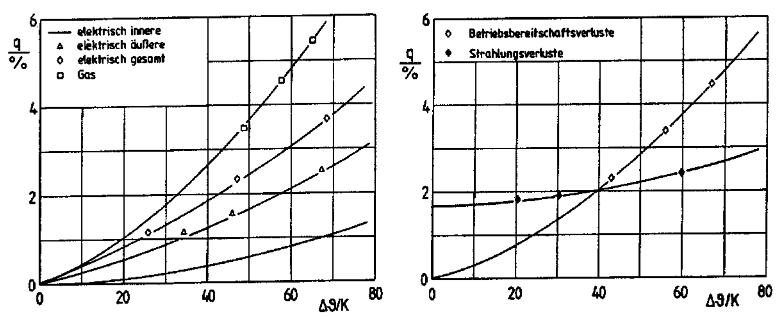

Figure 2.2: Measured heat losses from gas boilers

while the boilers own burner is used for the same purpose in the German test (German standard DIN 4702). This differences may explain the different results obtained applying the French and German stand-by tests.

The graph at the bottom right of the figure shows both the stand-by loss and the heat loss to the boiler room, and one clearly sees that the stand-by loss is much more temperature dependent. The curve shape is unique for each boiler model.

2.2 Building Parameters

The heat flows in a building form a complex pattern. In figure 2.3 a building and the different heat flows are shown. The heat demand consists of transmission loss $\dot{Q}_{trans}$ through walls, windows, floor and roof, controlled ventilation loss $\dot{Q}_{vent,1}$ and uncontrolled ventilation loss $\dot{Q}_{vent,2}$ due to leakage

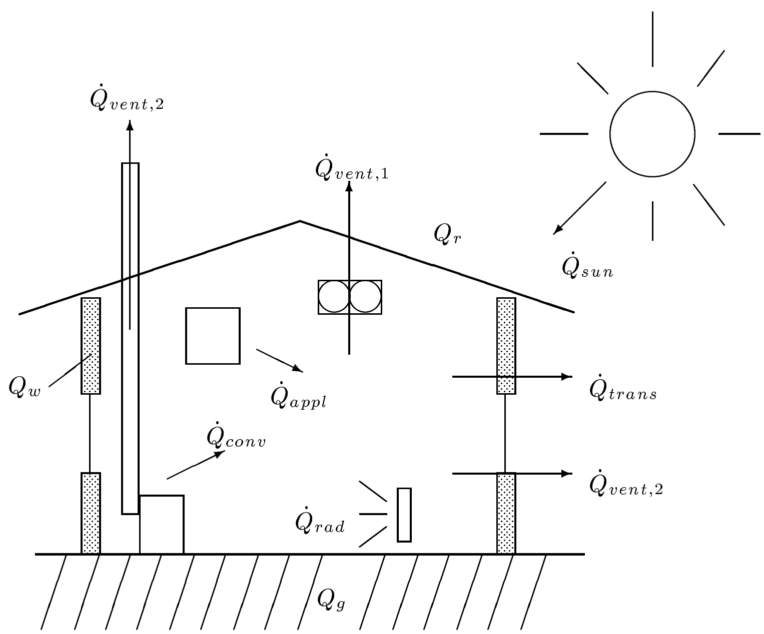

Figure 2.3: Heat flows in a building

in for example window openings. In general, the walls including windows, roof and floor have quite different heat insulation qualities and heat storage capacities. Heat from the heating system $\dot{Q}_{rad}$ is normally responsible for the major part of the space heating. The indoor air is also heated by heat losses from the boiler to the boiler room $\dot{Q}_{conv}$ ($\dot{Q}_{lh} + \dot{Q}_{lw}$), heat from electric appliances $\dot{Q}_{appl}$, heat from occupants and solar radiation $\dot{Q}_{sun}$.

The boiler operating conditions generated by the building can be described by simple steady-state expressions for heat load and heating system temperatures. The heat load may be calculated from the annual net heat demand and the outdoor or ambient temperature assuming a linear relationship. This can be done if a period of several hours are considered or if the building has no habitants. The radiator system temperatures are easily calculated, see for example Ransmark [67]. These data can then be used for an analysis of the boiler operation.

Effects of night setback on the boiler efficiency and gas consumption need a more detailed, dynamic, building description. For this, dynamics due to heat stored in walls Q_w, roof Q_r, floor and ground Q_g and indoor air Q_{air} need to be considered as well as the changes in radiator temperatures. A further discussion is made in the derivation of the building model, see page 66.

The different parts of the building and the heating system in which the boiler is installed influence the entire system performance, e.g. the annual efficiency. The parts considered are shown in figure 2.4.

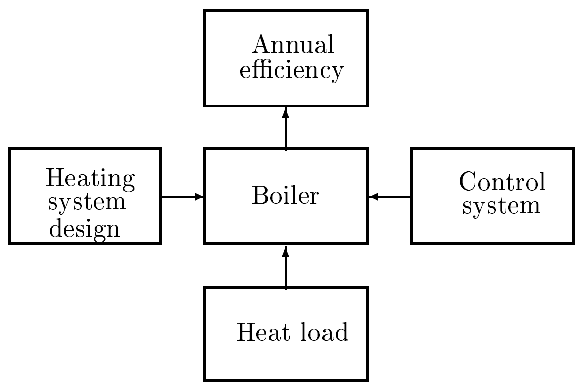

Figure 2.4: The boiler and the environment influencing the annual efficiency

The following boiler parameters are assumed to have an influence on the efficiency: the heat exchanger design, the burner input and the excess air ratio, the heat losses, the boiler heat capacity and the boiler thermostat characteristics.

The control system also influence the efficiency. The boiler operating conditions are not the same when different control systems are used. They can use for example a boiler thermostat only, a room thermostat or an outdoor temperature controlled thermostat. Also, a circulation pump with either a timer or a variable speed are sometimes included in the control system and it can also influence the boiler operating conditions.

The heat load is defined by the house design and the climate as well as the possibility to use night setback. The heating system includes important factors as the design temperatures, the heat capacity and the water flow.

2.3 Gas Boiler Electricity Consumption

Electric power consumption for the combustion fan and circulation pump is necessary for the generation and distribution of heat. These devices are also responsible for the major part of the electric power consumption in gas-fired boilers. It is therefore of interest to investigate the power consumption as well as the gas cost. Especially in low energy houses and in countries where the ratio between electricity and gas prices is high the cost for the electricity consumed is not negligible compared to the gas cost. The electric power consumption P_{tot} is composed of

$$P_{tot} = P_{fan} + P_{ign} + P_{control} + P_{pump} \tag{2.4}$$

where subscripts *fan*, *ign*, *control* and *pump* denote the combustion fan, the flame ignition, the control system and the electronic devices in the boiler and finally the water circulation pump respectively. In a warm-air heating system the circulation pump is replaced by an air circulation fan.

The power consumption for each device is either constant or dependent on the burner operation. A modulating burner and a variable speed circulation pump may give a power consumption which is not constant at each operating condition. However, even in these cases the power consumption can be described by much simplier expressions than the transient heat transfer processes in the boiler.

3

Models for the Prediction of Boiler Performance

To what extent is it possible to predict the boiler performance in different situations? In this chapter are models for the prediction of boiler performance described and commented. The description is limited to typical model structures and thus no standards or regulations are described. Models used to predict boiler performance can be divided into two types:

- Models to be used for existing boilers. Measured heat flows are used in the predictions.
- Models for prediction of the performance of an arbitrarily chosen boiler design. Design specification and heat transfer correlations are used in the predictions. The design specification includes the heat exchanger geometry.

Most models, independent of the above mentioned types, only deal with heat transfer in the boiler. The electricity consumed, necessary for the boiler operation is seldom considered. A simple model for the electricity consumption is therefore also presented in this chapter.

3.1 Models for Existing Boilers

Several purposes for the use of measured or predicted part-load performance can be mentioned. Among them are consumer information, fulfilling appliance standards e t c]. Models and testing procedures used for official efficiency data or labelling are not discussed. Instead, different approaches are discussed. Models for annual efficiency prediction are often based on simple equations for the part-load efficiency.

The main error source in all models is the estimation of the boiler heat losses which normally only are a minor part of the energy input. Therefore will even the simpliest model in most cases seldom give errors exceeding a few percent. However, if a few test measurements are to be used for an annual efficiency prediction or for quality rating, the model must have an accuracy equivalent to the test accuracy, i.e. not worse than approximately 2–3%.

Several models for part-load performance prediction have been presented. They can be divided into one group containing models based on a steady-state approach and one group where the models include dynamics.

Simple models based on steady-state heat balances cannot take transient effects into considerations. It is therefore difficult to rely on these models if the operating conditions differ much from the test conditions. More detailed models are easier to improve due to their often physically better description of the heat transfer. Dynamic models give the opportunity to an even more detailed description of the boiler performance.

3.1.1 Steady-State Models

An easy-to-use model for annual efficiency predictions was derived by Dittrich in 1972 [18]. The model is based on the assumption of two steady-state conditions, full load and stand by, see figure 2.1 on page 27. During a period t of full-load operation the boiler input energy Q_1 with η_b boiler efficiency equals

$$Q_1 = t\,\frac{\dot{Q}_{out}}{\eta_b} \tag{3.1}$$

where $\dot{Q}_{out}$ is the heat output. Convective losses are included in η_b. During the stand-by period, $t_{tot} - t$, the energy Q_2 is supplied to compensate for the stand-by loss represented by q_{sb}

$$Q_2 = (t_{tot} - t)\, q_{sb}\, \frac{\dot{Q}_{out}}{\eta_b} \tag{3.2}$$

which gives the annual efficiency η as

$$\eta = \frac{Q_1\,\eta_b}{Q_1 + Q_2} = \frac{\eta_b}{1 + \left(\frac{t_{tot}}{t} - 1\right)\, q_{sb}} \tag{3.3}$$

This way of predicting the annual efficiency assumes a linear relationship between heat losses and operating time. It is only accurate if a constant boiler temperature is used. An advantage is the use of easily measured parameters but fixed values are used for the full-load efficiency and stand-by loss. Plate and Tenhumberg [64] improved the model by introducing heat load dependent functions for heating system temperatures, stand-by loss and full-load boiler efficiency. These changes made it possible to predict the efficiency for boilers with load dependent temperatures as well, for example when using an outdoor temperature controlled flow temperature. This is a step towards a performance prediction where all heat flows are separated and individually described. However, in the Dittrich model, with and without improvements, the heat losses are included in the full-load efficiency and the stand-by loss.

Separating the losses makes it possible to describe the part-load operation more in detail. Models with a steady-state approach including a detailed description of the heat losses have been developed by for example de Wit and Paulsen [17] and the author [56]. The heat losses are in these models separated into $\dot{Q}_{lw}$, $\dot{Q}_{lh}$, and $\dot{Q}_{lf,off}$. The different expressions used are shown in equations 3.4–3.8. de Wit and Paulsen calculate the stand-by loss $\dot{Q}_{lf,off}$ as

$$\dot{Q}_{lf,off,[17]} = (1.0 - I)\,\dot{Q}_{lf,ref}\left(\frac{T-20}{45}\right)^{1.3} \tag{3.4}$$

where I is a relative load ($\dot{Q}_{rad}/\dot{Q}_b$) based on heat load and burner input and $\dot{Q}_{lf,ref}$ is the stand-by loss at the reference condition (65°C). The author has chosen equation 3.5 for the calculation of the stand-by loss

$$\dot{Q}_{lf,off,[56]} = k_1 \Delta T^n \tag{3.5}$$

The difference between the average boiler temperature and the room temperature is denoted ΔT. The constant k_1 and the exponent n are determined by stand-by tests at different boiler temperatures.

Heat loss from the boiler surface $\dot{Q}_{lw}$, is in both models calculated in analogy with heat transfer from heating system radiators as

$$\dot{Q}_{lw,[17]} = \dot{Q}_{lw,ref}\left(\frac{T-20}{45}\right)^{1.3} \tag{3.6}$$

and

$$\dot{Q}_{lw,[56]} = k_2\,\Delta T^{1.3} \tag{3.7}$$

Heat loss from hot spots occurs only during burner operation and is according to de Wit and Paulsen directly proportional to the relative load I. It is written as

$$\dot{Q}_{lh,[17]} = I\,\dot{Q}_{lh,nom} \tag{3.8}$$

where $\dot{Q}_{lh,nom}$ is the nominal loss (continous burner operation).

3.1.2 Models Including Dynamics

The steady-state performance models do not directly take dynamic behaviour into consideration with a few minor exceptions. A model by van Rij and Overman [81] contains a parameter for start-stop effects, i.e. changes in the steady-state heat balances only depending on the cycling frequency. The model by de Wit and Paulsen [17] includes a calculation of the heat loss caused by pre-purge ventilation. The boiler heat capacity is used in a simple expression for the cycling frequency at a known heat load.

The newly developed SAVE model described by Schweitzer [72] is based on steady-state heat balances. The average flue gas temperature is calculated using time constants for the heating and cooling of the heat exchanger. The time constants are determined from a 30% heat load test.

Laret [43] has developed a model which includes the dynamic behaviour. Basic thermodynamic relations are used for the boiler description. A first order differential equation is used to characterise the dynamic behaviour. The water and the heat exchanger are together considered as the boiler heat capacity. All terms such as heat flows, temperatures e t c are assumed to be proportional to the relative operating time. The model is calibrated using data from a full-load and a part-load test. A time constant for the heat capacity is obtained from the part-load data and further used to determine the dynamic characteristics. Describing the heat exchanger by means of the total heat transfer (UA) also gives the possibility to analyse boilers with modulating burners. Laret claims that the accuracy is better than 1% for predictions covering a wide range of operating conditions.

Claus and Stephan [13] developed a model for furnaces and boilers. The transient heat transfer analysis included a first order differential equation; the boiler is treated as a single heat capacity. Temperatures and draught in the chimney are also calculated in order to calculate air flow during the burner stand-by period. As in the previous model, experimental data are used to fit the model to the test results.

Lebrun et al. [44] found that the steady-state approach gave fully satisfactory efficiency values if long periods are considered. However, it is claimed that a dynamic boiler model is necessary to evaluate all topics in an integrated boiler and building system. Two heat capacities are used in the model, the flue gases and the heat exchanger including the water.

Transient heat transfer and boiler efficiency for larger boilers, >200 kW, with fan assisted burners has been investigated by Pfeiffer [60]. This model is however not general in the sense that it can be used for any boiler together with a few calibrating test results, it is rather a model for carefully described boilers.

The model includes radiation heat transfer from the flame to the combustion chamber walls, convective heat transfer in the combustion chamber and the heat transfer in the convective parts of the heat exchanger. The surface shape can also be sufficiently described, for example taking fins into account. Good agreement with manufacturers' data is reported. Purposes mentioned for this model are to studies of the gas temperature and retention time in the combustion chamber for NO_x formation reasons, and wall temperatures when modulating burners are used.

The last example of models shows some additional uses for detailed boiler analysis that can be performed with a more detailed physical description. The main disadvantage of models of this kind is their limited use to only one or a few boilers. The particular model however, describes a widely used boiler design and can therefore be adapted to more boilers than most similar models.

3.1.3 Models for Other Fuels

Gas or oil fired boilers are easier to model compared to for example wood fired residential boilers. This is due to the ease to measure and keep constant the firing rate. Problems arising when modelling wood fired boilers regard the heat input, unburnt fuel and CO. Examples on the modelling and testing of such boilers are one model by Ahmad [1] and a testing procedure by the National Swedish Testing Institute [78].

3.1.4 Comments on Part-Load Efficiency Models

Part-load efficiency models usually use an approach of comparing steady-state heat flows at full-load and part-load conditions. In most cases the accuracy of the predicted part-load efficiency could be within a ±3–4% range. A comparison between calculated and measured efficiencies for several models is reported by Koot et al. [39]. Largest differences between the predictions and the measurements occured in part-load conditions for a boiler with high, not directly measured, heat losses. However, when all operating conditions during the heating season are taken into account the deviation from measured values decrease to a maximum of 3–4%. The boilers with high heat losses, used to test model limits, show differences up to 10% between measurements and calculations. All models used in the investigation were based on steady-state approaches.

Models based on a transient heat transfer approach are more often based on thermodynamic relationships which make them easier to improve. Often, they are used to predict the performance of non-existing boilers. The use of such models is normally restricted to overall system studies instead of being used as tools for the engineer or installer.

Heat Losses

The flue loss during burner operation is the easiest loss to measure. In condensing boilers this loss is equivalent to, or often lower than other losses. In models based on steady-state heat balances the average flue gas temperature during the burner operation is seldom possible to calculate. Instead, the steady-state value is used which gives an error in the flue loss prediction. Using overall heat transfer characteristics and a transient heat transfer approach give a way to better predict the average flue gas temperature.

Heat loss due to the convection and radiation from the boiler surface and heat loss due to the cooling of the boiler interior during the burner stand-by time are based on different temperatures. These are the heating system return or flow water temperatures or the average value of these temperatures.

Expressions for the different losses in steady-state models often lack a thermodynamic base and are fitted to a few test results. In a boiler the heat exchanger surface temperature during the burner stand-by period will increase at a higher cycling frequency, see Koot, Koschowitz and Näslund [40]. A model including transient heat transfer capability was developed and used for evaluation of the influence from cycling frequency[1]. In figure 3.1 flue gas temperature and heat exchanger temperature near the outlet are shown. The graphs show the result for a 17 kW boiler (35% excess air) at 52% load. Cycling frequencies are 2.5, 10 and 30 operating cycles per hour. In table 3.1 average material temperatures are shown. Segment 1 and 3 represent the inlet and outlet of the heat exchanger.

Table 3.1: Average flue gas and material temperatures (°C) in a non-condensing boiler for different cycling frequencies

	Cycling frequency (cycles/h)		
Period	2.5	10	30
Segment 1			
cycle	159.5	146.8	145.2
on-time	183.4	149.4	147.5
off-time	133.4	144.6	148.8
Segment 2			
cycle	72.1	69.9	70.2
on-time	74.5	70.0	69.6
off-time	69.6	69.9	70.6

The table shows that the largest differences occur between 2.5 and 10 cycles/h. Further, the differences between the average values are more pro-

[1] The model is a simplified version of the boiler model described in the next chapter.

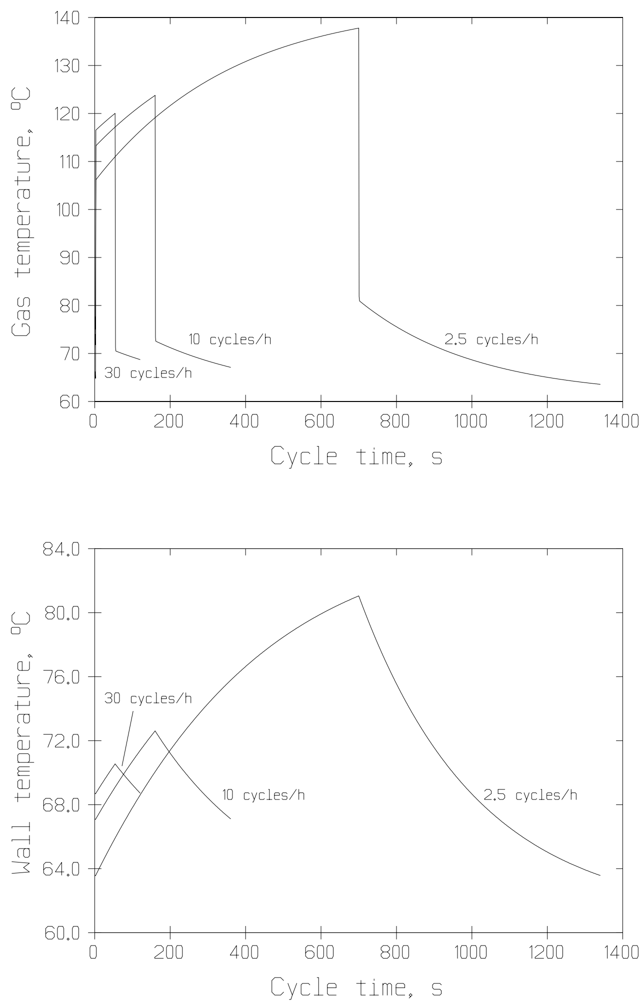

Figure 3.1: Flue gas temperatures (top) during the burner operation and wall temperatures near the outlet (bottom) at different cycling frequencies. Calculated values for a boiler with 17 kW gas input and 52% load.

nounced in the first part of the heat exchanger. The most interesting temperature for the stand-by loss is maybe the material temperature during the stand-by time. This temperature is increasing for an increased cycling frequency. We also observe a tendency to a lower flue gas temperature for the higher cycling frequencies. In a boiler with an atmospheric burner it is likely that an increased cycling frequency results in a higher stand-by loss due to the higher heat exchanger surface temperature. No model studied based on steady-state heat balances seems to include this effect. In boilers with fan assisted burners the effect on stand-by loss is probably negligible. However, the heat loss during the burner pre-purge time may be affected.

Control System

Several methods of adapting the boiler operation to the heat load are possible. The most commonly used involve a boiler thermostat alone, a room thermostat or an outdoor temperature controlled thermostat. The method used is often dependent on the country of operation. For example, in Sweden and Germany an outdoor temperature controlled flow temperature is often used while room thermostats are widely used in the Netherlands. Often are the part-load models not able to take different control systems into account. An exception is the earlier mentioned SAVE model.

It is not unlikely that new control strategies will be introduced or gain market share. Two examples are adaptive control systems and control systems developed within the smart house concepts. To the latter may belong a control systems for individual room heating. This means that performance models need to be continously improved in order to be up to date with commercial boilers.

Environment

The environment is in this context defined by the heating system and the building. It determines the boiler temperature and to some extent also the flue gas temperature and thus the maximum obtainable efficiency and some of the heat losses. Models which use the boiler temperature for the calculation of stand-by and convection heat losses are able to take the effect of different heating systems into consideration. However, heating systems which have considerably different water flows compared to those of the efficiency tests may increase or decrease the start and stop loss without any possibility to predict this in many models.

Concluding Remarks

The comments made on models, and calculation of different heat flows and losses, point towards the use of a dynamic heat transfer approach if a wide range of operating conditions, also except those few in the laboratory tests, shall be possible to treat accurately. A steady-state approach is sufficient if losses are separated and part-load efficiency for an existing boiler sought for. However, the need for a dynamic model is greatly reduced if simple expressions for as many boiler characteristics as possible are included in a static, or steady-state, model.

3.2 Models for New Boilers and as Design Tool

A survey of existing models for calculating the performance of condensing boilers or heat exchangers is presented in this section. These models are based on a boiler or heat exchanger design specification rather than measured heat flows as in the previous models. The purpose is to show some data about their aim, design, restrictions, results and accuracy. The presented models often use heat transfer correlations developed for dehumidifiers or heat pumps, not correlations especially designed for the heat transfer between the flue gases and heating system fluid. The influence on the boiler performance from the different boiler parts can be evaluated using these models. The possibility to evaluate parts or details depend on the accuracy of the boiler description.

3.2.1 Gaz de France

At the French gas company Gaz de France a model for condensing heat exchangers has been developed, and described by Pelloux-Prayer [59].

The model applies to separate heat exchangers connected after a conventional gas boiler. Mass transfer is calculated from known heat transfer correlations for non-condensible heat transfer and using the Chilton-Hougen analogy between heat and mass transfer. Since the gas inlet temperature is low, 150–250°C, no attention needs to be paid to gas radiation and flame radiation. The overall steady-state efficiency for a boiler and a condensing heat exchanger is said to be calculated with an accuracy of ±1%.

Furthermore, the influence of tube design, smooth or finned tubes, was investigated. Two heat exchangers, one with finned tubes and one with smooth tubes, with the same performance in non-condensing operation were compared in condensing operation. Best result was obtained with the smooth tubes due to decreased fin efficiency in the presence of condensation for the finned tubes.

3.2.2 USA

A number of condensing heat exchanger models have been developed in USA. Among them are a model for oil furnaces and boilers by Ball and

White [4] and three models for warm-air furnaces by Lux et al. [45], Fischer and Stickford [22] and Aronov and Sheridan [2].

The model by Fischer and Stickford, CONDHX, deals with a finned tube heat exchanger in a cross flow for warm-air furnaces and steady-state operation. Air is flowing outside the tubes while the flue gas flows inside the tubes. For the calculation of the air-side heat transfer coefficient, a heat pump model is used.

The authors recommend a calibration of the model to fit it to experimental data by adjusting a number of constants. The model will then be ready for the prediction of the effects due to changes in the operating conditions.

3.2.3 British Gas

At British Gas, a steady-state heat transfer model suitable for residential boilers has been presented by Newcombe and Dixon [50]. The purpose of the development of the model and a computer program was to provide reliable design data.

The authors mention the possibility of using the model in a quasi-steady mode in order to describe the transient conditions found in commercial boilers. The simulated boiler is seen in figure 3.2. The burner fires downwards facing the heat exchanger which consists of finned tubes.

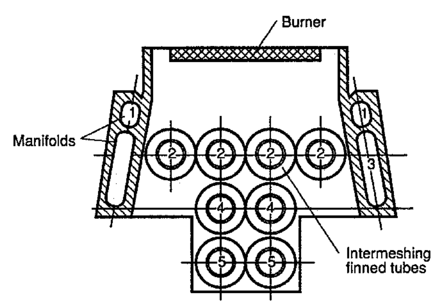

Figure 3.2: Boiler design used in British Gas' condensing heat exchanger model

The model uses correlations for convective heat transfer with and without condensation from previous work and radiative heat transfer. Heat is transferred to the heat exchanger as well as to the manifolds. Experiments showed a substantial deviation between model prediction and measured data. Heat transfer coefficients computed from measurements were 2–3 times the predicted coefficient. Experimental data were used to establish new heat transfer correlations. The heat transfer coefficient data is presented for Reynolds number Re = 300–750 (the characteristic length for calculating Re is not mentioned). The conclusion drawn is that empirical data must be obtained from specific tests.

Yau and Rose [85] have also studied the performance of condensing boilers of the same design. The calculations were made for steady-state conditions using the fin efficiency η_f for the heat transfer to the tubes. They studied three heat exchanger configurations, one identical with figure 3.2 and the other two had three and two tubes in the first row, the latter a pure in-line configuration. Best performance was shown for the configuration with three tubes in the first row despite less heat exchanger area. The largest difference between the configurations, measured as heat output, was approximately 5%. This difference decreased as return water temperature increased. The study shows that a substantial reduction in heat exchanger area is possible by rearranging the heat exchanger tubes and thus improving the performance.

3.2.4 Danish Technological Institute

The most detailed model for performance calculation is the model from Danish Technological Institute (DTI) by Gundtoft [26]. It is applicable for non-condensing boilers. In figure 3.3 the system of boiler and heating system is shown. The boiler model allows calculation of time resolved temperatures of flue gases and boiler water in an well defined environment comprising the heating system and the building. The stand-by loss is also calculated thus making a calculation of boiler efficiency possible at an arbitrarily chosen operating condition.

Equation 3.9 is the basic equation for the modelling of the boiler. As seen in figure 3.3 the boiler is divided into three parts. For the first of these three parts a heat balance is written as

$$\begin{aligned}
&\overbrace{\frac{T_{b1,new} - T_{b1,old}}{\Delta t}\,\frac{m_b}{3}\,c_{p,H_2O}}^{\text{Heat transfer to the boiler material}} \quad + \\
&+ \overbrace{\dot{m}_{H_2O,tot}\,c_{p,H_2O}(T_{b1,old} - T_{ret,BP})}^{\text{Heat transfer to the boiler water}} = \\
&= \underbrace{U\,(T_{ret,1} - T_{b1,old})}_{\substack{\text{Heat transfer from the}\\ \text{flue gases to the boiler}}} - \underbrace{\frac{\dot{Q}_{conv}}{3}\left(\frac{(T_{b1,old} - T_{cc})}{40}\right)^{1.3}}_{\text{Convective loss}} \qquad (3.9)
\end{aligned}$$

where $T_{b..}$ is the temperature of each boiler part, T_{cc} is the gas temperature in the combustion chamber, $T_{ret..}$ is the water temperature in the by-pass pipe or in the heating system return pipe, m_b is the total boiler mass,

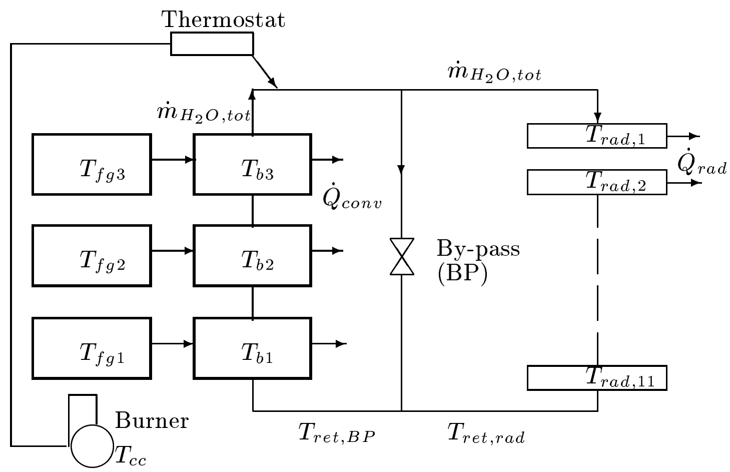

Figure 3.3: The division of a boiler into different parts according to the model from Danish Technological Institute

$\dot{m}_{H_2O,tot}$ is the water mass flow in the boiler and U is the overall heat transfer coefficient. One purpose of the model development was to get a tool to improve the boiler efficiency by evaluating changes in the burner control system, the pre-purge time and the outdoor temperature boiler control.

3.2.5 Error Sources

It is not the intention in this thesis to derive more accurate correlations for the heat transfer in residential gas boilers, but an attempt to explain the differences between model results and actual measurements is made. The differences are assumed to exist on the flue gas side in the heat exchanger.

Experiments for the correlation of heat and mass transfer data have most certainly been made with uniform inlet flow conditions. In gas boilers we often find flow fields which may not be in accordance with the assumed flow fields in the heat transfer correlations that have been used in the various models.

Calculations of the flow field in a tube bundle can be used to evaluate possible sources for model errors. The computer code FLUENT [16] was used for a short study of the flow fields in in-line and staggered tube arrangements. Inlet flow conditions simulating different burner cross sections were also used.

The tube arrangements studied are shown in figures 3.4 and 3.5[2]. The domain cross section is 185×305 mm and has a length of 185 mm. 6 rows of tubes are included; 4 tubes per row in the in-line arrangement and 3 and 4 tubes in the staggered tube arrangement. The tubes have sharp edges as seen in the figures. This is due to the fact that the FLUENT version used did not allow for body fitted coordinates (BFC) and that the number of cells was limited to 20 000. Only cold flow fields were calculated; i.e. no heat transfer. The flow assumed was set to 25 m^3/h. Inlet flow conditions were set by assuming three burner types, a burner covering the entire cross section, a line burner over a third of the cross section and finally a square opening simulating a fan assisted burner. From the calculations, flow fields are showed for two cases. These are the flows in the two tube arrangements and inlet flow as if a burner covering the entire cross section (a uniform inlet flow field) was used, see figures 3.4 and 3.5.

The two figures show the flow field at the center of the domain. Significant differences between the tube arrangements are clearly seen. The flow closer to the walls is similar to that at the center with this simulated burner. Larger differences are found when the assumed burner does not give a uniform inlet flow. Especially when in-line tube arrangement is considered, the flow is concentrated to the domain center. Large differences in the flow fields between the center and the walls where the tubes are connected are also observed.

It seems interesting to perform a more in-depth study of the interaction between the tube arrangement, the burner type and the flow field. This may also include measurements, for example Laser Doppler Anemometry (LDA), to verify the calculations.

3.2.6 Concluding Remarks

Models that can be used as design tools for gas fired boilers are much more limited to a particular design than the previous steady-state or dynamic models. The more detailed models described in this chapter give more in-depth information about the boiler characteristics, for example the local temperatures. In general, these models are not complicated and the calculations are straightforward. Well known heat transfer correlations are normally used.

The need for calibration or correction in some of the models clearly illustrate the complicated heat transfer processes involved in condensing boiler or furnace designs. It also shows the difficulty of using heat transfer data and correlations obtained from carefully controlled experiments in boiler models. Differences explaining the need for calibration may exist in the flow field and in the temperature distribution.

[2] They are the same as the boiler model in the next chapter.

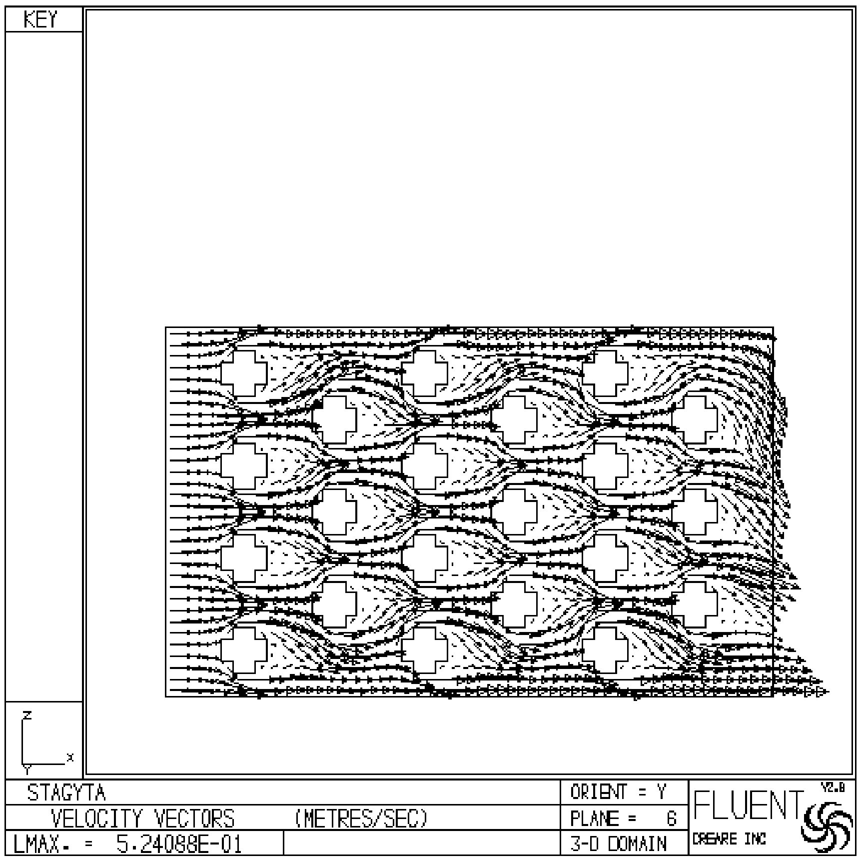

Figure 3.4: Cold flow field calculated for a staggered tube arrangement. Uniform inlet flow, center of domain. Re = 550

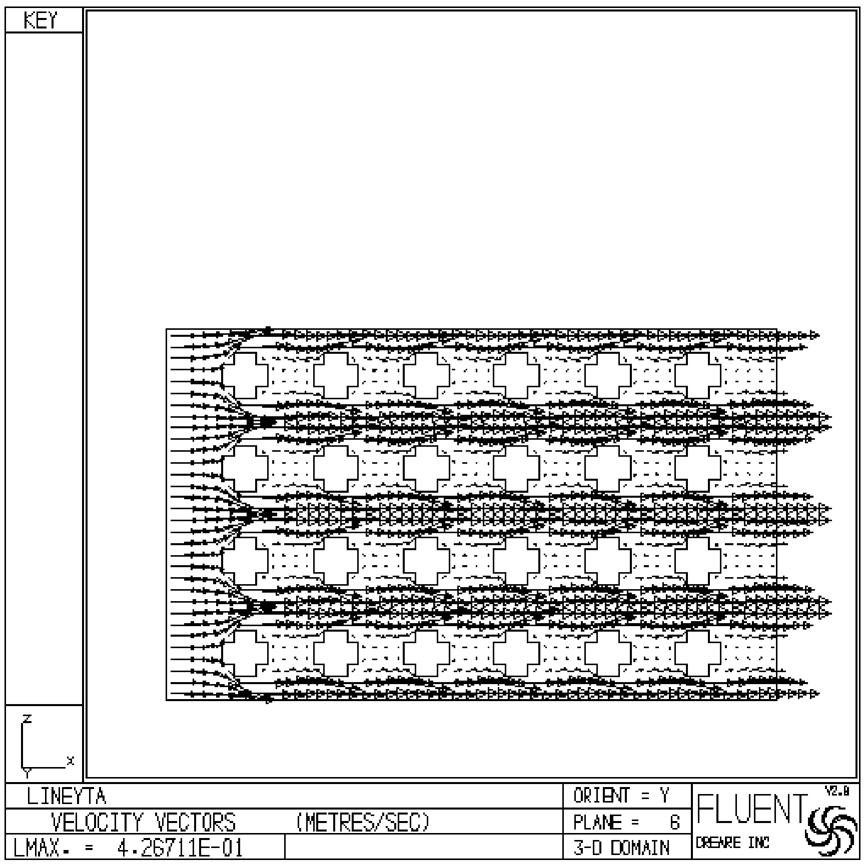

Figure 3.5: Cold flow field calculated for an in-line tube arrangement. Uniform inlet flow, center of domain. Re = 550

3.3 Electricity Consumption

The performance models described in this chapter do not include calculations of the electricity consumption. This must be done if the total energy consumption and the total energy cost are to be determined. A model for the electricity consumption will be presented here. The combustion air fan, the circulation pump, the flame ignition and the control system are dealt with separately. This model can easily be included in models for existing boilers.

3.3.1 Combustion Air Fan

Calculating the total fan operating time including the pre-purge time, requires knowledge of the number of burner starts during a certain time period. The hourly heat delivered to the house, Q_{rad}, is

$$Q_{rad} = \dot{Q}_b \, \tau \, \eta_b \, 3600 \tag{3.10}$$

where the relative time τ is defined as

$$\tau = \frac{t_{on}}{t_{on} + t_{sb}} \tag{3.11}$$

and t_{on} and t_{sb} are defined as the burner operating time and burner stand-by time in an operating cycle. The number of cycles n during one hour is

$$n = \frac{3600}{t_{on} + t_{sb}} \tag{3.12}$$

and the total fan operating time per hour, t_{fan}, becomes

$$t_{fan} = n \, (t_{on} + t_p) \tag{3.13}$$

where t_p denotes the pre-purge time. The hourly electrical energy W_{fan} supplied to the fan with electrical input P_{fan} is

$$W_{fan} = P_{fan} \, n \, (t_{on} + t_p) \tag{3.14}$$

An expression for the share of the combustion fan electricity consumption to the energy output Q_{rad} then reads

$$\frac{W_{fan}}{Q_{rad}} = \frac{P_{fan} \, n \, (t_{on} + t_p)}{\dot{Q}_b \, \tau \, \eta_b \, 3600} \tag{3.15}$$

and finally by combining equations 3.12 and 3.15

$$\frac{W_{fan}}{Q_{rad}} = \frac{\frac{P_{fan}}{t_{on}+t_{sb}}\,(t_{on} + t_p)}{\dot{Q}_b\,\tau\,\eta_b} \tag{3.16}$$

The electrical energy required for the combustion air fan is shown in figure 3.6. Equation 3.16 was used to calculate the curves. The electrical input to the fan is 20 W and the burner input is 10 kW. The pre-purge time is set to 30 seconds and boiler part-load efficiencies η_b of 80% and 90% are used. The results are shown with the electrical input as percentage of the heat output. It is clearly seen that the combustion air fan consumption is lower than 0.5% of the heat output as long as the burner operating time, t_{on}, exceeds 20 seconds in each operating cycle. Only at extremely short burner operating times the consumption reaches values exceeding 1%. A reduced pre-purge time, for example 5–10 seconds, will reduce the electricity consumption.

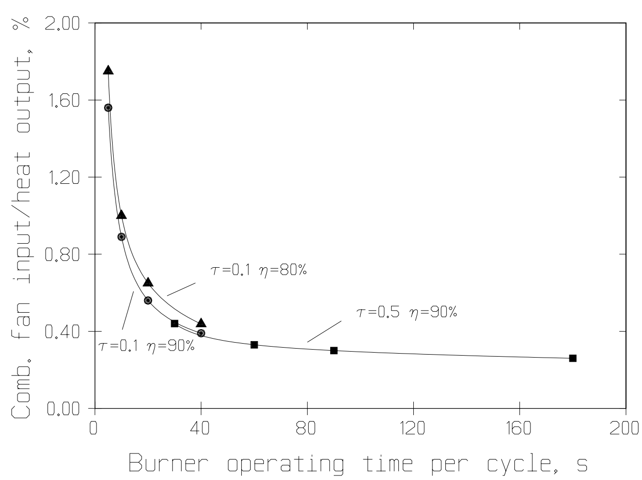

Figure 3.6: Combustion fan electricity consumption as function of heat output. The fan is assumed to have an electrical input of 20 W and the burner input is 10 kW. The pre-purge time is set to 30 seconds.

As seen in equation 3.16, the burner operating time has to be known. A simple expression for the cycling frequency, N, in a period has been presented by de Wit and Paulsen [17]. For space heating only, it is written as

$$N = \frac{1}{C\Delta T_{thermo}} \left(1 - \frac{\dot{Q}_{rad}}{\dot{Q}_b}\right) \dot{Q}_{rad} \tag{3.17}$$

where N is given in s^{-1} and C denotes the boiler heat capacity (kJ/K) and ΔT the boiler thermostat temperature hysteresis. The number of starts per hour n thus becomes

$$n = 3\,600\, N \tag{3.18}$$

This discussion has shown that the electricity consumption is dependent on parameters such as burner design, boiler heat capacity and parts of the control system.

3.3.2 Circulation Pump

The circulation pump is either operating continously or switched off some time after the end of the burner operation. A variable speed pump can also be used. Here, only pumps operating with a fixed capacity will be dealt with. For continous operation, the electrical energy consumption is

$$W_{pump} = t\, P_{pump} \tag{3.19}$$

The electricity consumption when the circulation pump can be switched off is dependent on heat load and the number of burner starts per time unit. The burner stand-by time, $t_{sb,cycle}$, is calculated as

$$t_{sb,cycle} = \left(1 - \frac{\dot{Q}_{rad}}{\eta_b\, \dot{Q}_b}\right) \frac{3\,600}{n} \tag{3.20}$$

for an operation with n burner cycles per hour. Equations 3.17 and 3.18 are used to calculate n. The circulation pump will only operate intermittently if $t_{sb,cycle}$ exceeds the time set by the timer, $t_{pump,off}$. The electricity consumption for the circulation pump is calculated according to equation 3.21 if intermittent operation is possible.

$$W_{pump} = P_{pump} \left[\left(1 - \frac{\dot{Q}_{rad}}{\eta_b\, \dot{Q}_b}\right) \frac{3\,600}{n} - t_{pump,off}\right] \tag{3.21}$$

3.3.3 Flame Ignition and Control System

For completeness, the electricity required for flame ignition and the boiler control system must also be included in a detailed model. The ignition electrical energy consumption per hour, W_{ign}, becomes

$$W_{ign} = n\, t_{ign}\, P_{ign} \tag{3.22}$$

A constant power consumption for the control system is assumed, i.e.

$$W_{control} = t\, P_{control} \tag{3.23}$$

3.3.4 Total Hourly Electricity Consumption

Combining the equations above gives an expression for the total electrical energy consumption during one hour, $W_{el,hour}$.

$$\begin{aligned} W_{el,hour} &= P_{fan}\, n \left(\frac{t_{on}}{3600} + \frac{t_p}{3600}\right) + 3600\, P_{pump} + n\, t_{ign}\, P_{ign} + \\ &+ 3600\, P_{control} = P_{fan}\, n \left(\frac{t_{on}}{3600} + \frac{t_p}{3600}\right) + \\ &+ 3600\, (P_{pump} + P_{control}) + n\, t_{ign}\, P_{ign} \end{aligned} \tag{3.24}$$

or

$$\begin{aligned} W_{el,hour} &= P_{fan}\, n \left(\frac{t_{on}}{3600} + \frac{t_p}{3600}\right) + n\, t_{ign}\, P_{ign} + 3600\, P_{control} + \\ P_{pump} &\cdot \left[\left(1 - \frac{\dot{Q}_{rad}}{\eta_b\, \dot{Q}_b}\right) \frac{3600}{n} - t_{pump,off}\right] \end{aligned} \tag{3.25}$$

when the circulation pump is switched off during a part of the burner stand-by time, i.e. $t_{sb,cycle} > t_{pump,off}$.

3.4 Conclusions from this Chapter

In this chapter the discussion have dealt with characteristics such as operating conditions and efficiency, and the influence from different parts in the building and in the boiler. Models for the prediction of the part-load efficiency and the annual efficiency have also been described and commented. These models can be used for existing as well as non-existing or future boilers. The part-load performance of existing boilers can be sufficiently well predicted by models based on steady-state heat balances. This requires a detailed description of the different heat flows. Models based on a transient heat transfer approach are well suited for system studies. These models use overall boiler characteristics.

Models suitable as design tools often use a detailed description of the burner and heat exchanger design. Heat transfer correlations from literature can then be used. Large deviations between predicted and measured heat transfer coefficients have been observed which illustrate the complex heat transfer processes in a boiler. It was also shown that the flow field in a heat exchanger changed considerably when different burner outlets were assumed. Flow fields different from those in tests for development of heat transfer correlations are probably present in many commercial boilers.

4

Development of a New Boiler Model and Modelling Results

Several models for the design of condensing boilers or furnaces have been presented. A common characteristic of almost all of these models is that only the condensing heat exchanger design is dealt with. The heating system and the building are seldom included as shown previously. In order to evaluate the effects of the boiler design, a quite detailed description of the parts involved is necessary. The model shall make it possible to vary the heat exchanger design, i.e. tubes and fins, mass flow and flue gas properties as well as the material properties.

The boiler model developed within this work is used for the calculation of the total energy use, gas and electricity, required by a well defined boiler installed in a well defined building and a certain control system. Three parts are therefore necessary in the model. They are:

- A submodel describing the transient heat and mass transfer processes in the boiler
- A submodel describing the house and the heating system
- A submodel describing the control system

Each submodel is described in the chapter as well as a general description is given of heat transfer in tubes with annular fins. A boiler with a heat exchanger consisting of tubes with annular fins was chosen for three main reasons:

- Heat transfer correlations are easily found in literature
- It is a common design among commercial boilers
- It is possible to build a flexible laboratory boiler of this design

Some of the tasks for such a detailed model are:

- Analysis of the overall performance
- Evaluation of material temperatures in order to avoid overheating of the fins
- Investigation of where the condensation starts and point out possible areas for corrosion

The first task, analysis of the boiler performance, is one of the two main topics of this thesis. It is possible to adapt the heat and mass transfer model to other heat exchanger designs. This adaptation requires known correlations for the heat and mass transfer in the new heat exchanger design.

4.1 Modelling the Performance of a Condensing Boiler

The heat transfer model described in this chapter is not intended to be an improvement of previous work on heat transfer in finned tube heat exchangers. Heat transfer correlations from other researchers are used for the modelling of the heat exchanger performance.

Investigations on the heat exchanger design considered, tube bundles of in-line or staggered configurations, have been made for applications such as gas turbine regenerators, power plant heat exchangers, heat pumps and air conditioning appliances. Two early examples are studies by Huge [31] and Pierson [62] on bundles consisting of smooth tubes in different arrangements and tube spacings.

4.1.1 Modelling Approach

The boiler to be modelled in this work consists of a bundle of finned tubes in an insulated box. Vessels outside the box connect the tube rows. The burner is located at the top firing downwards. This form a cross flow finned heat exchanger with multiple passes on the water side. Figure 4.1 shows a part of the assumed boiler design, two tube rows and the connecting vessel.

The burner is modelled as a source of a flue gas flow where gas input, excess air and radiation characteristics can be varied. The system controlling the boiler operation is idealised, i.e. the characteristics of real sensors are not taken into consideration. Instead, thermostats in for example the boiler and in rooms switch when boiler water and room temperature settings are reached without considering response times in these sensors. Future work could include studies of the influence of real sensor characteristics on the boiler performance.

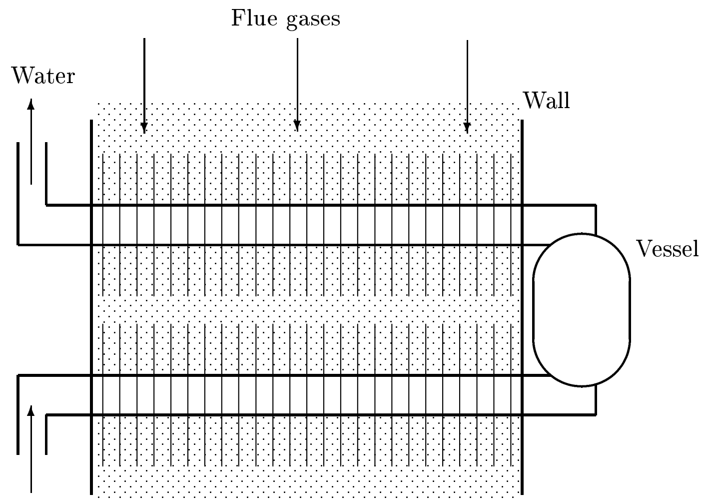

Figure 4.1: Assumed boiler design in the simulation model

4.1.2 Overall Heat Balance

Basically, a transient heat transfer model can evolve from a set of differential equations based on a small heat exchanger segment as shown in figure 4.2. In this approach three heat capacities are used, the heat exchanger material, the water and the flue gases.

A heat balance around the heat exchanger segment gives the following set of first order differential equations for changes in average heat exchanger temperature T_m, water temperature T_{H_2O} and flue gas temperature T_{fg}.

$$\frac{\partial T_m}{dt}(m\,c_p)_m = h_{fg}A_{fg}(T_{fg} - T_m) - h_{H_2O}A_{H_2O}(T_m - T_{H_2O}) \tag{4.1}$$

$$\begin{aligned}\frac{\partial T_{H_2O}}{dt}(m\,c_p)_{H_2O} = {} & h_{H_2O}A_{H_2O}(T_m - T_{H_2O}) + \\ & + \dot{m}_{H_2O}c_{p_{H_2O}}(T_{H_2O,in} - T_{H_2O})\end{aligned} \tag{4.2}$$

$$\frac{\partial T_{fg}}{dt}(m\,c_p)_{fg} = h_{fg}A_{fg}(T_m - T_{fg}) + \dot{m}_{fg}c_{fg}(T_{fg,in} - T_{fg}) \tag{4.3}$$

where subscript *in* denotes properties for fluid entering the segment. The heat transfer in the vessel is treated in an analogous way.

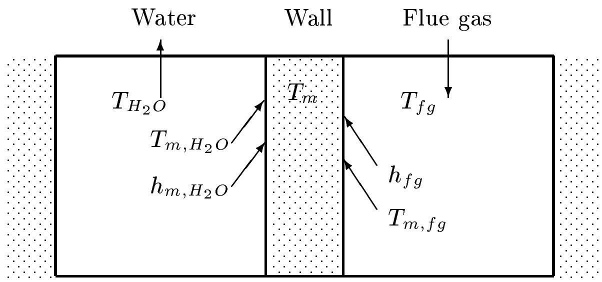

Figure 4.2: Heat balance around a heat exchanger segment in the boiler

4.1.3 Flue Gas Side Heat Transfer in Finned Tubes

In order to reach the goal of evaluating the influence of heat exchanger design on the boiler performance, it is necessary to calculate the radial fin temperature. The temperature may affect the condensate evaporation and heat loss during the pre-purge period. The text below shows different ways of calculating fin temperatures in steady-state and transient conditions. Further, only heat exchanger fins thin enough to have a constant temperature across the fin at a certain radius are considered in this work, i.e. fins having a small Biot number. The Biot number is defined as

$$\mathrm{Bi} = \frac{h\,b}{k} \tag{4.4}$$

where h is the heat transfer coefficient, b is the fin thickness and k is the thermal conductivity. If Bi<0.1, a constant temperature across the material can be assumed.

Analytical Description of Steady-State Temperatures in Annular Fins

The radial temperature distribution from the fin base at steady-state operation is described as follows. Consider a tube with annular fins of constant thickness, see figure 4.3. A heat balance around a small element in the fin gives

$$\dot{Q}_r = \dot{Q}_{r+dr} + d\dot{Q}_A \tag{4.5}$$

$$\mathrm{d}A = \frac{dA}{dr}\,dr \tag{4.6}$$

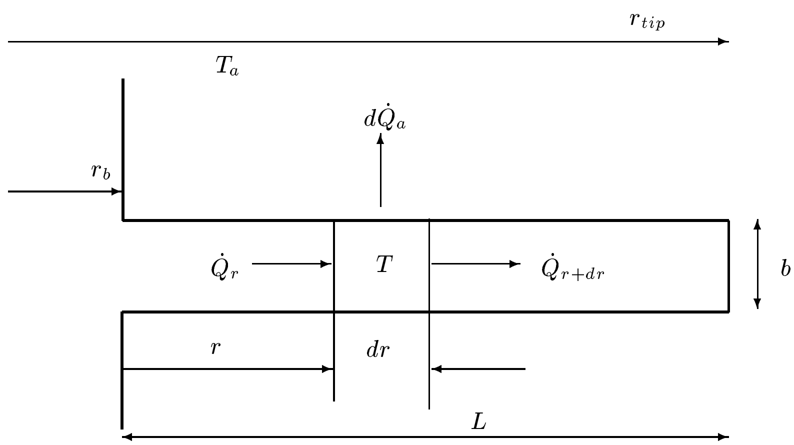

Figure 4.3: Heat exchanger tube with annular fins of constant thickness

This gives, see for example a paper by Gardner [23] and textbooks by Stasiulevičius [77] and Kern and Kraus [37]

$$\frac{d^2\Theta}{dr^2} + \frac{1}{r}\frac{d\Theta}{dr} - \frac{2\,h}{k\,b}\Theta = 0 \tag{4.7}$$

where $\Theta = T - T_{amb}$. The boundary conditions are

$$\begin{array}{ll} r = r_b & \Theta = \Theta_b \\ r = r_{tip} & \frac{d\,\Theta}{d\,r} = 0 \end{array}$$

The solution to equation 4.7 is

$$\Theta(r) = \Theta(r_b)\frac{K_1\,(m\,r_{tip})\,I_0\,(m\,r) + I_1\,(m\,r_{tip})\,K_0\,(m\,r)}{I_0\,(m\,r_b)\,K_1\,(m\,r_{tip}) + I_1\,(m\,r_{tip})\,K_0\,(m\,r_b)} \tag{4.8}$$

where I_0, I_1, K_0 and K_1 are zero and first order Bessel functions and

$$m = \sqrt{\frac{2\,h}{k\,b}} \tag{4.9}$$

where h is the heat transfer coefficient, k is the fin thermal conductivity and b is the fin thickness. Equation 4.8 describes the radial temperature distribution along the fin radius without condensation.

Discretisized Description of Steady-State Temperatures in Annular Fins

Dividing the fin into a finite number of elements or nodes gives another way of calculating heat transfer from the fin to the tube, see figure 4.4.

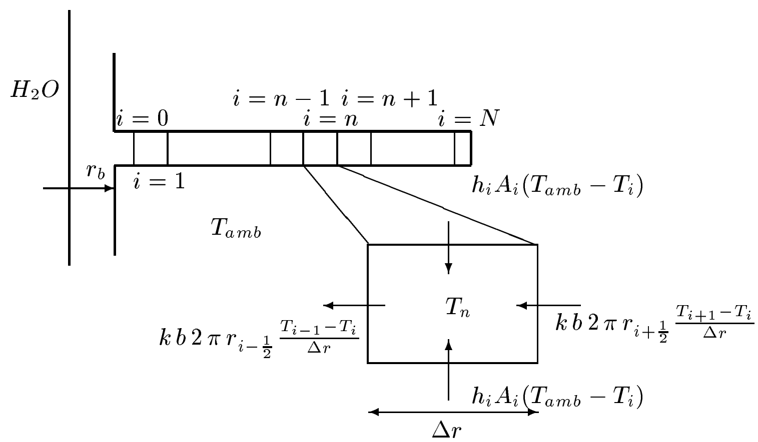

Figure 4.4: An annular fin and its elements

Assuming steady-state thermal conduction, a heat balance around fin node i gives

$$\begin{aligned} & k\,b\,2\,\pi\,r_{i-\frac{1}{2}}\frac{T_{i-1}-T_i}{\Delta r} + k\,b\,2\,\pi\,r_{i+\frac{1}{2}}\frac{T_{i+1}-T_i}{\Delta r} + \\ & +2\,h_i\,2\,\pi\,r_i\,\Delta r(T_{amb} - T_i) = 0 \end{aligned} \tag{4.10}$$

for $i = 1, 2, \ldots, N-1$. Multiply equation 4.10 with $\Delta r / k\,b\,2\,\pi$

$$r_{i-\frac{1}{2}}(T_{i-1} - T_i) + r_{i+\frac{1}{2}}(T_{i+1} - T_i) + \frac{2\,h_i\,r_i\,(\Delta r)^2}{k\,b}(T_{amb} - T_i) \quad = \quad 0 \tag{4.11}$$

where

$$r_{i-\frac{1}{2}} = r_b + (i - \frac{1}{2})\Delta r \tag{4.12}$$

$$r_{i+\frac{1}{2}} = r_b + (i + \frac{1}{2})\Delta r \tag{4.13}$$

For node $i=0$ the temperature is equal to the base temperature, i.e. $T_0=T_b$, and for node $i=N$ the temperature is equal to the tip temperature T_N which give for node N

$$
\begin{aligned}
&k\,b\,2\,\pi\,r_{i-\frac{1}{2}}\frac{T_{N-1}-T_N}{\Delta r}+h_{tip}\,2\,\pi\,r_N\,b\,(T_{amb}-T_N)+\\
&+2\,h_N\,2\,\pi\,r_{N-\frac{1}{4}}\frac{\Delta r}{2}(T_{amb}-T_N)=0
\end{aligned}
\tag{4.14}
$$

Multiply equation 4.14 with $\Delta r/2\,k\,b\,\pi$

$$
\begin{aligned}
&r_{N-\frac{1}{2}}(T_{N-1}-T_N)+\frac{h_{tip}\,\Delta r}{k}r_N(T_{amb}-T_N)+\\
&+\frac{h_N\,(\Delta r)^2}{k\,b}r_{N-\frac{1}{4}}\,(T_{amb}-T_N)=0
\end{aligned}
\tag{4.15}
$$

where

$$
r_{N-\frac{1}{2}}=r_b+(N-\frac{1}{2})\Delta r \tag{4.16}
$$

$$
r_{N-\frac{1}{4}}=r_{tip}-\frac{\Delta r}{4} \tag{4.17}
$$

Radial Temperature Distribution in Annular Fins in Transient Conditions

Transient conditions give for the same case for node i in analogy with equation 4.10

$$
\begin{aligned}
&\frac{dT_i}{dt}c_{p,i}\,V_i\,\rho_i=k\,b\,2\,\pi\,r_{i-\frac{1}{2}}\frac{T_{i-1}-T_i}{\Delta r}+\\
&+k\,b\,2\,\pi\,r_{i+\frac{1}{2}}\frac{T_{i+1}-T_i}{\Delta r}+2\,h_i\,2\,\pi\,r_i\,\Delta r\,(T_{amb}-T_i)
\end{aligned}
\tag{4.18}
$$

for $i=1,2,3,\ldots,N-1$. Analogous with steady-state conditions this gives after multiplication with $\Delta r/k\,b\,2\,\pi$

$$
\begin{aligned}
&\frac{c_{p,i}\,\rho_i\,(\Delta r)^2\,r_i}{k}\frac{dT_i}{dt}=r_{i-\frac{1}{2}}(T_{i-1}-T_i)+\\
&+r_{i+\frac{1}{2}}(T_{i+1}-T_i)+\frac{2\,h_i\,r_i\,(\Delta r)^2}{k\,b}\,(T_{amb}-T_i)
\end{aligned}
\tag{4.19}
$$

where

$$
V_i=2\,\pi\,r_i\,\Delta r\,b \tag{4.20}
$$

is used for the node volume i. For node $i=0$ the temperature is equal to the base temperature, i.e. $T_0=T_b$ and for node $i=N$ the temperature is equal to the tip temperature T_N which yields

$$\frac{dT_N}{dt} c_{p,N}\, V_N\, \rho_N = k\, b\, 2\,\pi\, r_{N-\frac{1}{2}} \frac{T_{N-1}-T_N}{\Delta r} + \\ + h_{tip}\, 2\,\pi\, r_N\, b\, (T_{amb}-T_N) + 2\, h_N\, 2\,\pi\, r_{N-\frac{1}{4}} \frac{\Delta r}{2} (T_{amb}-T_N) \tag{4.21}$$

and can as before be rewritten as

$$\frac{dT_N}{dt} \frac{c_{p,N}\, \rho_N\, (\Delta r)^2\, r_{N-\frac{1}{4}}}{2\, k} = r_{N-\frac{1}{2}}(T_{N-1}-T_N) + \\ + \frac{h_{tip}\, \Delta r}{k} r_N (T_{amb}-T_N) + \frac{h_N\, (\Delta r)^2}{k\, b} r_{N-\frac{1}{4}} (T_{amb}-T_N) \tag{4.22}$$

where

$$r_{N-\frac{1}{2}} = r_b + (N-\frac{1}{2})\, \Delta r \tag{4.23}$$

$$r_{N-\frac{1}{4}} = r_{tip} - \frac{\Delta r}{4} \tag{4.24}$$

The method of calculating the fin temperatures in equations 4.18–4.24 is chosen in the boiler model. It makes it straightforward and easy to implement in a computer code with a satisfactory detailed description for calculation of various local temperatures and to evaluate the influence of heat exchanger design and material properties.

Fin Efficiency

The fin efficiency η_f is the ratio of the heat transfer from the fin or extended surface to the heat transfer that would occur if the entire fin surface has the same temperature as the base. For steady-state sensible heat transfer in annular fins of rectangular profile it may be expressed as

$$\eta_f = \frac{2\, r_b}{m\, (r_{tip}^2 - r_b^2)} \left(\frac{I_1\,(m\, r_{tip})\, K_1\,(m\, r_b) - K_1\,(m\, r_{tip})\, I_1\,(m\, r_b)}{I_0\,(m\, r_b)\, K_1\,(m\, r_{tip}) + I_1\,(m\, r_{tip})\, K_0\,(m\, r_b)} \right) \tag{4.25}$$

with m, I_0, I_1, K_0 and K_1 as before. Factors affecting the fin efficiency is the fin thermal conductivity k, the fin thickness b, the fin height $r_{tip}-r_b$

and the heat transfer coefficient to the finned surface h_f. Smooth tubes could be more efficient than finned tubes for steady-state operation and condensation, for example in power plant condensors where smooth tubes are used. As previously written, this has also been found in experiments performed at Gaz de France [59].

Heat Transfer Coefficients for Finned Tubes

Correlations for heat transfer in finned tube bundles are difficult to find if the conditions are equivalent to those in a residential gas boiler. A comprehensive investigation of the heat exchanger design and its implications on boiler performance requires correlations for a number of tube arrangements. However, correlations found in the literature often deal only with in-line and staggered tube bundles. Correlations including fin parameters are few.

In the developed model, two tube arrangements are possible, in-line or staggered tubes. These arrangements are shown in figure 4.5. The distances of interest are the transversal tube spacing s_1, the longitudinal tube spacing s_2 and the tube diameter d. The uniform flue gas flow has the velocity c.

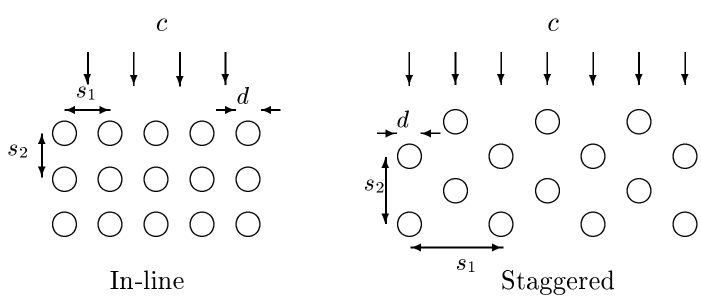

Figure 4.5: Heat exchanger tube arrangements

For bundles of finned tubes, heat transfer in this model is calculated in accordance with correlations given by Žukauskas [86] and VDI-Wärmeatlas [82]. For staggered tube bundles for $\mathrm{Re} = 200$–$20\,000$ the average Nusselt number for the finned tubes is calculated as [86]

$$\mathrm{Nu} = 0.192 \left(\frac{a}{b}\right)^{0.2} \left(\frac{s}{d}\right)^{0.18} \left(\frac{h}{d}\right)^{-0.14} \mathrm{Re}^{0.65}\, \mathrm{Pr}^{0.36} \left(\frac{\mathrm{Pr}}{\mathrm{Pr}_w}\right)^{0.25} \tag{4.26}$$

where $a = s_1/d$, $b = s_2/d$, s is the fin spacing and subscript w denotes wall conditions. For in-line tube arrangement the Nusselt number is expressed as [82]

$$\mathrm{Nu} = 0.3 + \sqrt{\mathrm{Nu}_{lam}^2 + \mathrm{Nu}_{turb}^2} \tag{4.27}$$

where

$$\mathrm{Nu}_{lam} = 0.664\,\sqrt{\mathrm{Re}}\,\sqrt[3]{\mathrm{Pr}} \tag{4.28}$$

and

$$\mathrm{Nu}_{turb} = \frac{0.037\,\mathrm{Re}^{0.8}\,\mathrm{Pr}}{1 + 2.443\,\mathrm{Re}^{-0.1}\,(\mathrm{Pr}^{2/3} - 1)} \tag{4.29}$$

Equation 4.29 is valid for one tube row. Corrections are made for the number of tube rows and the heat exchanger void fraction. For details, see [82].

The heat transfer coefficient h is given by

$$h = \frac{2\,\mathrm{Nu}\,k}{\pi\,d} \tag{4.30}$$

Since no correlation for the Nusselt number Nu at simultaneous heat and mass transfer in finned tubes was found in the literature the approach used by Coney et al. [15] was used. The total heat flux $\dot{Q}_{tot}$ is the sum of the sensible heat flux $\dot{Q}_{conv}$ and the latent heat flux $\dot{Q}_{cond}$.

$$\begin{aligned} \dot{Q}_{tot} &= \dot{Q}_{conv} + \dot{Q}_{cond} = h\,(T_{amb} - T_s) + \frac{h\,r_{H_2O}}{c_{p,amb}}(\omega_{amb} - \omega_s) = \\ &= h\left[1 + \frac{r_{H_2O}}{c_{p,amb}}\left(\frac{\omega_{amb} - \omega_s}{T_{amb} - T_s}\right)\right](T_{amb} - T_s) \end{aligned} \tag{4.31}$$

where r_{H_2O} is the water vapour latent heat and ω is the humidity. Subscripts amb and s denote ambient and saturated state at the surface temperature respectively. This equation gives the total heat transfer coefficient h_{tot} as

$$h_{tot} = h\left[1 + \frac{r_{H_2O}}{c_{p,amb}}\left(\frac{\omega_{amb} - \omega_s}{T_{amb} - T_s}\right)\right] \tag{4.32}$$

which describes the influence of the water vapour partial pressure.

A Very Short Review of Some Work on Finned Tubes

A number of investigations on heat transfer in finned tubes have been reported. Some of them are cited here. Investigations with geometries similar to those in heating boilers are rare and even fewer regarding transient conditions.

Among reported studies on steady-state heat transfer are two often cited papers by McQuiston [47, 48] which deal with finned tube bundles intended for dehumidification and cooling applications. Compared to boilers this involves a low water content on the corresponding flue gas side. In [47] it is shown that the fin efficiency decreases when mass transfer occurs and in [48] correlations for heat and mass transfer and pressure drop are presented for plate fin tube heat exchangers.

Coney et al. [15] gives a general description and numerical calculation results of heat and mass transfer. The temperature difference between fluid and fin material is small and the air flow is laminar. The influence of dry bulb temperature, air velocity and moisture content are investigated. Both the air flow and the humid air properties are shown to be important for the heat and mass transfer.

Idem [32, 33] investigated the performance of a finned tube heat exchanger in a boiler. The geometry chosen, two tube rows in an in-line arrangement, makes this work closely linked to the work in this thesis. The results are presented as Colburn j-factor ($j = \mathrm{Nu}/\mathrm{Re}\,\mathrm{Pr}^{1/3}$ for sensible heat transfer) for both the sensible heat transfer coefficient and the mass transfer coefficient. Pressure drop is also shown. The work was carried out together with Teledyne Laars, a company that has developed a condensing boiler of similar design described by McGlothin [46].

These cited works assume constant fluid properties along the fin radius despite the differences in local fin temperature. Chen et al. [10] calculated the fin efficiency assuming that the air properties also were different along the fin. The authors point out large differences between their results at low relative humidities and earlier work. They claim that the 2-dimensional approach may answer questions from earlier 1-dimensional analysis.

All of the above cited investigations deal with steady-state heat transfer. The transient behaviour of cross flow heat exchangers is described in a limited number of published reports. Aziz [3] studied annular fins in a single tube with a periodically varying temperature around an average value at the fin base. Tube bundles are concerned in the studies by Spiga and Spiga [75, 76] and Chen and Chen [11]. These papers do not consider condensation and analyses the temperature dependence of a step, ramp or exponential change in inlet conditions. The changes are made on the flow inside the tubes. The heat transfer coefficient h is fixed.

4.1.4 Water Side Heat Transfer

The heat transfer at the smooth inner surface of the circular tubes assumed in the boiler is determined by the following expressions for the Nusselt number Nu. For fully developed laminar flow and thermal field Nu is expressed as

$$\mathrm{Nu} = 3.656 \tag{4.33}$$

at constant wall temperature and for fully developed turbulent flow Nu is calculated using

$$\mathrm{Nu} = 0.023\,\mathrm{Re}^{0.8}\mathrm{Pr}^{0.4} \tag{4.34}$$

In the boiler, the water flow is turbulent. A water mass flow of 0.1 kg/s in four tubes of 16 mm inner diameter yields Re = 79 500.

4.2 Building Modelling

The building model consists of a heating system model and a house model. The models of the heating system and the house are both developed by other authors, and are here used as tools for simulating the environment around the boiler. The heating system model as well as the house model are developed by Paulsen and Gundtoft [58] and later further developed by Winberg [84].

4.2.1 Heating System Model

A two-string hydronic heating system is simulated in a model where the heating system is discretisized into a number of elements, and for each of these a heat balance is calculated. Used parameters are shown in figure 4.6.

The assumptions in the heating system model are:

- No heat conduction in the water flow direction
- No mixing in the water flow direction
- No temperature gradient across the water flow
- Water and heating system material have equal temperatures

The energy equation gives for the first element in figure 4.6.

$$C_N \frac{dT_2}{dt} = \dot{m}_{H_2O}\, c_{p_{H_2O}}\,(T_1 - T_2) - H_2\,(T_2 - T_{air}) \tag{4.35}$$

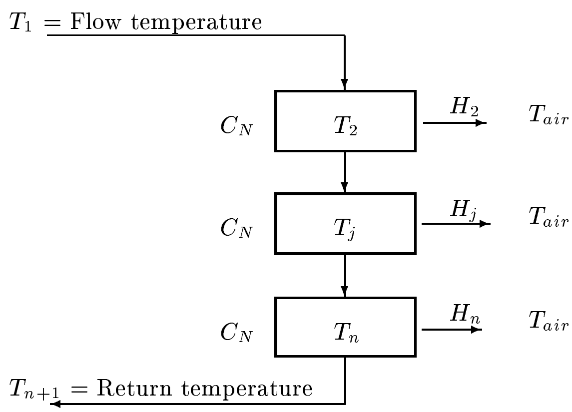

Figure 4.6: Model for a two-string hydronic heating system

where C_N is the heat capacity of element N, $\dot{m}_{H_2O}$ is the heating system mass flow, H_2 represents the heat transfer between water and air and T_{air} is the room temperature. Further, in the model is dT_2 set to

$$dT_2 = T_{2,i+1} - T_{2,i} \tag{4.36}$$

T_1 and T_2 equal the average temperature during one time step. Subscripts i and $i+1$ denote the conditions in two consecutive time steps.

$$T_{2,\,i+1} = \frac{T_{1,i+1} + T_{1,i} + 2\,\frac{H_2}{\dot{m}\,c_p}\,T_{air}}{\left[2\,\frac{\tau_0}{\Delta t} + 1\right]\left[1 + \frac{H_2}{\dot{m}\,c_p}\right]} + T_{2,i}\,\frac{2\,\frac{\tau_0}{\Delta t} - 1}{2\,\frac{\tau_0}{\Delta t} + 1} \tag{4.37}$$

where $\Delta\, t$ is the time step and

$$\tau_0 = \frac{\frac{C_N}{\dot{m}\,c_p}}{1 + \frac{H_2}{\dot{m}\,c_p}} \tag{4.38}$$

When the flow water temperature and the water flow are measured or calculated the return temperature may be calculated. Correct operating conditions for the boiler are then determined. This gives a model that takes into account dynamic characteristics and also is easily implemented in a test set up.

4.2.2 House Model

The house is simplified to consist of a single room with walls to the outdoor air at all sides. The heat transfer coefficient is constant at all walls. The building model includes two heat capacities, the indoor air and the building material. One radiator represents the heating system. The convective part of the heat emitted from the radiator is denoted f. The radiative part $(1-f)$ is assumed to be directly transferred to the building material. A ventilation air flow $\dot{m}_{air}$ is also included in the model. A schematic of the building model is shown in figure 4.7.

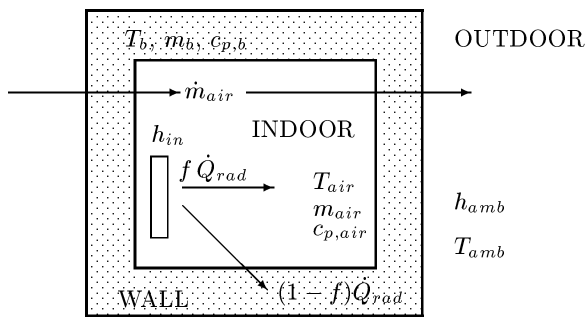

Figure 4.7: The simplified house as used in the house model

Heat balances for temperature changes in the building material m_b and the indoor air m_{air} give

$$\frac{dT_{air}}{dt}\, m_{air}\, c_{p,air} = h_{in}\, A_b(T_b - T_{air}) + \dot{m}_{air}\, c_{p,air}(T_{amb} - T_{air}) + f\,\dot{Q}_{rad} \tag{4.39}$$

$$\frac{dT_b}{dt}\, m_b\, c_{p,b} = h_{amb}\, A_b(T_{amb} - T_b) + h_{in}\, A_b(T_{air} - T_b) + (1-f)\,\dot{Q}_{rad} \tag{4.40}$$

One physical constant of the building is missing in this model, the wall thermal conductivity. The overall heat transfer coefficient U needs this value and the wall thickness. The wall thermal conductivity and the wall thickness are taken care of by adjusting the true values of h_{in} and h_{amb}. The model allows the effects of for example night setback to be taken into consideration.

Energy for space heating is only supplied by the heating system. Neither convective/radiative loss from the boiler nor heat from chimney walls are considered as useful in this approach. Excessive heat from electric appliances is also not included in the heat supplied for space heating.

4.3 Boiler Model Design

The equations describing the heat transfer in the different parts have been shown. This section contains the implementation of the equations into a computer code. The main parts are heat transfer from flue gases to heat exchanger material and water and heat storage in the heat exchanger and the water vessels. Tube and fin temperatures are calculated using the method described in equations 4.18–4.24. The fin is divided into 5 parts and the tube in a single part, i.e. 8 equations. The equations are solved using the NAG routines D02BAF and D02EAF. One tube row is treated as a unit. This means that temperatures of material segments, water and flue gases are equal regardless of the location throughout the cross section. It is a simplification made due to computer time required. Water and material temperatures in the vessel connecting tube rows are calculated using equation 4.1 with the flue gas term excluded and equation 4.2 which describe the heat transfer between water and material. The water side heat transfer coefficient is set constant to 1 500 W/m^{2}K. The vessel area is also set constant to 0.248 m^2. Increased boiler heat capacity is obtained through an increased water volume in the vessel. The heat loss from vessel n is calculated as

$$\dot{Q}_{loss,n} = C_1 \left(T_{ves} - T_{air}\right)^{1.3} \tag{4.41}$$

which is subtracted on the right hand side in equation 4.1.

The model described was implemented in a simulation program, CONDBOIL, written in FORTRAN. A simplified program, GASPANNA, was also developed. Results from the latter program have been shown in a previous chapter regarding heat transfer effects of burner cycling frequency (see page 39). Figure 4.8 shows the boiler design assumed and figure 4.9 shows the flow chart for the computer code CONDBOIL.

The simulations are ended when the cycle-to-cycle variations are considered small; the simulations start at cold conditions (20°C). The cycle-to-cycle variations are considered small enough when two consecutive cycles differ less than 1.0 second. In addition to this, the temperature difference

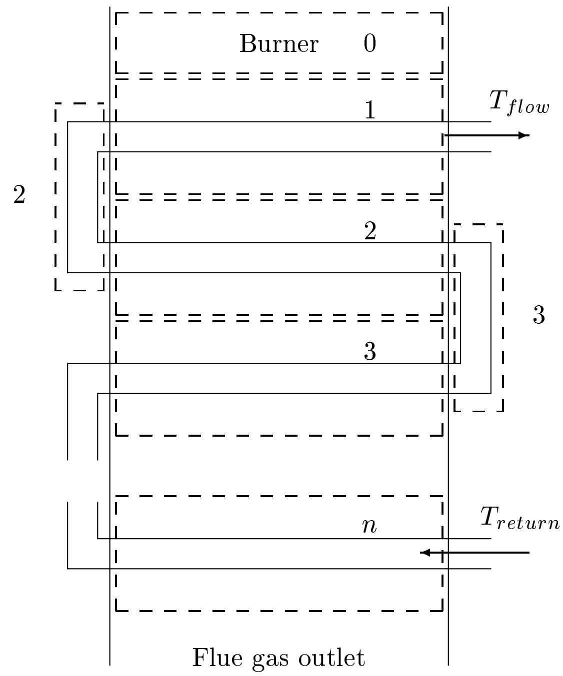

Figure 4.8: Boiler segment assumed in the computer program CONDBOIL

in outlet flue gas and flow water should be less than 0.2°C for each time step.

An IBM workstation RS6000/530 was used for the calculations. Execution time is dependent on heat exchanger size (number of tube rows), the heat load and the boiler heat capacity. The latter is a key parameter for the cycle time and the computational time. The time for a completed simulation varied between approximately 30 minutes and 24 hours.

4.4 Simulation Data Input

The data required for the simulations are collected in this section. Data input concern the burner, the heat exchanger, the building and its heating system and finally the boiler control system.

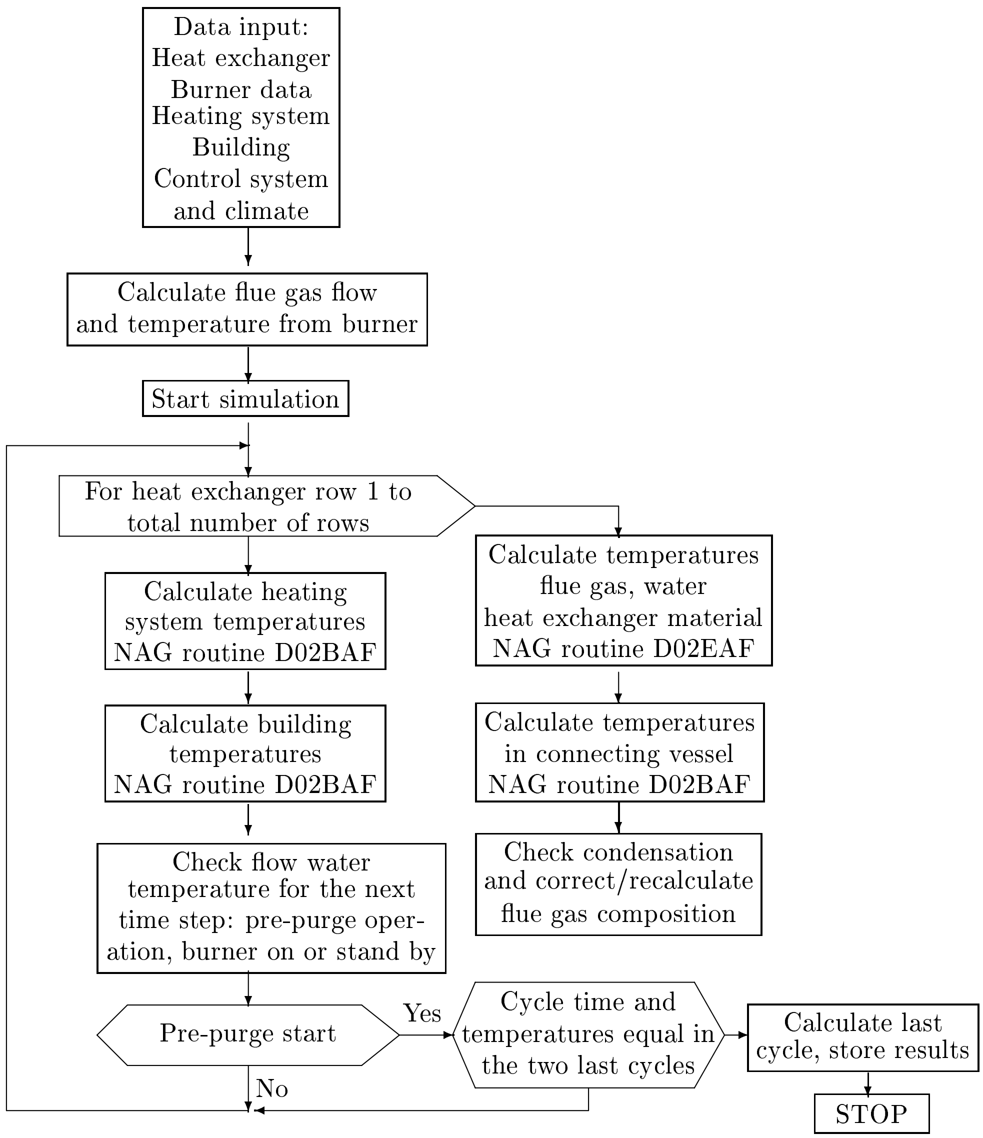

Figure 4.9: Flow chart for the boiler simulation program CONDBOIL

4.4.1 Burner

Burner gas input is kept constant at 18 kW. However, in steady-state calculations other gas inputs are used as well. The heat radiated from the burner surface is assumed to be 40% of the gas input. Stoichiometric condition is assumed which gives a water vapour dew point of 59.1°C. The combustion air temperature is 20°C (50% relative humidity).

A boiler with an 18 kW burner will be oversized for the building studied. However, this burner input will be suitable if sanitary hot water production with a storage tank is used. Further, the calculations will be made for a quite low heat load which reflects the usual boiler operating situation.

4.4.2 Heat Exchanger

In the simulations a finned tube consisting of a copper core and an aluminium fin is used. The tube has an inner diameter of 16.0 mm and a 2.0 mm wall thickness. A number of fin heights and thicknesses are also used in the simulations. Material properties are shown in table 4.1.

Table 4.1: Material properties for finned tubes used in simulations

Tube part	Material	Density (kg/m^3)	Heat capacity (J/kg K)	Thermal conductivity (W/m K)
Core	Copper	8930	390	390
Fin	Aluminium	2750	960	170

Fin sizes are shown in table 4.2. The tube spacings, both transversal and longitudinal, are chosen so the distance between fin tips always is 1 mm. The distances a_1 and a_2 are also shown in table 4.2.

4.4.3 Building, Heat Loads and Control Systems

The single-family house considered in the calculations are a one-storey brick house assumed to been built between 1950 and 1970. The U-values are 0.61 W/m^2K for the walls, 3.0 W/m^2K for the double-glazed windows and 0.27 W/m^2K for the roof, giving a heat loss of 6.29 kW at −14°C outdoor temperature. These values give a heat demand of 202 W/K (i.e. the temperature difference between the indoor and outdoor temperature) which corresponds to an annual heat demand of 15000 kWh/year in southern Sweden (3100 degree days annually).

Calculations are made for three heat loads. These are chosen as the heat loads representative for the design outdoor temperature (−14°C) and the two average outdoor temperatures in southern Sweden for the periods November until February and September, October, March, April and May.

Table 4.2: Fin profiles used in system simulations

Fin profile	Tube outer diameter (mm)	Fin diameter (mm)	Fin height r_{tip}/r_b (–)	Fin thickness (mm)	Heat capacity 100 mm tube (J/K)	a_1 (mm)	a_2 (mm)
1	20.0	27.0	1.5	0.5	60.1	28.0	28.0
2	20.0	36.0	2.0	0.5	89.2	37.0	37.0
3	20.0	45.0	2.5	0.5	126.5	46.0	46.0
4	20.0	27.0	1.5	1.0	73.9	28.0	28.0
5	20.0	36.0	2.0	1.0	184.4	37.0	37.0
6	20.0	45.0	2.5	1.0	205.1	46.0	46.0
7	20.0	27.0	1.5	2.0	91.2	28.0	28.0
8	20.0	36.0	2.0	2.0	163.8	37.0	37.0
9	20.0	45.0	2.5	2.0	257.1	46.0	46.0

The average temperature for the winter period then becomes 1.7°C and 6.9°C for the rest of the heating season. Heat loads in the building are 3.1 kW and 2.0 kW. The data input regarding the house and the hydronic systems are listed in table 4.3. The different heat loads and heating system temperatures used in the calculations are summarised in table 4.4. An outdoor temperature controlled flow temperature is used in all calculations. The water flow temperatures in the table are calculated from expressions for the steady-state flow and return temperatures in radiator systems. Two thermostat hysteresis are used, $\Delta T_{thermo} = 3$°C and $\Delta T_{thermo} = 6$°C.

Table 4.3: Parameters used in building and heating system models

Parameter		Heating system A	Heating system B	Heating system C	Unit
Radiator elements	J	10	10	10	–
Radiator exponent	n	1.3	1.3	1.3	–
Radiator heat capacity	C_N	285	285	190	kJ/K
Radiator output, full load	$\dot{Q}_{rad}$	15	15	10	kW
Radiator convective part	f	1.0	1.0	1.0	–
Building heat capacity	$c_{p,b}$	0.75	0.75	0.75	kJ/kg K
Building wall area	A_b	278	278	278	m^2
Building mass	m_b	60000	60000	60 000	kg
Indoor air heat capacity	$c_{b,air}$	1.00	1.00	1.00	kJ/kg K
Indoor air mass	m_{air}	280	280	280	kg
Outdoor heat transfer coefficient	h_{amb}	1.46	1.46	1.46	W/m^2K
Indoor heat transfer coefficient	h_{in}	1.46	1.46	1.46	W/m^2K
Ventilation air flow	$\dot{m}_{air}$	0.0389	0.0389	0.0389	kg/s
Indoor room temperature	T_{air}	20.0	20.0	20.0	°C

Table 4.4: Heating system data for part-load analysis

Heating system	Heat load at design point (kW)	Flow temperature (°C)	Return temperature (°C)	Water flow (kg/s)
A	15.0	80.0	60.0	0.179
–14°C		49.7	41.3	
1.4°C		36.8	32.7	
6.9°C		32.1	29.4	
B	15.0	70.0	55.0	0.239
–14°C		44.1	37.8	
1.4°C		33.7	30.6	
6.9°C		29.8	27.8	
C	10.0	55.0	40.0	0.239
–14°C		44.8	38.6	
1.4°C		34.1	31.0	
6.9°C		30.2	28.1	

4.5 Steady-State Performance

A baseline design with a fuel input of 18 kW and a heat exchanger consisting of 6 tube rows with 4 tubes in the first row was used. Effects of heat exhanger size, fin profiles, heating system return temperatures, changes in fuel input and rearrangement of the heat exchanger tubes were evaluated.

4.5.1 Baseline Configuration

Steady-state performances for all 9 fin profiles are shown for two water return temperatures, 30°C and 60°C. In figures 4.10–4.11 flue gas temperature at the boiler outlet as function of total tube length is shown. The length is related to the length of 6 rows of staggered tubes, 305 mm long. The first row always contains four tubes. In a staggered arrangement three tubes is used in the second, fourth row e t c, and in the in-line arrangement four tubes are used in all rows. The curves are created from calculations of tube bundles with 1 to 7 rows, i.e. a stepwise heat exchanger area increase. Observe that the heat exchanger cross section is not fixed in the calculations. Tip distance between two tube rows is fixed at 1.0 mm distance resulting in heat exchangers almost as compact as the the fin height allows.

It is seen that best performance is obtained in heat exchangers with high fins, i.e. largest heat exchanger area. The heat exchanger area seems to be of greater importance than increased heat transfer coefficient obtained in the tube bundles with low fins. However, The Reynolds number Re is quite low for these cases, $\mathrm{Re} = 230$–370. The conclusion regarding the heat exchanger area is that a staggered tube arrangement reduces the heat exchanger area by approximately 15–20% compared to an in-line arrangement for equal performance.

The radial fin temperatures for fins 4–6 are shown in figures 4.12–4.14. Each heat exchanger has 7 tube rows and the curves show fin temperature from the fin base ($r/r_b = 1.0$) to the fin tip ($r/r_b = 1.5$ and 2.5).

The calculations show that the radial fin temperature is almost constant except for the first row. This is caused by the low heat transfer coefficient and thus the low heat flux. The results for fins 1–3 and 7–9 are similar. Fins 1–3 show slightly lower temperatures while fins 7–9 show higher temperatures.

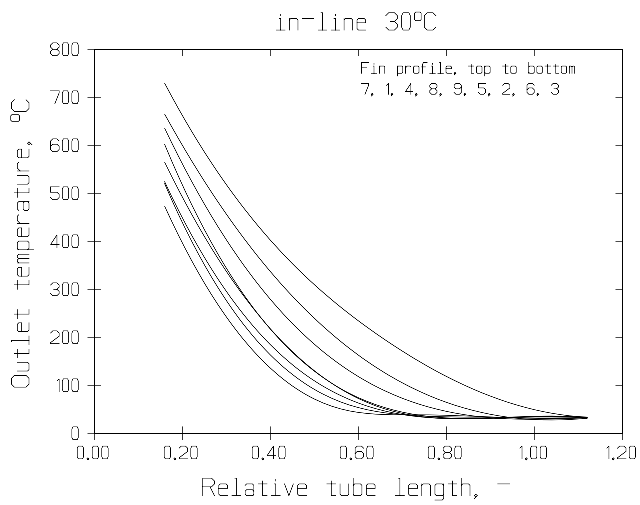

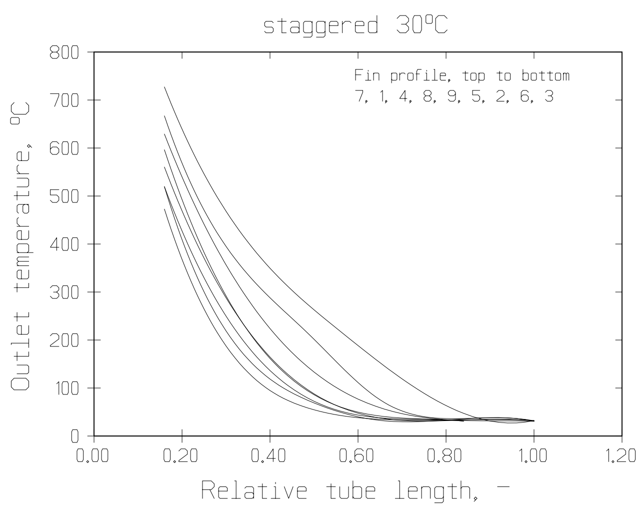

Figure 4.10: Steady-state performance as function of tube length for the 9 fin profiles. Return water temperature is 30°C. Performances for in-line tube arrangement are shown in the top graph while staggered tube arrangement performance are shown in the bottom graph.

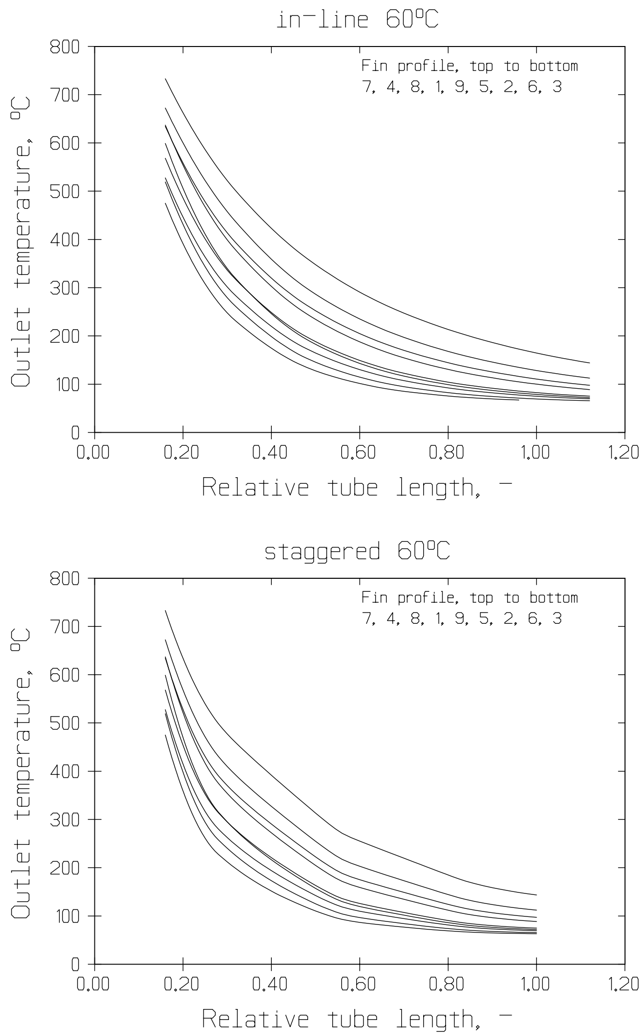

Figure 4.11: Steady-state performance as function of tube length for the 9 fin profiles. Return water temperature is 60°C. Performances for in-line tube arrangement are shown in the top graph while staggered tube arrangement performance are shown in the bottom graph.

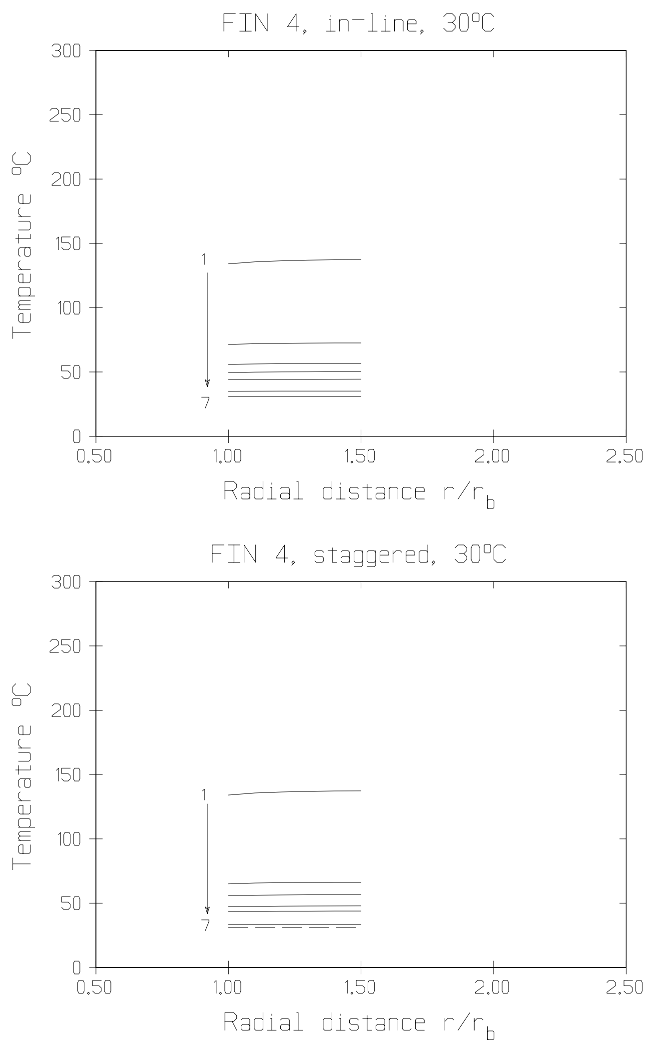

Figure 4.12: Fin temperature as function of the radial distance to the fin base, fin 4 row 1–7

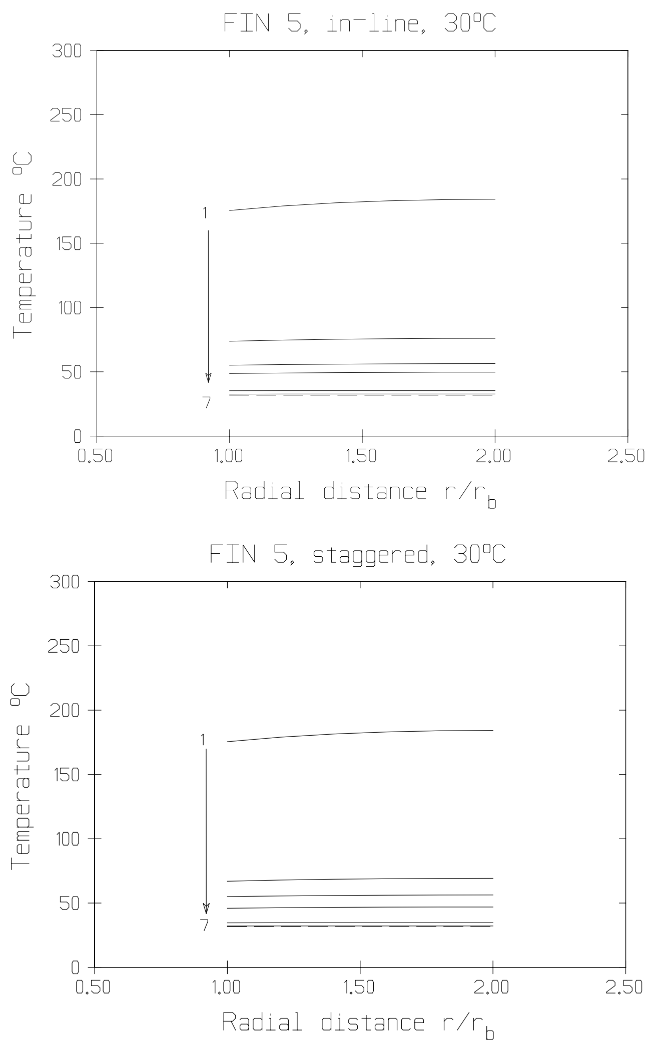

Figure 4.13: Fin temperature as function of the radial distance to the fin base, fin 5 row 1–7

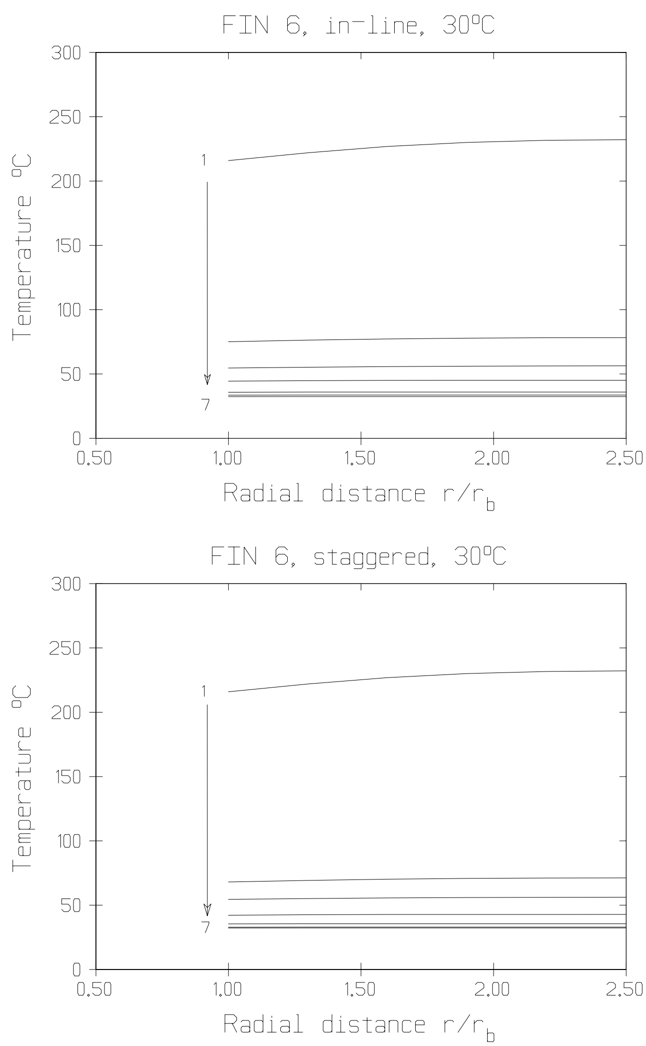

Figure 4.14: Fin temperature as function of the radial distance to the fin base, fin 6 row 1–7

4.5.2 Effects of Changes in Fuel Input

The sensitivity to changes in heat input was also studied. Fuel input in the baseline design was changed to 13 kW and 25 kW at stoichiometric conditions. This gives a Reynolds number range of Re = 170–570. The Reynolds number Re is put on the x-axis instead of the burner input due to different cross section areas. The distance between fin tips is always 1.0 mm regardless of the fin height. The results, shown as outlet temperatures are seen in figure 4.15. All fin profiles show similar heat exchanger characteristics.

4.5.3 Effects of Changes in Heat Exchanger Configuration

The baseline heat exchanger configuration assumed four tubes in the first row. Changing the tube number change the Reynolds number Re because the cross section area and thus the gas velocity also is changing. Performance with tube bundles of 3 and 5 tubes in the first row was calculated and compared to the baseline performance. Tube bundles with 3 and 6 tube rows were evaluated. In figures 4.16–4.20 the results are shown as function of the relative tube length. As before, the baseline configuration (relative tube length = 1.0) consists of 6 rows of tubes in a staggered arrangement with 4 tubes in the first row. The curve in each graph shows results for the baseline design. Below the curve are results for tube bundles with 3 tubes in the first row shown and above the curve are results for the 5 tubes design shown. Reynolds number Re are shown for each point.

An increased Reynolds number when the tube bundles are rearranged reduces the necessary heat exchanger area significantly. For equal performance approximately 15–20 % less area can be used. The gain seems to be larger for low fins than for high fins.

Fin temperatures are also shown. In figures 4.21–4.22 three fin profiles are shown as an example of this. The fin profiles not shown have a similar temperature distribution. The radial fin temperature distribution has approximately the same shape as in the baseline design except that the values are lower in the baseline design.

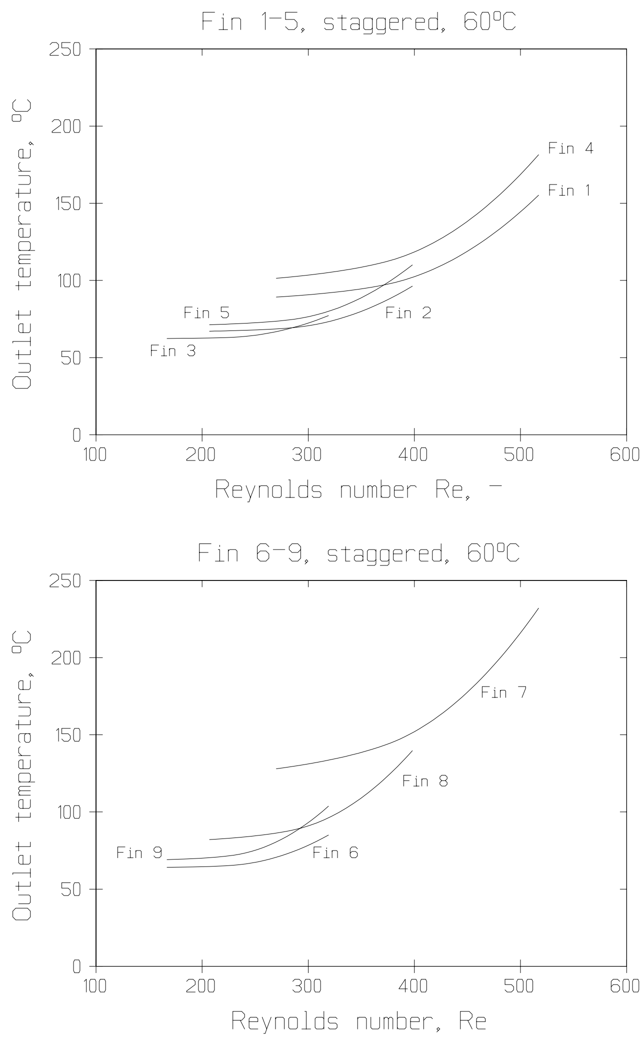

Figure 4.15: Outlet flue gas temperature as function of the Reynolds number for fins 1–9 (changed due to varying burner input)

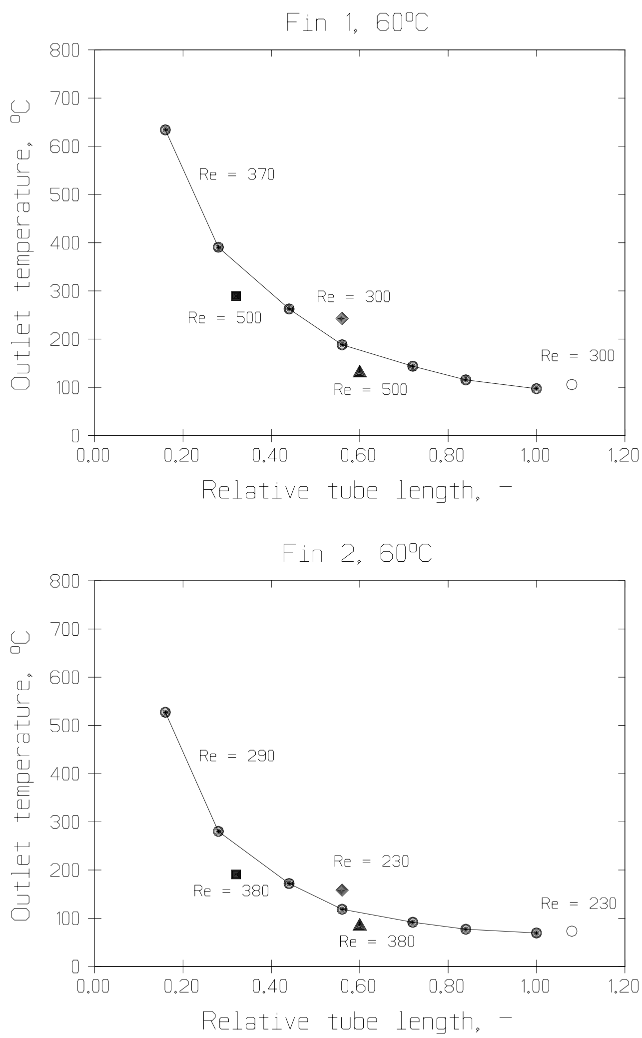

Figure 4.16: Outlet flue gas temperature as function of the relative tube length when rearranging the tubes in the baseline configuration, fins 1 and 2.

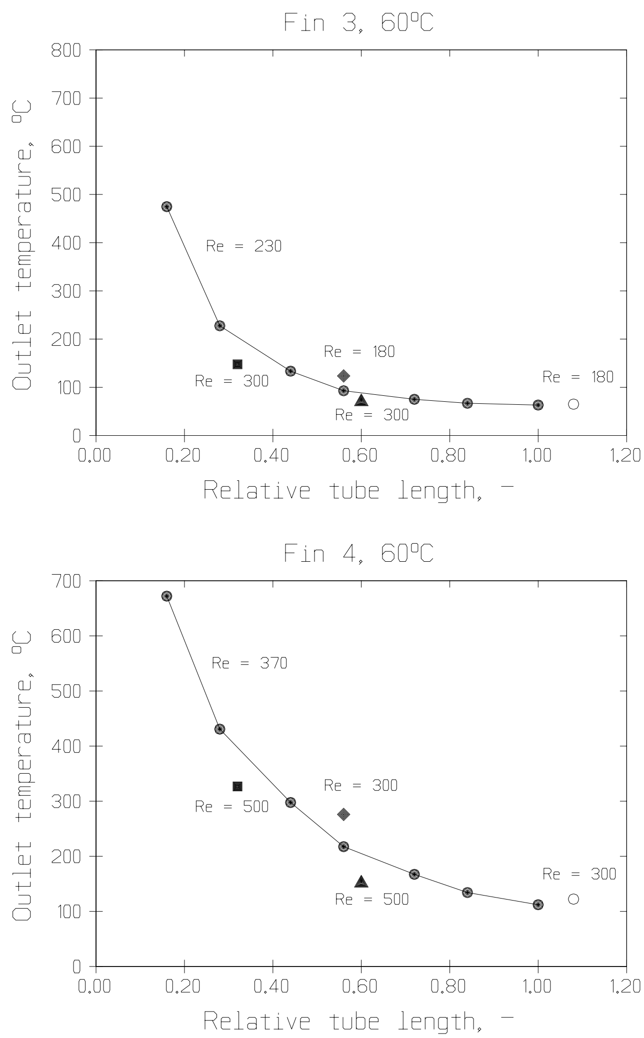

Figure 4.17: Outlet flue gas temperature as function of the relative tube length when rearranging the tubes in the baseline configuration, fins 3 and 4.

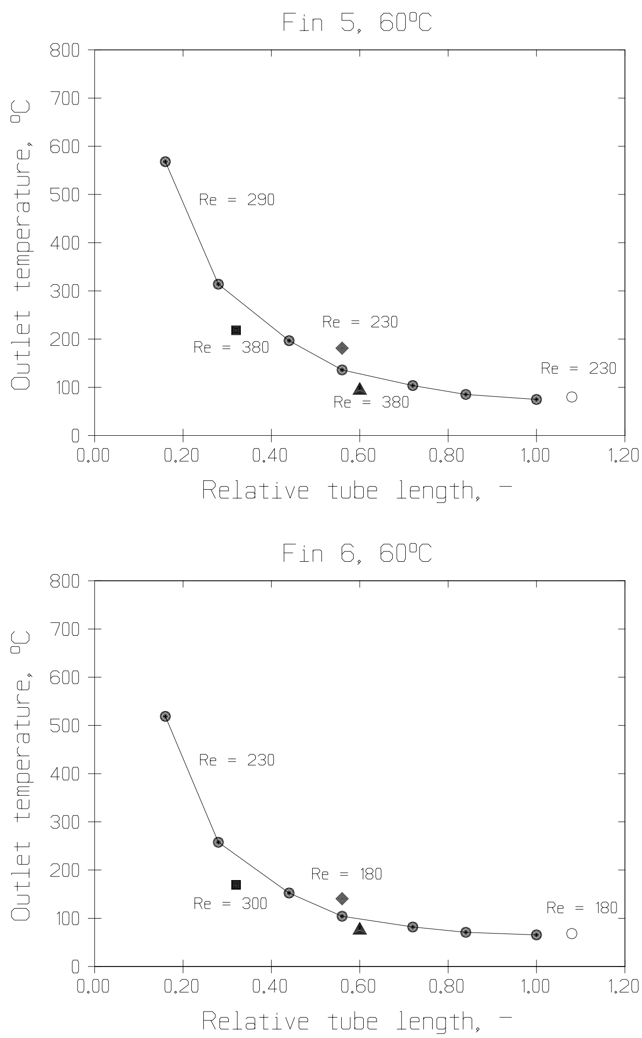

Figure 4.18: Outlet flue gas temperature as function of the relative tube length when rearranging the tubes in the baseline configuration, fins 5 and 6.

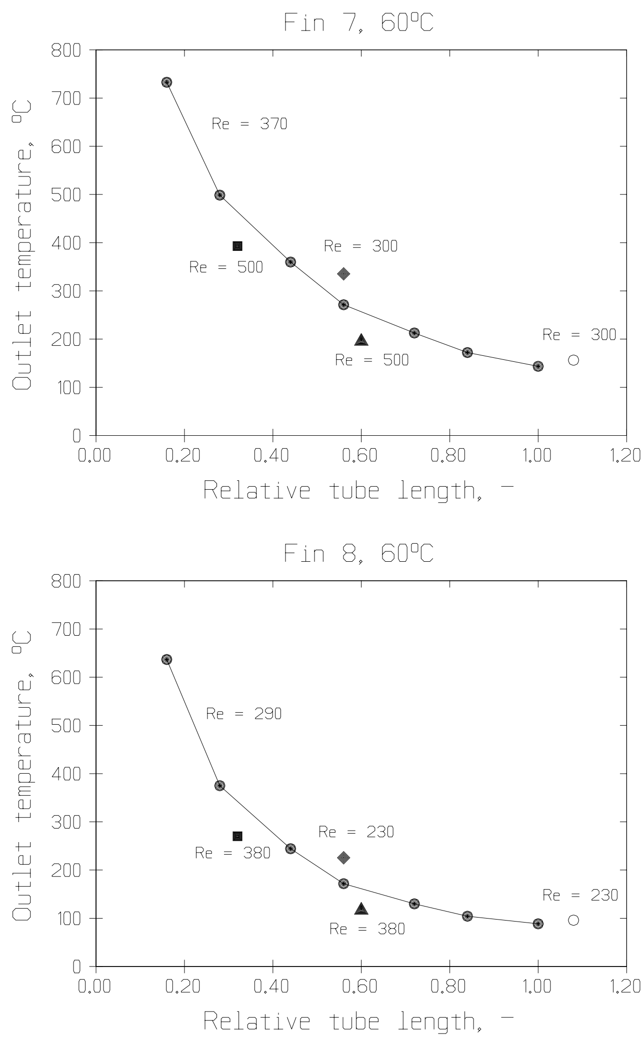

Figure 4.19: Outlet flue gas temperature as function of the relative tube length when rearranging the tubes in the baseline configuration, fins 7 and 8.

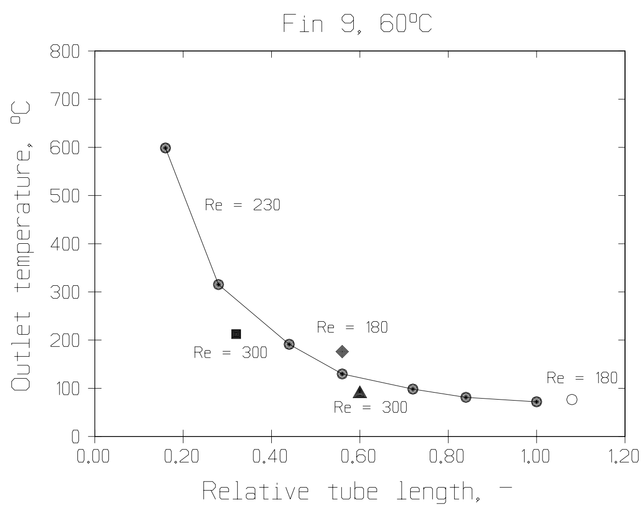

Figure 4.20: Outlet flue gas temperature as function of the relative tube length when rearranging the tubes in the baseline configuration, fin 9

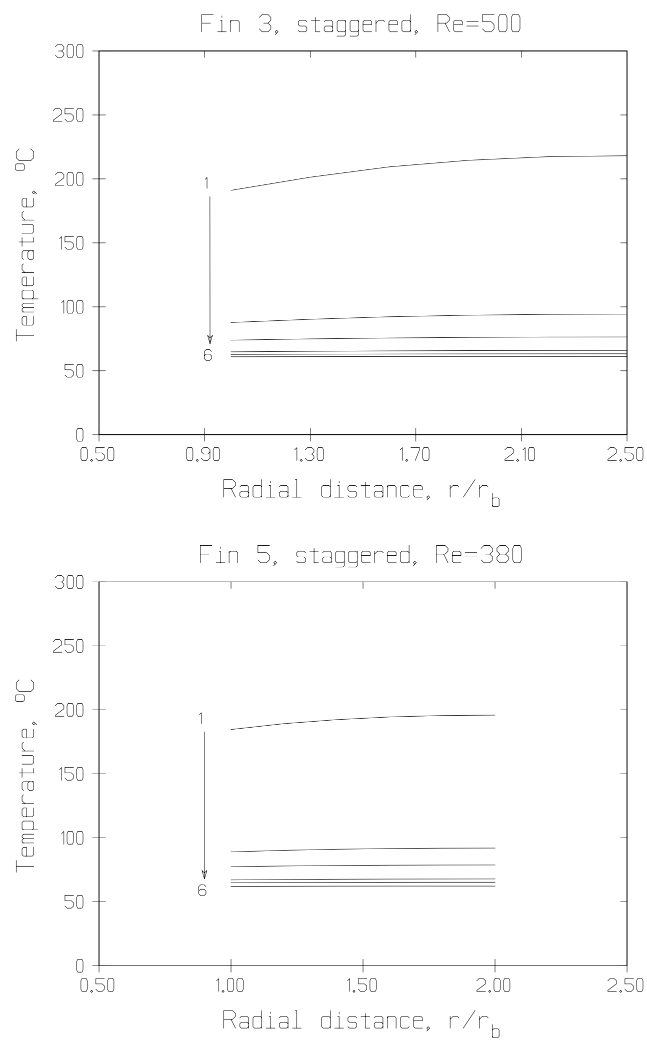

Figure 4.21: Local fin temperature as function of the radial distance when rearranging the tubes in the baseline configuration, fins 3 and 5. The curves represent tube row 1–6.

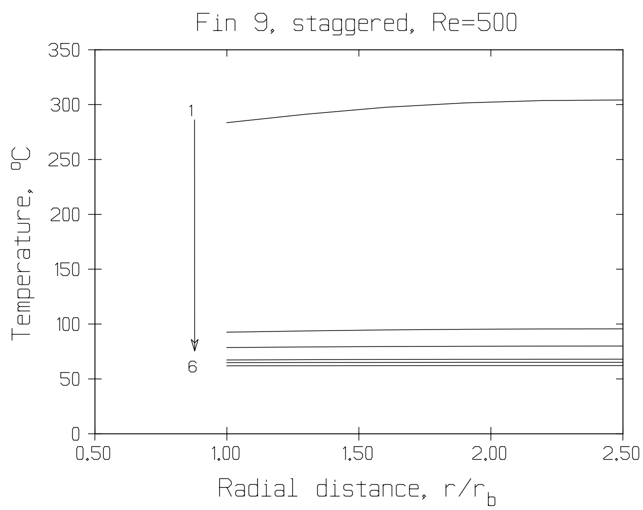

Figure 4.22: Local fin temperature as function of the radial distance when rearranging the tubes in the baseline configuration, fin 9. The curves represent tube row 1–6

4.5.4 Conclusions — Steady-State Performance

The conclusions regarding boiler heat exchanger design are based on investigations on fin design, tube arrangement and heat load. Only tube bundles with constant cross sections are studied. Not surprisingly, the staggered tube arrangement facilitates a smaller heat exchanger without lowering the steady-state thermal performance.

Rearranging the heat exchanger tubes can improve the steady-state thermal performance. This is achieved if the number of tubes in the first row is reduced which increases the Reynolds number. An increased Reynolds number due to a higher heat input in a fixed tube arrangement leads to an increased outlet flue gas temperature.

The difference between the return water temperature and the flue gas temperature is smaller for low return water temperatures.

4.6 Part-load Performance

The transient heat transfer and the performance during part-load operation are evaluated at the operating conditions presented earlier and for a number of boiler designs. The different boiler designs are shown in table 4.5. The performance of each boiler design is calculated with a few different boiler heat capacities and, as mentioned before, two thermostat hysteresis settings, 3°C and 6°C. Fin 3 is used in all calculations of boiler part-load performance.

The results from the transient analysis of part-load operation will be shown as follows:

- A detailed description of one studied part-load situation
- Overall performance for the different chosen designs
- In-depth analysis of the different heat transfer parts

The reason for this way of showing the results is to concentrate the presentation in a way that allows a direct comparison between overall part-load performance for the different designs.

Table 4.5: Boiler designs used in transient analysis

Boiler design	Tube rows	Tubes in rows	Relative tube length	Heating system
1	5	4 + 3	0.857	A
2	6	4 + 3	1.000	A
3	7	4 + 3	1.190	A
4	5	3 + 2	0.619	A
5	6	3 + 2	0.714	A
6	7	3 + 2	0.857	A
7	5	4 + 3	0.857	B
8	6	4 + 3	1.000	B
9	7	4 + 3	1.190	B
10	5	3 + 2	0.619	B
11	6	3 + 2	0.714	B
12	7	3 + 2	0.857	B
13	5	4 + 3	0.857	C
14	6	4 + 3	1.000	C
15	7	4 + 3	1.190	C
16	5	3 + 2	0.619	C
17	6	3 + 2	0.714	C
18	7	3 + 2	0.857	C

4.6.1 Detailed Description of One Part-Load Case

In this detailed description will the performance for the boiler designs be shown for heating system B and an outdoor temperature of 1.7°C. The boiler designs are number 7–12 in table 4.5.

In figure 4.23 burner operating times and average flue gas temperatures are shown for the different boiler designs. Heat capacity is increased by assuming larger water vessels connecting the tube rows. This means that the boiler heat capacity is concentrated to the water parts of the boiler. Parts in contact with flue gases, i.e. the heat exchanger tubes, are only responsible for a minor part of the overall heat capacity.

The burner operating time in each cycle is longer at higher heat capacities. The relationship is not linear due to the changes in efficiency for the various heat capacities. A boiler thermostat with high hysteresis gives longer operating times, approximately 25–50% longer. The calculations also show that the average flue gas temperature increases for large boiler heat capacities. Lowest flue gas temperature is obtained in boilers with low heat capacities and small thermostat hysteresis. This is due to the shorter burner operating periods and consequently a lower average flue gas temperatures.

Figure 4.24 shows the boilers part-load efficiency for designs 7–12. It is clearly seen that the efficiency is decreasing at larger heat capacities. The explanation is the the higher average flue gas temperature as shown in figure 4.23. We also see a significant difference between the designs regarding the slope of the efficiency curve. Generally, boilers with large heat exchangers are less sensitive to changes in the heat capacity. It is interesting to compare boiler designs 7 and 12 since they have heat exchangers with the same relative length, but differently arranged. Design 12, which has a 3+2 arrangement, shows both a higher boiler efficiency and a lower sensitivity to changes in the heat capacity.

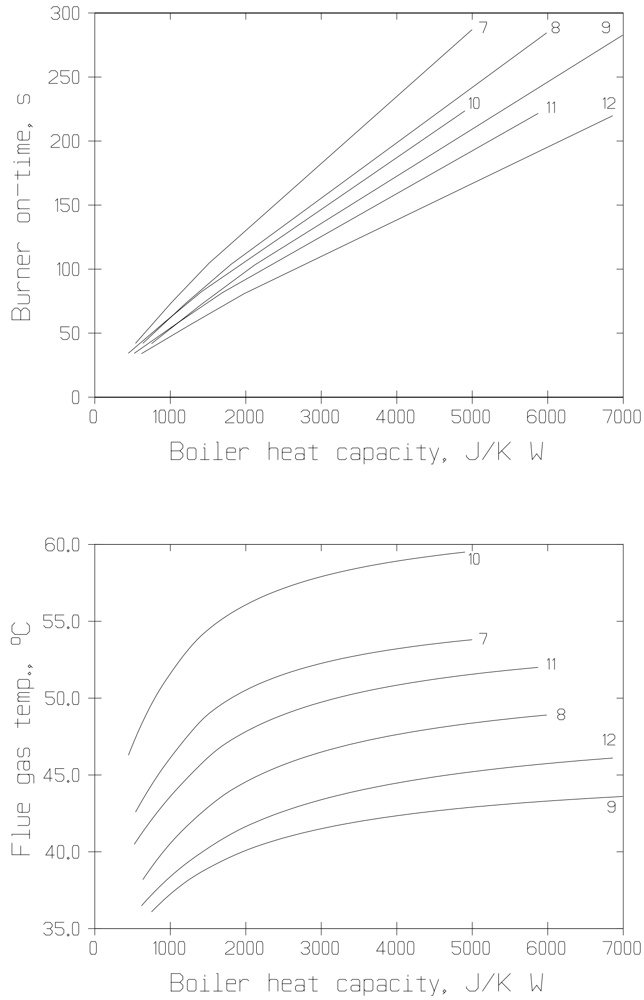

Figure 4.23: Burner operating time (on-time) and average flue gas temperature as a function of the boiler heat capacity for boilers designs 7–12. Heating system B and 1.7°C outdoor temperature.

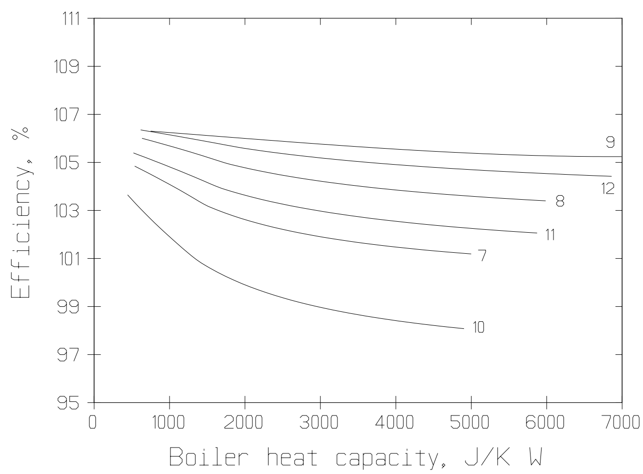

Figure 4.24: Part-load boiler efficiency as a function of the boiler heat capacity for the boilers designs 7–12. Heating system B and 1.7°C outdoor temperature.

4.6.2 Performance of the Different Designs

The evaluation of the part-load performance is done on the performance for boilers with heat capacities of 1 500–2000 J/kW K. Due to the stepwise increase of heat capacity and the varying number of tube rows, fixed heat capacity is not possible to get in the calculations.

Boiler Efficiency

In tables 4.6 and 4.7 are calculated boiler efficiencies shown. For all designs the convective loss from the boiler casing was small. Expressed as an efficiency loss, it was limited to 0.2–0.3%.

Tables 4.6 and 4.7 show that the efficiency decreases when the thermostat hysteresis ΔT_{thermo} is increased from 3°C to 6°C. The difference is approximately 0.3–1.5%. The largest performance difference between the 3 heat loads, for identical boilers, is found in boilers with small heat exchangers and in high temperature heating systems. Heat exchangers with higher heat fluxes (3+2 tubes instead of 4+3 tubes) show a slightly larger performance difference between low and high heat load. These differences increase as ΔT_{thermo} gets larger.

Table 4.6: Part-load efficiencies for the boiler designs, $\Delta T_{thermo} = 3$°C

Boiler design	Outdoor temperature –14°C	1.7°C	6.9°C
1	100.40	102.74	103.60
2	102.98	104.67	105.34
3	104.16	105.55	106.01
4	97.78	100.38	101.48
5	101.53	103.64	104.44
6	103.52	105.20	105.80
7	101.99	104.75	104.90
8	104.08	105.58	106.08
9	105.15	106.40	106.66
10	99.46	102.29	103.27
11	102.95	104.81	105.46
12	104.65	105.89	106.41
13	102.03	105.33	104.83
14	104.04	104.12	106.06
15	105.02	106.17	106.64
16	99.36	104.37	103.19
17	102.85	102.91	105.43
18	104.61	106.00	106.39

Table 4.7: Part-load efficiencies for the boiler designs, $\Delta T_{thermo} = 6°C$

Boiler design	Outdoor temperature		
	–14°C	1.7°C	6.9°C
1	99.49	101.51	102.30
2	102.33	103.87	104.53
3	104.09	105.91	105.99
4	97.81	98.55	99.63
5	100.75	102.58	103.31
6	103.00	104.47	105.07
7	101.42	103.25	104.08
8	103.25	104.99	105.60
9	104.78	105.89	106.42
10	98.31	100.91	101.98
11	102.21	103.99	104.75
12	104.19	105.51	106.11
13	101.27	103.17	104.00
14	103.52	104.92	105.56
15	104.80	105.97	106.37
16	98.27	100.82	101.89
17	102.14	103.92	104.64
18	104.13	105.59	106.06

Figure 4.25 shows the part-load efficiency for boiler designs 7–12 as a function of the relative tube length. It is clearly seen that a rearrangement of the heat exchanger in order to increase the Reynolds number also increases the part-load efficiency. This is in agreement with the results for steady-state operation. The heat exchanger area can be decreased appoximately 25% for equal performance.

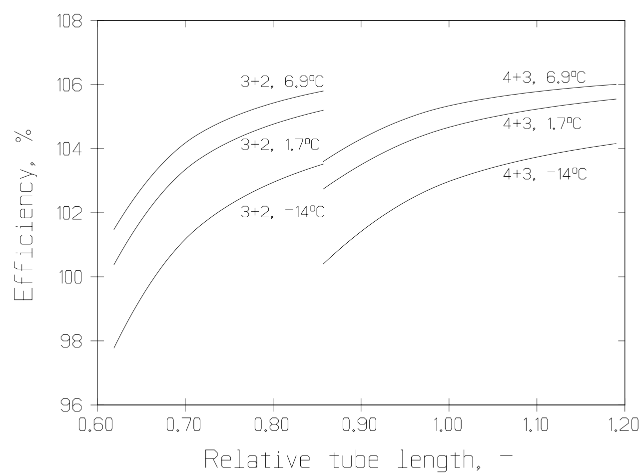

Figure 4.25: Part-load boiler efficiencies for various heat exchanger sizes (relative tube length). Boiler designs 13–15 (4+3) and 16–18 (3+2) and the three different heat loads used in the text.

Heating Costs

The cost for each unit energy from the heating system is shown in tables 4.8 and 4.9. The gas energy is calculated using the efficiency in tables 4.6 and 4.7. The electrical power consumption was also calculated in the boiler simulations, using 75 W for the circulation pump and 0.2% of the gas input for the combustion fan. For the different designs, and heat capacities, electricity consumption varied between 1.5% and 4% of the gas input. Generally, lower values are found in high heat capacity boilers. At lower heat loads the electricity consumption increases because heat from the circulation pump represents a larger share of the heat required. Assuming equal rates for gas and electricity ($c_{el}/c_{gas}=1.0$) and a electricity rate twice the gas rate ($c_{el}/c_{gas}=2.0$) give the values in the tables 4.6 and 4.7. The lower value corresponds to $c_{el}/c_{gas}=1.0$.

Highest heating costs are often found at the lowest heat load. For the higher electricity rate this is always the case. The difference in cost is 3–4% for the higher electricity rate. Sometimes, a weak cost minimum is seen at the heat load corresponding to the 1.7°C outdoor temperature.

Table 4.8: Heating cost per unit output energy. $\Delta T_{thermo}=3$°C. Heating costs are shown for $c_{el}/c_{gas}=1.0$ and $c_{el}/c_{gas}=2.0$ for each case

Boiler design	Outdoor temperature		
	–14°C	1.7°C	6.9°C
1	1.0135/1.0280	1.0006/1.0279	1.0046/1.0439
2	0.9861/1.0011	0.9835/1.0116	0.9898/1.0303
3	0.9754/0.9907	0.9768/1.0057	0.9851/1.0269
4	1.0371/1.0515	1.0233/1.0504	1.0242/1.0630
5	0.9998/1.0147	0.9928/1.0207	0.9976/1.0377
6	0.9813/0.9966	0.9793/1.0080	0.9866/1.0280
7	0.9950/1.0097	0.9846/1.0141	0.9965/1.0397
8	0.9973/0.9938	0.9837/1.0149	0.9878/1.0329
9	0.9700/0.9870	0.9739/1.0061	0.9838/1.0279
10	1.0213/1.0372	1.0074/1.0372	1.0114/1.0545
11	0.9877/1.0113	0.9872/1.0113	0.9859/1.0320
12	0.9724/0.9892	0.9718/0.9996	0.9851/1.0304
13	0.9952/1.0103	0.9786/1.0079	0.9943/1.0347
14	0.9752/0.9924	0.9887/1.0170	0.9852/1.0275
15	0.9682/0.9842	0.9720/1.0021	0.9789/1.0201
16	1.0214/1.0364	0.9834/1.0122	1.0094/1.0497
17	0.9877/1.0031	1.0061/1.0340	0.9901/1.0317
18	0.9713/0.9867	0.9731/1.0028	0.9830/1.0261

Table 4.9: Heating cost per unit output energy. $\Delta T_{thermo} = 6°$C. Heating costs are shown for $c_{el}/c_{gas} = 1.0$ and $c_{el}/c_{gas} = 2.0$ for each case

Boiler design	Outdoor temperature		
	–14°C	1.7°C	6.9°C
1	1.0195/1.0339	1.0119/1.0387	1.0149/1.0523
2	0.9920/1.0068	0.9904/1.0181	0.9953/1.0339
3	0.9801/0.9952	0.9808/1.0093	0.9872/1.0268
4	1.0367/1.0510	1.0413/1.0679	1.0419/1.0801
5	1.0074/1.0222	1.0022/1.0296	1.0074/1.0468
6	0.9860/1.0011	0.9855/1.0138	0.9922/1.0327
7	1.0026/1.0192	0.9982/1.0279	1.0020/1.0432
8	0.9817/0.9980	0.9837/1.0149	0.9946/1.0374
9	0.9711/0.9878	0.9764/1.0084	0.9838/1.0279
10	1.0329/1.0486	1.0207/1.0504	1.0225/1.0644
11	0.9946/1.0108	0.9923/1.0230	0.9984/1.0421
12	0.9764/0.9930	0.9796/1.0114	0.9875/1.0326
13	1.0024/1.0173	0.9973/1.0253	1.0014/1.0413
14	0.9814/0.9968	0.9823/1.0115	0.9852/1.0275
15	0.9700/0.9858	0.9736/1.0035	0.9825/1.0249
16	1.0324/1.0472	1.0192/1.0465	1.0221/1.0627
17	0.9942/1.0094	0.9910/1.0197	0.9975/1.0397
18	0.9760/0.9917	0.9768/1.0065	0.9865/1.0301

Two possible measures to take in order to decrease the heating cost, related to the electricity consumption, are the use of a pulse combustor or a circulation pump timer. An atmospheric burner is not a realistic alternative for condensing boilers with this performance. The pulse combustor does not need a combustion air fan after the combustion has started. The possible reduction is illustrated with an example where a pulse combustor is used in boiler design 1 and $\Delta T_{thermo} = 3°C$. The electricity consumptions are 1.45% and 3.93% of the gas consumption at –14°C and 6.9°C outdoor temperature. The use of a pulse combustor (where the combustion air fan is shut off 3 seconds after the flame ignition) lowers these values to 1.25% and 3.73%. The total heating costs are then reduced to 1.0085/1.0210 (–14°C) and 1.0026/1.0399 (–14°C), i.e. a reduction of approximately 0.5%. It is likely that a circulation pump timer will reduce the costs more. However, the heating system characteristics will then not be the same as in the simulations and no values of cost savings will therefore be presented.

4.6.3 In-Depth Analysis of the Heat Transfer

The heat transfer differences between steady-state and part-load operation will be discussed in this section. The topics are: flue gas temperature, fin temperatures during the operating cycle and the air temperature during the pre-purge period and associated losses. Boiler designs 14 (4+3 tubes and 6 tube rows) and 17 (3+2 tubes and 6 tube rows) with low and high heat capacities are chosen for the discussion. Heat capacities for design 14 are 1 200 J/kW K and 6 000 J/kW K whereas they are 1 100 J/kW K and 5 900 J/kW K for design 17. The cycle times are 425 and 1 517 seconds for design 14 and 330 and 1 172 seconds for design 17.

Flue gas temperature

Table 4.6 showed an increasing efficiency for low boiler heat capacities. The reason for this is the lower average flue gas temperature. For example, design 14 has an average flue gas temperature of 41.6°C at 1 200 J/kW K and 48.9°C at 6 000 J/kW K (1.7°C, 3.1 kW heat load). The lower temperature corresponds to an efficiency of 106.1% while the second temperature corresponds to 103.7%

The flue gas temperatures for designs 14 and 17 with the high heat capacities are shown in figure 4.26. It is clear that design 17 (3+2 tubes) shows a more rapid temperature rise. A lower heat capacity also result in a slightly higher flue gas temperature due to shorter cooling periods. This is equal to a higher cycling frequency. Boilers with high heat transfer coefficients will not show as high efficiency gains as boilers with low heat transfer coefficients due to a lower average flue gas temperatures.

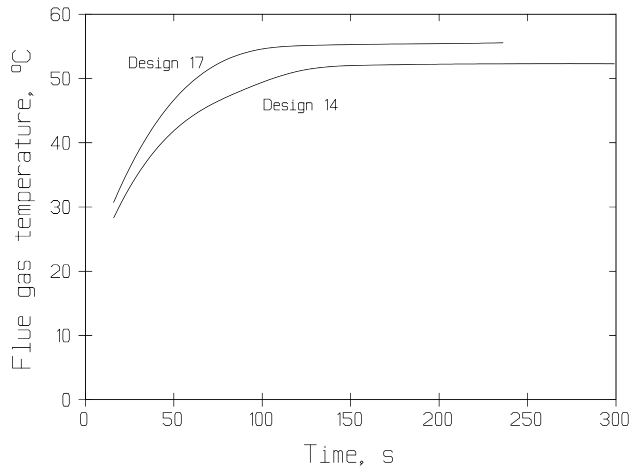

Figure 4.26: Flue gas temperatures during burner operation for design 14 and 17 with high boiler heat capacities

Fin Temperatures

Fin temperatures are important for the condensation rate and the stand-by loss. The radial temperature distributions for fins in the first and last tube row in designs 14 and 17 are shown in figures 4.27 and 4.28. The curves show temperatures at 10% increments of the burner cycle. For design 14 the cycle is 425 seconds and for design 17 it is 330 seconds. At the end of burner operation the temperature is shown, time 0.173 in figure 4.27 and time 0.187 in figure 4.28. The different times are caused by varying efficiencies.

Fin temperatures are rapidly increasing after the burner has started for both boiler designs. The temperature gradient is slightly larger for design 17 (3+2 tubes) due to a higher heat flux at the fin base. During the stand-by period the temperatures are decreasing quickly and they are close to the water temperature a long time before the pre-purge period starts. For both designs the temperatures in the last row are well below the dew point (59.1°C) during the whole cycle.

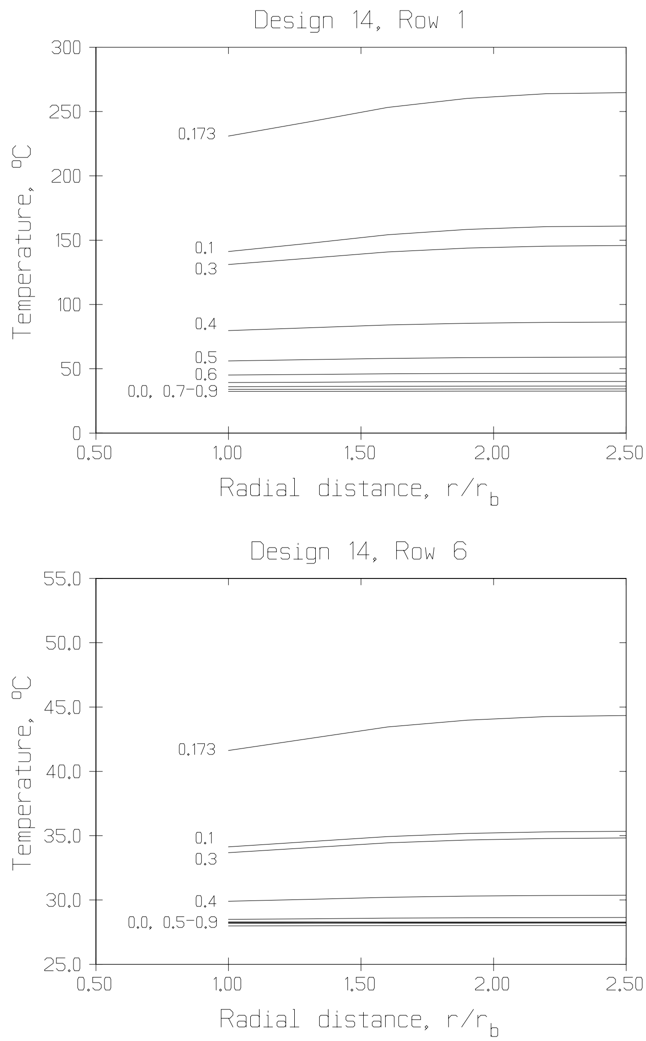

Figure 4.27: Fin temperatures at different points during the whole burner cycle. The lines represent temperatures at 10% time increment from pre-purge start (0.0), design 14. Heat capacity is 1200 J/kW K

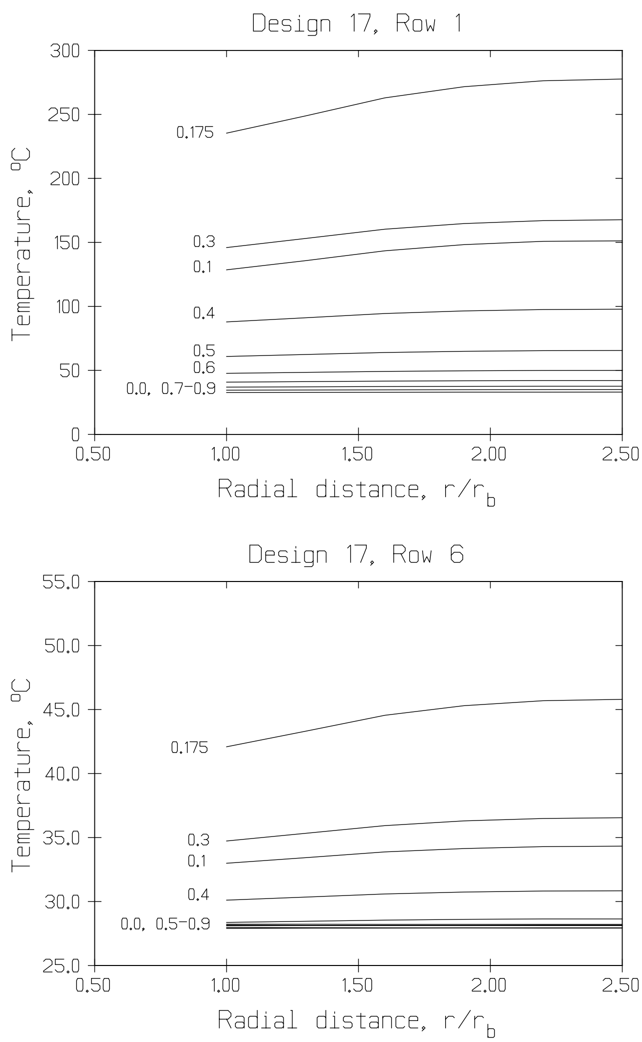

Figure 4.28: Fin temperatures at different points during the whole burner cycle. The lines represent temperatures at 10% time increment from pre-purge start (0.0), design 17. Heat capacity is 1100 J/kWK

Pre-Purge Time Air Temperature

During the pre-purge period will the heat exchanger be cooled and this causes a heat loss. In condensing boilers also evaporation of condensate will occur. In figure 4.29 is the air outlet temperature for low and high heat capacities, boiler designs 14 and 17, shown for the whole pre-purge period. A slightly higher temperature is observed for the low heat capacity boilers due to the higher cycling frequency.

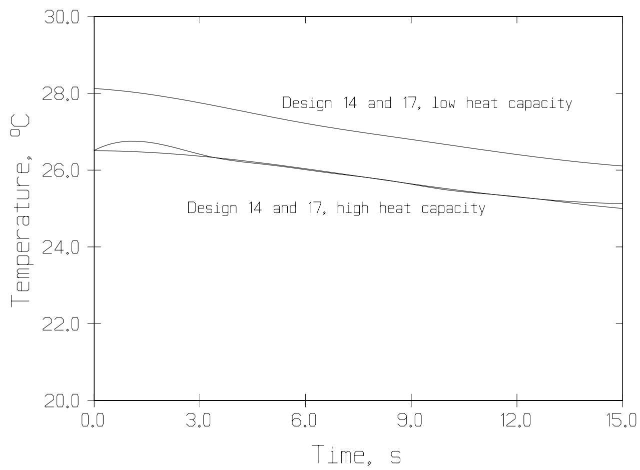

Figure 4.29: Air temperature at the boiler outlet during the pre-purge period for design 14 and 17

The air temperature along the heat exchanger in design 14 is shown in figure 4.30. The curves show the temperatures 5, 10 and 15 seconds after the pre-purge start. The graph shows that heat is transferred downstream the heat exchanger. The air temperature at the outlet is close to the heat exchanger temperature. In design 17 a sligthly lower temperature, <0.5°C, is observed.

In figure 4.31 is the pre-purge heat loss plotted for different heat capacities for design 14 and 17. A very strong increase of this loss is observed at low heat capacities. This is caused by the higher cycling frequency due to lower heat capacity.

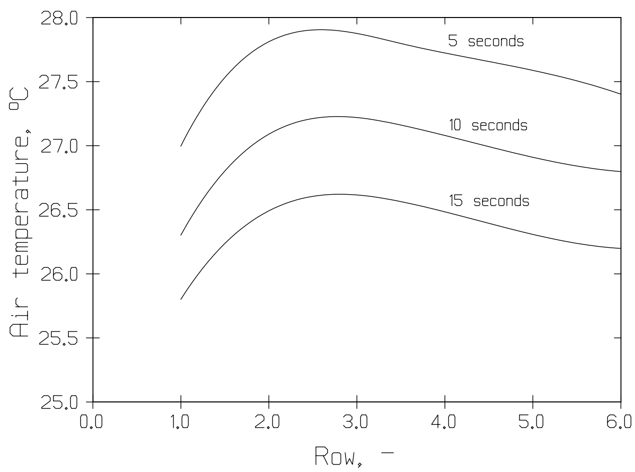

Figure 4.30: Air temperature along the heat exchanger at 5, 10 and 15 seconds after pre-purge period beginning. Design 14 (1 200 J/kW K)

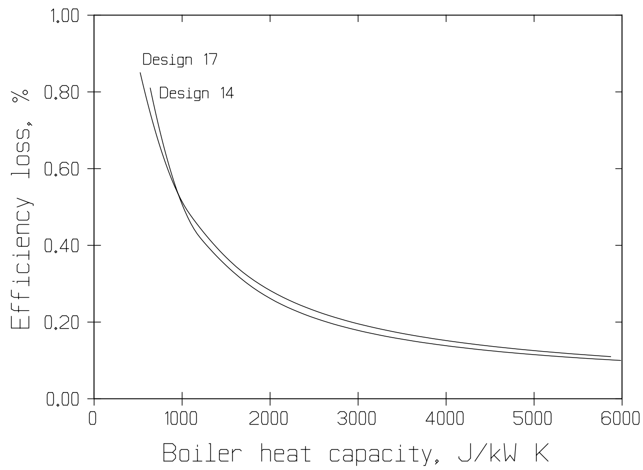

Figure 4.31: Efficiency loss due to pre-purge air flow at different boiler heat capacities, design 14 and 17

4.6.4 Differences due to Boiler Heat Capacity

The performance figures presented have mostly dealt with boilers with heat capacities in the 1 500–2 000 J/kW K range. Further, the presentation has also focussed on heating system B and 1.7°C outdoor temperature. Differences in performance due to other heat loads and heat capacities will be shortly commented in this section.

The calculations also included heat capacities slightly above 1 000 J/kW K and up to 5 500–6 000 J/kW K. Lower boiler heat capacities increase the boiler efficiency since the pre-purge loss was not large enough to outweigh the gain due to a lower average flue gas temperature. The efficiency difference between the heat loads increased for boilers of the same design but with lower heat capacity. For example, the efficiency difference between −14°C and 6.9°C for design 1 in table 4.6 increases from 3.20% to 3.48% when the heat capacity is reduced. For a 3+2 tube arrangement the differences are even larger. Design 4 shows an increase from 3.70% to 5.47%. For heating systems B and C, the differences are smaller than found for heating system A. Consequently, boilers with higher heat capacities than covered in tables 4.6 and 4.7 show smaller differences between the three different heat loads.

4.7 Conclusions About the Efficiency Sensitivity

This chapter has dealt with the first aim of the thesis, a study of boiler performance in different installations. A transient heat transfer model is used and boiler performances at full load and part load are evaluated.

The boilers simulated have a one-step burner of 18 kW gas input and 0% excess air. Surface combustion is assumed with a 40% radiation efficiency. The heat exchangers have a staggered tube arrangement with either 4+3 tubes or 3+2 tubes.

The part-load simulations showed that a larger thermostat hysteresis gives a slightly lower efficiency, <1%, mainly due to a higher average flue gas temperature. The boiler least sensitive to changes in heat load is a boiler with a large heat exchanger with low heat transfer coefficients and a larger thermostat hysteresis. The boiler simulations showed an efficincy difference of 1.5–4% for heat capacities of 1 500–2 000 J/kW K. Regarding the heat exchanger size, the best boiler is one where the heat transfer rate is higher. Only a negligible efficiency reduction occurs, but this is only valid if material temperatures are close to the adjacent water temperature and the burner cycling frequency is not too high.

In no simulation was the pre-purge loss (as decreased efficiency) larger than around 1%. However, at shorter operating times (in seconds) due to less boiler heat capacity is the pre-purge loss rapidly increasing.

The calculation of total heating costs, including gas and electricity, showed that the highest costs occur at low heat loads due to the heat supplied by the circulation pump. This is more evident as the relation between gas and electricity rates increases. The electricity consumption can be reduced either by using a pulse combustor or a circulation pump timer. Using a pulse combustor may reduce the cost approximately 0.5% when the electricity rate is twice the gas rate. The potential of using a circulation pump timer was not evaluated but is probably larger than a change of burner.

5

Methods of Flue Gas Drying

The second aim of this thesis is to investigate the possibility of using and operating a condensing boiler without any modification to the chimney. A brick chimney or similar is assumed as the base case, i.e. a chimney of a material which is sensitive to condensate formation and has a high thermal conductivity. Masonry chimneys in Sweden often have a bent flue duct and space for a rigid smooth liner could be limited. Extensive work on the flue system may be needed.

Condensation of water in the boiler reduces the water vapour flow entering the flue system and simplifies the introduction of a drying system into the boiler design. The question to answer is whether or not it is possible to avoid condensation in a chimney when condensing boilers are used. The question arises only in case of a conversion from another fuel and when the boiler is located in the basement thus making a horisontal flue terminal impossible. Further, it is assumed that the water pipes to the boiler are not moved. This problem is dealt with in two chapters. This chapter contains a description of three possible methods. Boiler designs using these methods are described followed by a calculation of the heat transfer in chimneys in order to determine the necessary flue gas state at the boiler outlet. The chapter ends with a discussion about the boiler efficiency using drying methods. The results from chapter 5 and 6 are summarised in chapter 6. It also contains results from experiments performed on two boilers with drying capability.

This part of the thesis differs from the previous part because flue gas drying is mainly experimentally studied instead of theoretically analysed as the boiler performance. Flue gas drying should primarily be considered as a method of reducing the total cost when a horisontal flue terminal cannot be used, but it can also be considered as a way to make the condensing boiler installation less sensitive to the previous non-condensing installation.

Three technical solutions are suggested and discussed. One of these are also experimentally investigated. Parts of this chapter is also found in [53].

5.1 Drying Methods

Flue gas drying in this context is a notation for ways to create a flue gas state which allows an operation without condensate forming in the chimney. Possible ways are an increased flue gas temperature, a reduced water content or a combination of the these.

Three different methods of creating the desired flue gas state are listed below. They all involve heat transfer to the boiler flue outlet.

1. Flue gas reheating using a conventional heat exchanger
2. Flue gas reheating using heat pipes
3. Flue gas drying and heating using adsorbents

These designs will be discussed more in detail in the following text. Calculations of the flue gas state required for the desired operation will be shown.

The suggested boiler designs to obtain dry flue gases are unconventional in contrast with the boiler design chosen in the previous chapter. Boilers with flue gas reheating by means of a conventional heat exchanger were developed and tested. Test results are shown in the next chapter.

5.1.1 Reheating Process

Flue gas reheating in a condensing boiler means that the flue gases are heated after the condensation in order to achieve a temperature and water content which prevents condensate forming in the chimney. Figure 5.1 explains the process graphically. Reheating can be accomplished in a number of ways regarding the heat transfer process. Conventional heat exchangers and heat pipes are discussed in this thesis.

The heat used for reheating can be taken from for example boiler water, hotter flue gases or by using electrical heating. Heat produced in the combustion process, from boiler water or flue gases, is here called internal heat. Heat produced outside the combustion process, for example electrical heating, is called external heat. The influence of different types of internal or external heat on the boiler efficiency is discussed on page 130.

As can be seen in figure 5.1, a boiler could theoretically be designed to allow a way directly from point 1 to point 4, i.e. reaching the desired temperature and humidity without reheating. This boiler design must allow condensate forming without the flue gas temperature dropping close to the dew point.

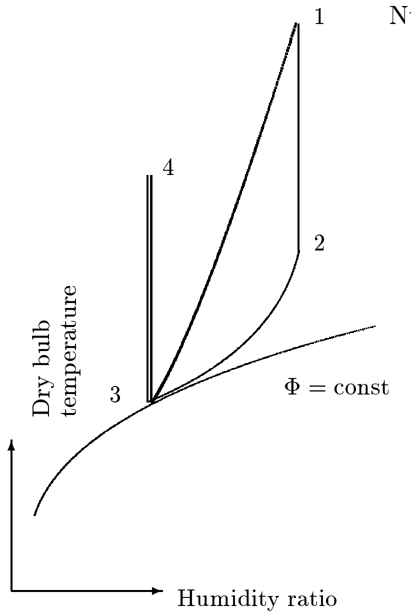

Numbers 1–4 indicate:

1. Flue gases from a non-condensing boiler
2. Condensation of water vapour in the boiler starts
3. Flue gases from a condensing boiler
4. Flue gases from a condensing boiler with reheated flue gases

Figure 5.1: The principle of reheating. The thin line represents a boiler using a heat exchanger design of one non-condensing and one condensing heat exchanger. The thick line represents a boiler where condensation can start early in the heat exchanger. Φ = relative humidity.

Alternative to Reheating

One slightly different alternative to reheating has been commercialised by Viessmann in Germany [83], the Viessmann Mirola. To avoid damages to the chimney, a small amount of flue gases are by-passed from the combustion chamber to the boiler outlet. In this arrangement, the flue gases from the condensing heat exchanger are mixed with the hotter flue gases to achieve a temperature sufficiently high to avoid condensate formation in the chimney. If the chimney later is changed to handle condensate, the by-pass line can be shut and full condensing operation can be used. The boiler design is also described by Rosa [69]. The design criterium according to Rosa is a difference between flue gas temperature and water dew point of at least 20°C.

5.1.2 Adsorbent Drying

Condensate formation in the chimney can also be avoided by reducing the water content in the flue gases, in this case by use of an adsorbent. The use of adsorbents will not only reduce the water content but also raise the flue gas temperature during the adsorption. The process is illustrated in figure 5.2.

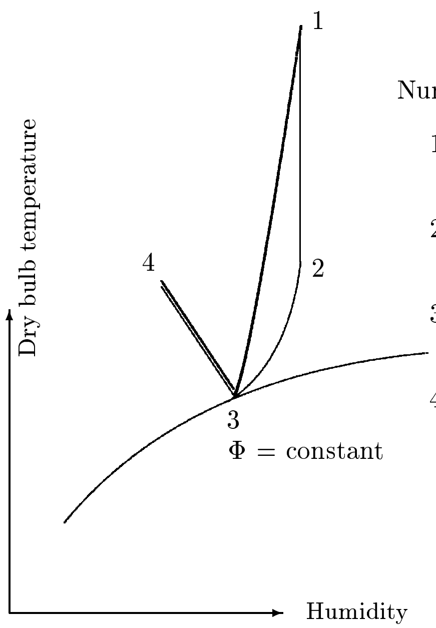

Numbers 1–4 indicate:

1. Flue gases from a non-condensing boiler
2. Condensation of water vapour in the boiler starts
3. Flue gases from a condensing boiler
4. Flue gases from a condensing boiler with adsorbent drying

Figure 5.2: The principle of adsorbent drying. The line from point 1 to point 3 represents a boiler using a heat exchanger design of one non-condensing and one condensing heat exchanger. The thick line represents a boiler where condensation can start early in the heat exchanger. Φ = relative humidity.

The adsorbent needs to be frequently regenerated in order to reduce the water content. The suggested boiler design described here involves a circular adsorbent bed, rotating between the flue and the boiler interior making adsorption and regeneration possible. The similarities with desiccant cooling and air preheaters in power plants are obvious. Possible adsorbents are for example zeolites and silica gel.

Zeolites

Zeolites, or molecular sieves, adsorb molecules in small cavities in their structure. The adsorption is a surface process, not a chemical reaction. The zeolite has a 3-dimensional structure and a well defined cavity size determined by the atoms in the stucture. The choice of adsorbent material determine the size of molecules to be adsorbed. Zeolite 4A is suitable for water adsorption and has a cavity of 4.1 Å (Ångström). Its chemical formula is

$$\mathrm{Na_{12}[(Al\,O_2)_{12}(Si\,O_2)_{12}]\cdot x\,H_2O} \tag{5.1}$$

The water molecules are removed from the zeolite by heating, also called regeneration. The well defined cavity diameter gives zeolites a high degree of selectivity and only molecules with a diameter equal to the cavity diameter or less can be adsorbed. Other molecules in flue gases, with similar molecular sizes to water are oxygen (2.8 Å), carbon monoxid (2.8 Å) and nitrogen (3.0 Å). Adsorption capacity of zeolites and alternative adsorbent materials are shown in figure 5.3 [24].

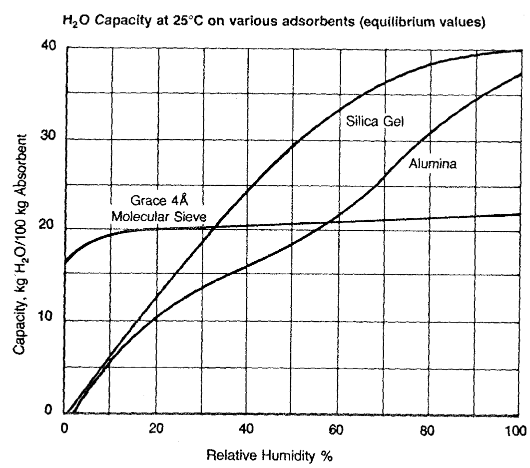

Figure 5.3: Water adsorption for zeolite 4A, silica gel and Alumina

Molecular sieves seem to be a better alternative than the other materials since the capacity is less affected by higher temperatures. Regeneration in a space heating boiler is most likely to be a thermal regeneration, i.e. the adsorbent is heated. The regeneration can be achieved in a wide temperature span. If it is done using hot flue gases, the bed temperature should be at least 300°C if the residual water content in the bed not should exceed approximately 5% [24]. The dew point of the regeneration fluid, i.e flue gases, is here an important factor.

It has not been further investigated if the operating conditions, for example the cycling frequency, are favourable for adsorbent use. However, communication with the company GRACE [25] indicate a reduced adsorbent lifetime for this application.

5.2 Suggested Boiler Designs

Among condensing boilers two basic types are found, see page 17. These types differ in the heat exchanger design. The first type, here called type I, has two clearly separated heat exchangers where all condensation takes place in the second one. In the second type, type II, all heat exchanger area is collected in one package, an integrated design. In this section reheating is commented for each basic type and suggested boiler designs are suggested.

5.2.1 Type I Boiler with Reheating

In a type I boiler, the reheating heat exchanger is naturally located between the first and second, condensing, heat exchanger. The engineer is somewhat tied to this design which have some disadvantages. The reheating heat exchanger more or less has to be located between the first and second heat exchanger. The flue gas temperature may therefore not be appropriate for an efficient reheating. Due to the fairly low temperature after the first heat exchanger the reheating heat exchanger area will be fairly large. In figure 5.4 a suggested design and the associated flow chart are shown. The burner in this design is assumed to be a conventional atmospheric burner.

However, this design is today obsolete for residential condensing boilers connected to hydronic systems. The interest for producing a boiler of this design should therefore be quite small.

5.2.2 Type II Boiler with Reheating

Two designs of type II boilers are suggested for flue gas reheating. The main difference is the burner geometry, either flat or cylindrical. This leads to different heat exchanger designs. The burners are assumed to operate in a fully premixed mode.

Several types of this basic design are found among the boilers on the European market. Many have a heat exchanger in one piece, for example founded in an aluminium alloy. A large number of boilers are described by

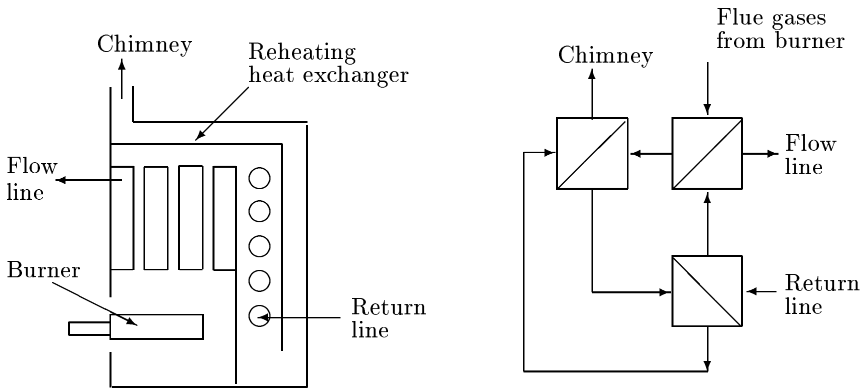

Figure 5.4: Suggested design of a type I condensing boiler with reheating

Jannemann [36]. These designs do not always offer the same opportunity to include reheating as the design discussed in this thesis.

Flat Burner

A flat burner can either be a radiant burner or a conventional blue flame burner. Combustion is taking place across the entire flat burner area. The burner is placed above the heat exchanger, which consists of a number of finned tubes. The reheating heat exchanger can in this design be placed at an arbitrary location based on wishes of material use and dynamic characteristics. Figure 5.5 shows the suggested design and the flow chart.

Cylindrical Burner

A cylindrical burner with flames around the perimeter is suggested to be surrounded by a finned helically shaped tube. The burner can also be surrounded by a smooth or surface extended water jacket, which will give a similar design. Convective heat losses are likely to be easier to reduce in the latter design. The reheating heat exchanger is located above the water side heat exchanger and thus facing uncooled flue gases. The boiler design using a cylindrical burner is shown in figure 5.6 below.

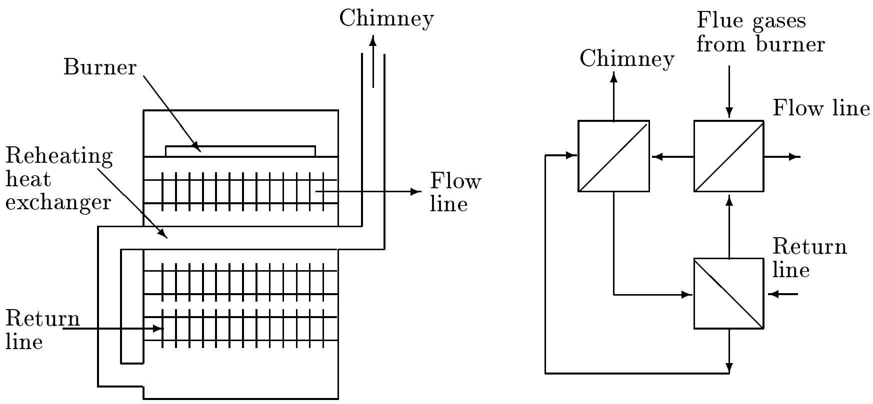

Figure 5.5: Suggested design of a type II condensing boiler with a flat burner and reheating

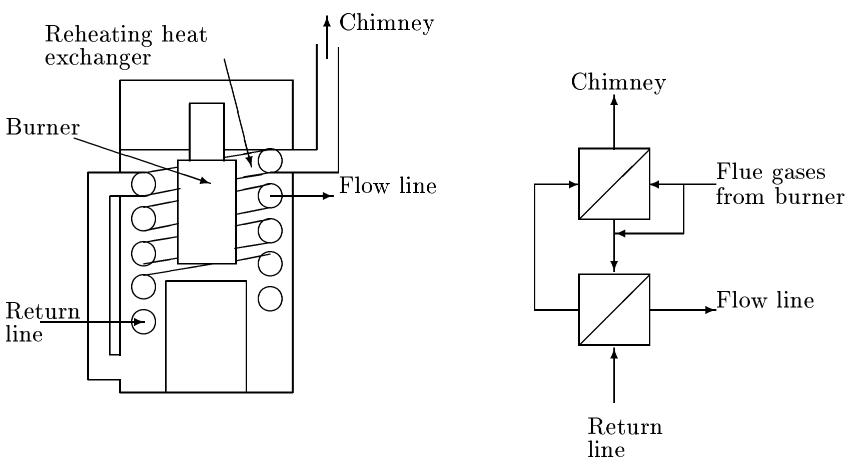

Figure 5.6: Suggested design of a type II condensing boiler with a cylindrical burner and reheating

5.2.3 A Boiler with Heat Pipes

Heat pipes offer a high heat transfer rate as a result of the extremely high "thermal conductivity" along the pipe or tube axis due to the evaporation and condensation of the working fluid within the tube. A simple and compact boiler design is possible. Heat pipes have been used in earlier studies of space heating systems, see for example Becker and Searight [5] and Ernst et al. [19] from 1981. The use of heat pipes in warm-air furnaces is described in these studies. In both cases the heat pipes are used to directly transfer the flue gas energy to the warm-air heating system. In these studies are heat pipes used instead of conventional heat exchangers. It is likely that the steady-state boiler performance is equal to the performance with a conventional heat exchanger. Dynamic characteristics may though be different.

Using heat pipes for reheating can simplify the boiler design compared to a design where a heat exchanger is used. The discussion about using heat pipes is limited to a suggested boiler design, see figure 5.7.

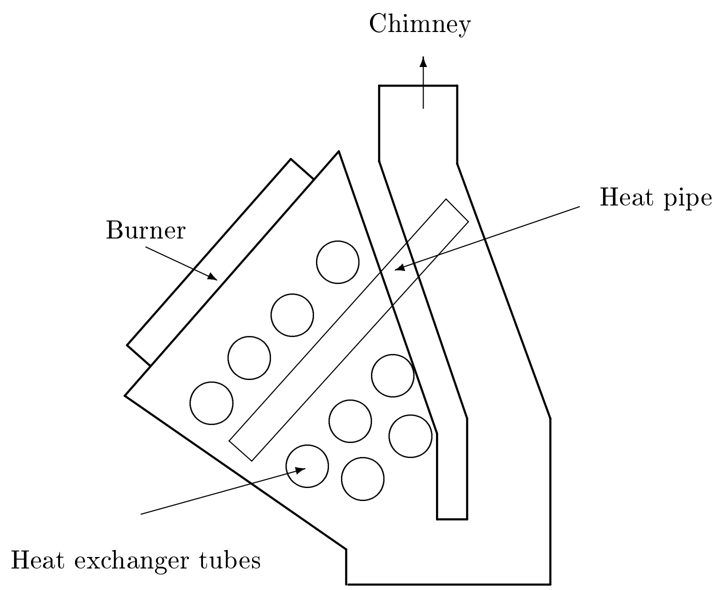

Figure 5.7: Possible design of a condensing boiler using heat pipes for flue gas reheating

The burner in this design is facing a staggered heat exchanger arrangement. Heat pipes are located between two rows in the beginning of the heat exchanger.

5.2.4 A Boiler with Adsorbents

Adsorbent drying can easily be included in a boiler using a flat burner. The main design difference is in this case a wheel containing adsorbent material. The wheel is located in a way which makes rotation possible between the flue gas outlet and a point with sufficiently high temperature for the regeneration. In figure 5.8 the boiler and adsorbent wheel design are shown.

In the design of the adsorbent wheel a couple of important parameters are identified. These are:

- High adsorption capacity, i.e. $\mathrm{kg}_{H_2O}/\mathrm{kg}_{ads}$
- Fast regeneration
- Efficient regeneration in a humid environment at temperatures found in a boiler

The boiler design is not further discussed in this thesis.

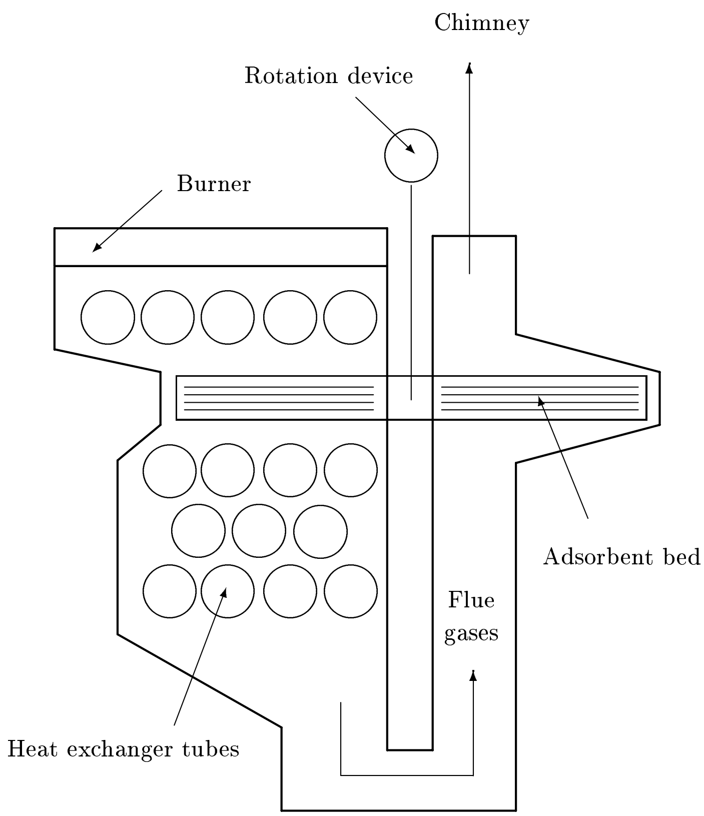

Figure 5.8: Possible design of a condensing boiler with an adsorbent bed for flue gas drying

5.3 Calculation of the Necessary Flue Gas State

In this section, a model is developed for calculation of heat transfer in chimneys. The necessary flue gas state, i.e. the temperature and relative humidity at the boiler outlet, is then determined. The values given refer to boilers with burner inputs of 15–20 kW and 25% excess air. The influence of burner input, excess air and heating system return temperature on the condensate formation in the chimney is also studied. This study of parameter importance is done for a condensing boiler with no flue gas drying. The model which has been used for calculating heat and mass transfer in the chimney is based on appropriate correlations from literature.

5.3.1 Parameters Affecting Flue Gas Drying

The different parameters of the building in which the boiler is installed influence the characteristics of the entire heating system as previously shown. In this section a number of possible parameters important for the flue gas drying are discussed. These parameters are the heat demand, the burner input, the heating system temperatures and the chimney size. In figure 5.9 the interaction between these components are made clear graphically.

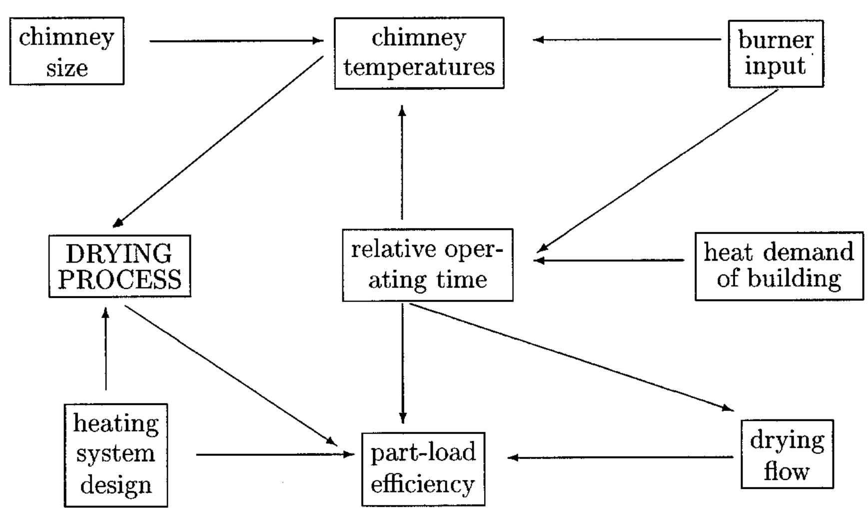

Figure 5.9: Parameters affecting the performance of flue gas drying

The component interaction can be described as follows. The burner input and the buildings heat load and the boiler efficiency give the relative operating time, τ, of the burner (one-step burner assumed). In the model this parameter is used to calculate the flue gas temperature at the boiler outlet for acceptable operation. The chimney size, cross section area and height, is also of importance for the flue gas temperatures and thus of interest for the calculation of necessary reheating. Evaporation of condensate formed during the burner operation is also taken into consideration in this calculation. The air flow through the boiler and chimney is determined from the flue system size and the relative operating time. The air flow leads to an increased heat demand. This has to be taken into consideration when comparing different boiler designs. Finally, the characteristics of the heating system are considered important for the calculation of necessary reheating. Since the heating system fluid return temperature directly affect the flue gas temperature, a low temperature system seems appropriate. Also, the aim of minimising the water content indicates certain characteristics of the burner, among them low excess air ratio.

Figure 5.9 shows that boiler, heating system and building, constitute a complex system. Consequently, each component has to be investigated before a suitable boiler design can be proposed. In the calculation of necessary flue gas temperature this investigation is made for the burner input, the excess air ratio and the heating system temperatures.

5.3.2 Chimney Heat Transfer Model

Calculations of heat and mass transfer in the chimney are simplified by use of a quasi-stationary approach. The model gives the average values of flue gas temperature T_{av} and inner wall temperature T_{in} during the burner cycle, i.e. the time between two burner starts.

Consider a circular chimney with r_{in} as the radius to the inner wall, r_{out} as the radius to the outer wall and Δx as a segment height. The thermal conductivity is k_{chi}. The chimney is shown in figure 5.10. The heat transfer from flue gas to the chimney outer wall is determined by equations 5.2–5.4. The equations show the heat transfer at the chimney inner wall $\dot{Q}_{in}$, through the chimney wall $\dot{Q}_{chi}$ and at the outer wall $\dot{Q}_{out}$. The inner and outer segment areas are denoted A_{in} and A_{out}.

$$\dot{Q}_{in} = h_{in}\,(T_{av} - T_{in})\,A_{in} \tag{5.2}$$

$$\dot{Q}_{chi} = 2\,\pi\,k_{chi}\,\Delta x\,\frac{T_{out} - T_{in}}{\ln(r_{out}/r_{in})} \tag{5.3}$$

$$\dot{Q}_{out} = h_{out}\,(T_{out} - T_{amb})\,A_{out} \tag{5.4}$$

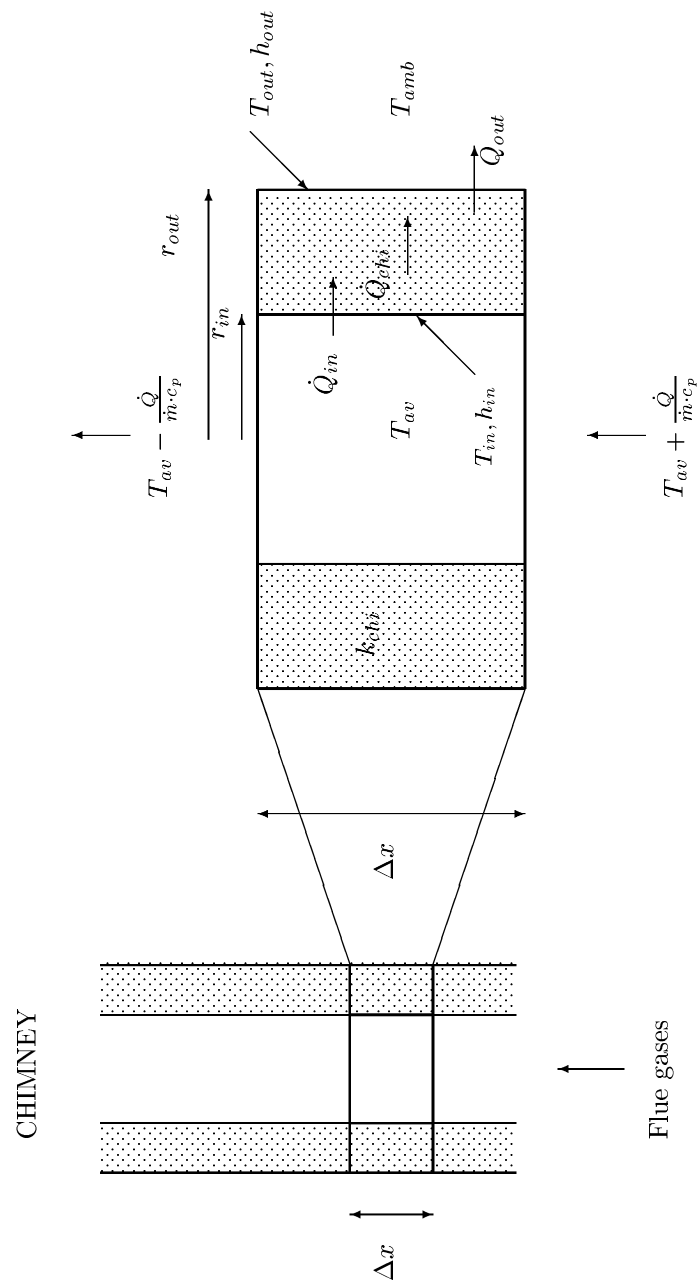

Figure 5.10: A section of a chimney. Used and calculated values and properties are marked

The heat transfer rates are equal in steady-state conditions. The heat transfer coefficient at the chimney inner wall, h_{in}, is calculated using equations 5.5–5.8. The calculations of Nusselt number Nu and Rayleigh number Ra for vertical surfaces take into account both heat and mass transfer, see Churchill and Chu [12]. Constant values for the outer wall heat transfer coefficient h_{out} are used for the indoor and outdoor part respectively.

$$\mathrm{Nu} = 0.68 + \frac{0.670\,\mathrm{Ra}^{\frac{1}{4}}}{\left[1 + \left(\frac{0.437}{\mathrm{Pr}}\right)^{\frac{9}{16}}\right]^{\frac{4}{9}}} \tag{5.5}$$

$$\mathrm{Ra} = \frac{g\,\beta\,(T_{in} - T_{av})\,d_{h,in}^3}{\nu\,h_{in}} \tag{5.6}$$

where g is the gravity, $d_{h,in}$ is the flue duct hydraulic diameter and ν is the kinematic viscosity. The thermal expansion factor β is calculated as

$$\beta = -\frac{1}{\rho_{av}}\left(\frac{\partial \rho_{av}}{\partial T}\right) \tag{5.7}$$

where ρ_{av} is the density of flue gases at the temperature T_{av} and finally

$$h_{in} = \frac{k_{av}\,\mathrm{Nu}}{d_{h,in}} \tag{5.8}$$

The one-step burner operation is taken care of through a quasi-stationary calculation method. This method is described by Plate and Tenhumberg [65] and Rosemann [70]. The heat transferred to the wall Q_{cycle} during burner operation t_{on} is

$$\frac{dQ_{cycle}}{t_{on}} = h_{in}\,(T_{av} - T_{in})\,A_{in} \tag{5.9}$$

Assuming constant inner wall temperature yields the heat transfer through the chimney during the whole burner cycle, $t_{on} + t_{off}$, as

$$\frac{dQ_{cycle}}{t_{on} + t_{off}} = 2\,k_{chi}\,\pi\,\Delta x\,\frac{T_{in} - T_{out}}{\ln(r_{out}/r_{in})} \tag{5.10}$$

A dimensionless time parameter, relative operating time, τ is introduced and defined as

$$\tau = \frac{t_{on}}{t_{on} + t_{sb}} \tag{5.11}$$

Equations 5.9–5.11 give the average chimney wall temperature T_{in} as

$$T_{in} = \frac{T_{out}\,\frac{2\,k\,\pi\,\Delta x}{\ln(r_{out}/r_{in})} + \tau\,h_{in}\,T_{av}\,A_{in}}{\frac{2\,k\,\pi\,\Delta x}{\ln(r_{out}/r_{in})} + \tau\,h_{in}\,A_{in}} \tag{5.12}$$

In case of water vapour condensation, the heat transferred to the wall due to convection and condensation can be written as in equation 5.13 according to Colburn and Hougen [14].

$$\begin{aligned} d\dot{Q} &= h_{in}\,(T_{av} - T_{in})\,dA + \\ &\quad K\,M_{H_2O}\,r_{H_2O}\,(p_{H_2O,av} - p_{H_2O,s,in})\,dA \end{aligned} \tag{5.13}$$

where $p_{H_2O,s,in}$ denotes the saturated water vapour partial pressure at T_{in}. The mass transfer coefficient K is written as

$$K = \frac{h_{in}}{c_p\,\Delta p_m\,M_{av}}\left(\frac{\mathrm{Pr}}{\mathrm{Sc}}\right)^{\frac{2}{3}} \tag{5.14}$$

where M is the molar weight and (Pr/Sc) is the Lewis number Le which is set equal to unity as the flue gases may be considered as humid air. The mass flow of condensate, $d\dot{m}_{cond}$, is

$$d\dot{m}_{cond} = \frac{d\dot{Q}_{cond}}{r_{H_2O}} \tag{5.15}$$

which yields

$$d\dot{m}_{cond} = \frac{M_{H_2O}}{M_{av}}\,\frac{h_{in}}{c_p\,\Delta p_m}\,(p_{H_2O,s,in} - p_{H_2O,av})\,dA \tag{5.16}$$

5.3.3 Computer Code and Calculation Results

The chimney model is implemented in a program, SKORSTEN, where the chimney is divided into 100 segments. Flue gas state at the boiler outlet acts as inlet conditions to the first segment. Boiler heat input and building heat demand, given as calculation input, are used to calculate the relative operating time τ. Influence of boiler oversizing can thus be evaluated. The output data are the flue gas temperature, the wall temperature and the condensate formed.

A flow balance based on the assumption that the pressure generated by the average flue gas temperature in the chimney and chimney height is equal to the flow resistance give the possible air flow through the chimney during the burner stand-by period. The air flow is calculated as

$$\rho_{av}\, g\, H = \xi\, \frac{\rho_{av}\, c^2}{2}\, \frac{H}{d_{in}} \tag{5.17}$$

where ξ is the friction factor, c is the air velocity and H is the chimney height.

The air flow is present when a boiler equipped with an atmospheric burner is used while no air flow is assumed when a fan assisted burner is used. Evaporation of condensed water vapour is then possible to calculate. The Nusselt number for heat transfer during the stand-by period (atmospheric burner) is calculated from the correlation used for the burner operating time. In case of a fan assisted burner, free convection ($\mathrm{Nu} = 3.664$) is assumed. The flow chart in figure 5.11 shows the program structure.

Experiments performed on a laboratory chimney showed an accuracy of 10–15°C [57]. The results were obtained in tests where boilers with a fan assisted burner and an atmospheric burner were used. Flue gas temperatures at steady-state conditions were 140–200°C. The accuracy is better at lower flue gas inlet temperatures. The chimney used in the experiments consisted of a metal tube with thin walls. It was used both without and with heat insulation. The tests showed that the assumption of constant inner wall temperature was reasonable. The main difference between measurements and calculations was the inner wall temperature in the chimney outdoor part. Calculated values were significantly lower than measured. The conclusions from the comparison between measurements and calculations were that overall heat transfer was reasonably calculated. Since calculated wall temperatures were lower than measured the necessary reheating later shown will be overestimated.

Comparisons with the American computer code VENT-II [71] show good agreement for condensing boilers. In VENT-II a transient heat transfer analysis is used and calculated temperatures from this code are cycle averaged and compared. For a condensing boiler at 45% load and an average flue gas temperature during burner operation of 37.0°C, a comparison showed differences not exceeding 2°C [53].

Another dynamic or transient heat transfer model for chimneys has been developed by Pitschak et al. [63]. In this model, the chimney is considered as a single wall shell radially divided in segments. Good agreement is shown between measured and calculated data. From the data shown it is difficult to judge if the assumption of constant inner wall temperature is verified. However, presented results show a temperature difference less than 10°C during the operating cycle. The chimney was cold from the beginning of the tests.

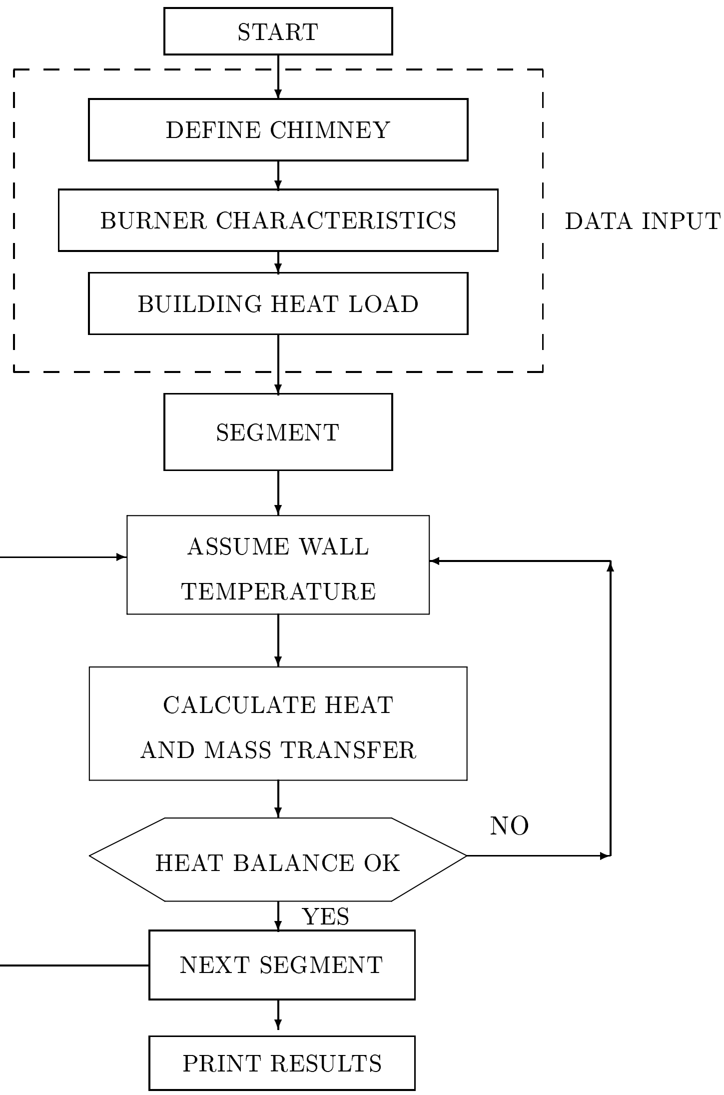

Figure 5.11: Flow chart describing the program SKORSTEN for calculating heat and mass transfer in a chimney

Influence from the Burner

The scope of studying the influence of the burner heat input and excess air ratio on temperatures and condensate formation in the chimney is to clarify if any combination of burner input and excess air is preferrable.

In the calculations are the heat demand and the chimney size fixed. The house has a heat demand of 13 kW at –14°C outdoor temperature. The chimney height is 7.5 m of which 6.5 m is indoors. The flue duct cross section is 150×150 mm. Heat transfer coefficients at the chimney outer wall are set to 5.0 W/m^{2}K and 15.0 W/m^{2}K for the indoor and outdoor part respectively. The boiler has a burner with either 15, 20 or 25 kW input. These burner inputs correspond to an oversizing of approximately 15%, 54% and 92%. The excess air ratio is 0% or 45% and the outdoor temperature is 0°C. The boiler efficiency is assumed constant for all calculated cases. No reheating is used. In figure 5.12 and 5.13 the chimney inner wall temperature and the accumulated condensate formation is plotted as a function of the chimney length.

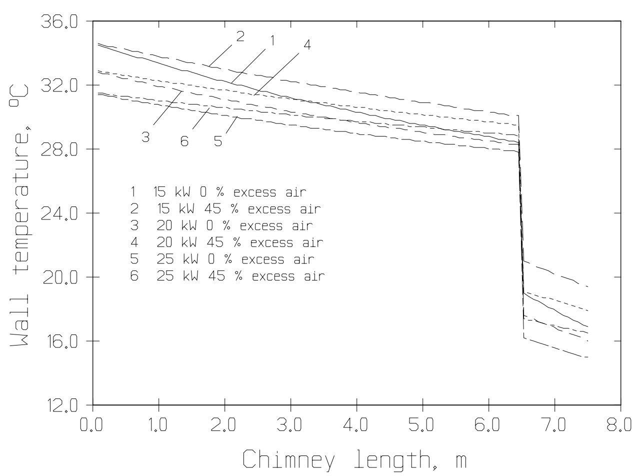

Figure 5.12: Chimney inner wall temperature at different burner inputs and excess air ratios. Flue duct cross section is 150×150 mm.

As seen in the first figure, the average inner wall temperature is hardly affected by the burner input. An increased burner input gives a lower av-

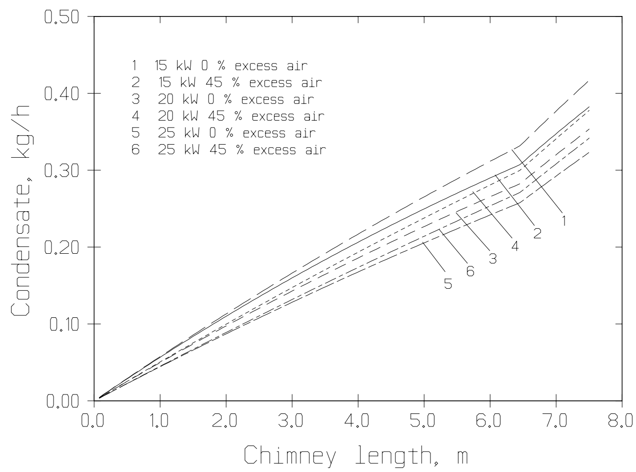

Figure 5.13: Accumulated condensate formation along the chimney at different burner inputs and excess air ratios.

erage inner wall temperature due to a reduced relative operating time τ. An increased flow given by a higher excess air ratio raises the temperature slightly. Figure 5.13 shows that the condensate formation has a minimum when the largest burner is used despite the lower wall temperature. However, a closer study shows that the condensate formation during the burner operating time is higher for large burners but shorter operating times give a smaller amount of condensate. The conclusion drawn from these calculations is that no major differences occur in wall temperatures and condensate formation due to reasonable changes in burner input and excess air.

Influence from the Heating System

There is a correlation between heating system temperatures and the flue gas temperature, and consequently the water vapour flow to the chimney. Saturated flue gases in all operating situations are assumed.

Here, the same building is used but the burner inout is fixed to 0 kW (45% excess air). The flue gas temperature after the condensing heat exchanger is varied between 30°C and 60°C. The outdoor temperature is 0°C. In figure 5.14 it is clearly seen that condensate formation is strongly dependent on the flue gas temperature at the boiler outlet.

It is an unpleasant fact that this strong dependency exists. Thus, also taking into consideration that the return temperature from an ordinary

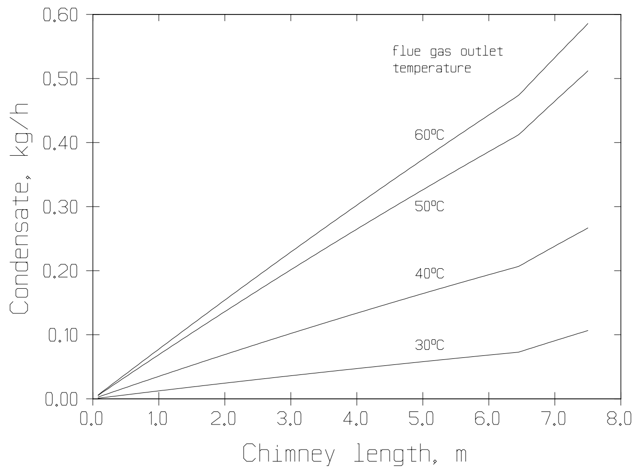

Figure 5.14: Accumulated condensate formation in the chimney as a function of the chimney length for different outlet temperatures from the boiler.

two-string hydronic system raises at higher load, it seems to be an obstacle getting a properly operating reheating and high efficiency at the same time. A way of removing this problem is to further reduce the flue gas temperature by means of the combustion air or the cold inlet sanitary water.

The examples given show that the most important building component regarding the condensate formation in the chimney, is the heating system and its return temperature. It is strongly desirable that the flue gas temperature after the condensing heat exchanger can be kept low and constant independently of the heating system characteristics.

5.3.4 Necessary Flue Gas Temperatures After Drying

The previous section dealt with the dependency of condensate formation in the chimney using a conventional condensing boiler and the building components. In this section we will show calculated values of the necessary flue gas temperature for operation with no condensate formation. The values given in table 5.1 are valid for boilers using burners in the 15–20 kW range, firing at 25% excess air. Other inputs are stated in the table caption.

No air flow through the chimney is assumed during the burner standby period, not even in the case of diluted flue gases, for example when a draught diverter is used. If such a flow is assumed in the calculations, a considerable reduction of reheating is possible. The necessary reheating is

Table 5.1: Necessary reheating calculated for boilers with 15–20 kW burner input. Reheating is given for a flue duct cross section area of 0.015 m^2 and 0.025 m^2. Chimney lengths are 6 and 8 m. The lowest flue gas temperature before reheating, T_{min}, is varied between 20 and 40 °C. The flue gases are either not diluted, $\lambda_{burner} = 1.25$, or diluted to $\lambda_{tot} = 2.5$, 3.0 and 3.5.

	Necessary reheating, °C							
	$\lambda_{tot} = \lambda_{burner}$		$\lambda_{tot} = 2{,}5$		$\lambda_{tot} = 3{,}0$		$\lambda_{tot} = 3{,}5$	
T_{min}, °C	6 m	8 m	6 m	8 m	6 m	8 m	6 m	8 m
0.015 m^2 flue duct								
20	35	55	30	30	30	30	30	30
30	70	90	35	45	30	40	30	35
40	90	130	60	75	50	65	50	60
0.025 m^2 flue duct								
20	50	65	30	30	30	30	30	30
30	90	100	55	70	40	50	40	50
40	95	155	80	110	70	90	65	75

then 40–50°C lower at 30°C and 40°C as the lowest flue gas temperatures. However, this air flow causes an increased heat demand which is dependent on chimney size and building tightness. The heat demand can in such cases increase by approximately 5% in a building with an annual heat demand of 20 000 kWh. The efficiency gain due to less reheating is smaller than the additional energy consumption, making the alternative of using air flow an uninteresting one.

The values presented are based on heat transfer in an uninsulated masonry chimney. This is the assumed typical installation and at the same time probably the most difficult case to handle. If other operating conditions are present, a significantly lower reheating is often sufficient. An example is a case where the flue gases are cooled by both the heating system and the cold inlet sanitary water. An insulated chimney is also connected to the boiler. If the cold sanitary water is stored, the influence of the heating system temperatures on the lowest flue gas temperature can be avoided. It is the possible to reduce the flue gas temperature to 20–30°C with this system design. The necessary reheating when an insulated chimney is used is approximately 20°C and can be accomplished by boiler water. KW Energiprodukter in Sweden [42] has used this design.

5.4 Flue Gas Drying and Boiler Efficiency

The suggested drying processes involve other heat flow patterns than discussed in earlier chapters. Due to the drying process heat is transferred to the outlet. This may introduce a new source for a heat loss. The heat transfer in the suggested boiler designs are discussed in this section.

5.4.1 Flue Gas Reheating and Boiler Efficiency

Looking only at the energy requirement for reheating, the boiler efficiency will of course decrease compared to an identical boiler with no reheating. The discussions about boiler efficiency are in this context always based on comparisons between two condensing boilers, one with flue gas reheating.

The energy requirement for reheating and the resulting decrease in boiler efficiency, theoretical efficiency decrease, are shown in figure 5.15. The theoretical efficiency decrease is plotted as a function of reheating, burner excess air and the flue gas temperature after the condensation in the boiler. The lower theoretical efficiency decrease at lower excess air ratos and flue gas temperatures is explained by the lower flue gas flow. The results in the figure are based on identical temperatures at every point in the two boilers except for the reheating heat exchanger.

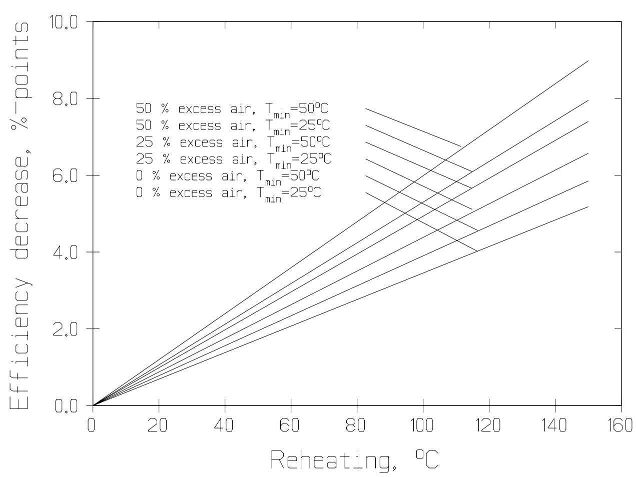

Figure 5.15: Theoretical efficiency decrease due to reheating

However, the outlet temperature from the heat exchanger is changed when flue gas reheating is added to an existing design. The discussion of changes in outlet temperature uses the term heat exchanger entalphy efficiency. Krighaar et al. [41] have discussed this for condensing boilers. The entalphy efficiency η_h is defined as

$$\eta_h = \frac{h_{in} - h_{out}}{h_{in} - h_w} \tag{5.18}$$

where h_{in} and h_{out} are the flue gas entalphy at the heat exchanger inlet and outlet. h_w denotes the enthalpy at water temperature. The entalphy efficiency is assumed to be constant for the operating conditions studied.

Heat exchangers suitable for type I boilers as well as type II boilers are considered, i.e. the chosen inlet temperatures are 300°C and 1 000°C. For each of these, different outlet characteristics are also chosen. In figure 5.16 the outlet flue gas temperature as function of the return water temperature is shown. In total, four heat exchangers are studied.

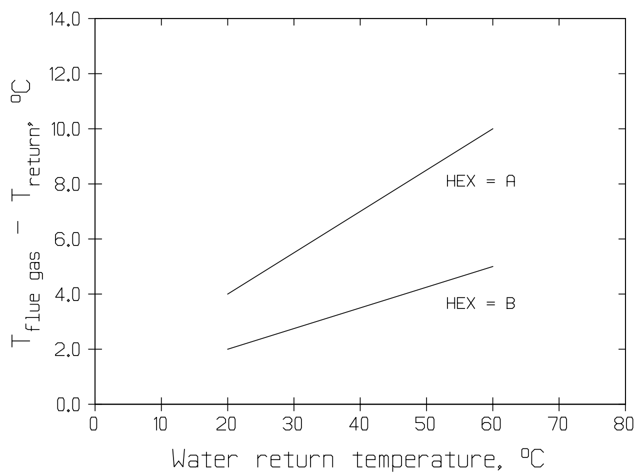

Figure 5.16: Assumed temperature difference between flue gas and return water temperature for heat exchangers studied regarding entalphy efficiency η_h

Chosen reheating levels are 75°C and 150°C. Excess air ratios are 1.0 and 1.3. The results are shown as efficiency gains in figures 5.17–5.18. These figures can be directly compared to figure 5.15 and thus can the total influence of adding flue gas reheating to an existing condensing boiler design be evaluated.

The graphs in figures 5.17 and 5.18 show that the efficiency gain is significantly higher if a type I boiler is simulated rather than a type II boiler. The gain increases as the excess air, reheating level and difference between return water and flue gas temperatures in the baseline case gets higher. All these factors make it possible to condense more water vapour.

The decrease in flue gas temperature at the heat exchanger outlet due to the added reheating is largest at 20°C return water temperature and decreases at higher temperatures. At 20°C, the temperature decrease is largest for 300°C baseline temperature and 150°C reheating and least at 1000°C and 75°C reheating. The changes are 5.42°C and 0.42°C. At 60°C return water temperature these temperature changes are 2.53°C and 0.17°C.

If the efficiency gains are compared with theoretical efficiency decrease it is obvious that only in boiler designs with two heat exchangers (type I) can the reduced temperature compensate the theoretical efficiency decrease to a substantial extent. Laboratory experiments performed on a converted Remeha 1HR [52] even showed an increased boiler efficiency. However, the conditions were more favourable than assumed in figures 5.17 and 5.18.

This discussion has shown that the boiler efficiency is reduced when flue gas reheating is added. However, the changed heat transfer in the boiler can reduce this efficiency loss. The boilers of interest for reheating do not allow any noticable reduction of this loss. This conlusion is valid for reheating using hotter flue gases.

The other proposed ways of accomplishing the reheating, using boiler water or electrical heating, do not affect the flue gas temperatures in a boiler with reheating. Thus, the efficiency decrease will be equivalent to the theoretical boiler efficiency decrease.

Keeping this discussion in mind, the influence of reheating on boiler efficiency can be estimated when looking at different boiler designs.

5.4.2 Adsorbent Drying and Boiler Efficiency

The use of an adsorbent requires a heat input for the regeneration process. This, and a possible new source for a heat loss (the adsorption device), constitute the base for efficiency influence using adsorbent drying.

When the water is adsorbed, latent heat is transformed to sensible heat and raising the adsorbent and the flue gas temperature. Assuming that all latent heat is used for heating the flue gases the graph in figure 5.19 can be drawn. It shows the flue gas temperatures after the adsorbent bed as a function of saturated flue gas temperature and the dew point after the adsorption. As seen in the figure, a dew point after the adsorption of approximately 0–5°C will be sufficient for trouble free operation.

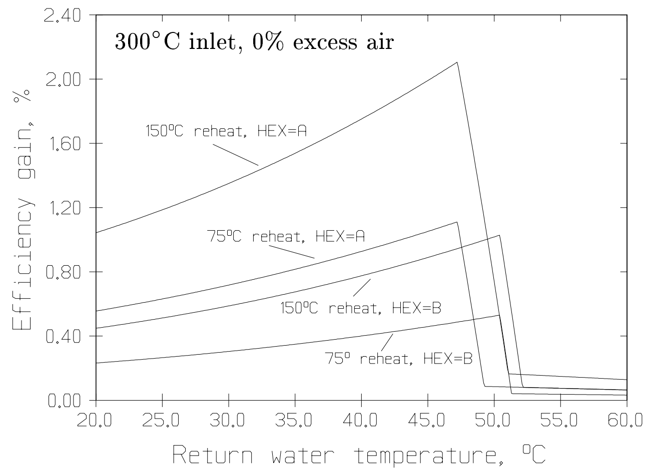

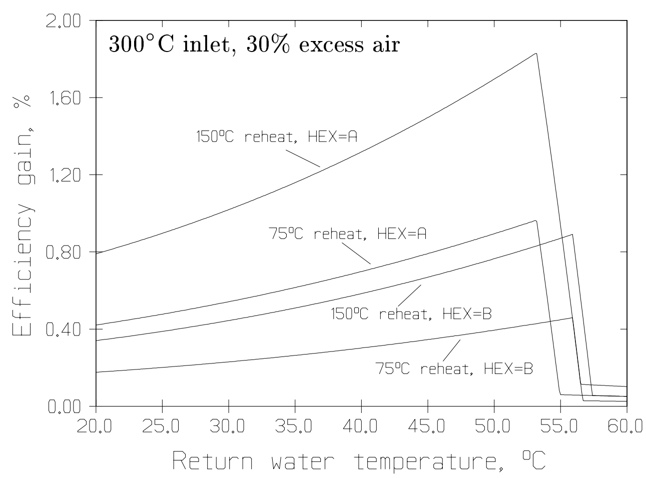

Figure 5.17: Efficiency gain due to changed flue gas temperature at the heat exchanger inlet. Baseline conditions are 300°C inlet temperature, 0% (top graph) and 30% excess air. Reheating is 75°C and 150°C. Lines marked with HEX=A represent the heat exchanger with larger difference between flue gas temperature and return water temperature

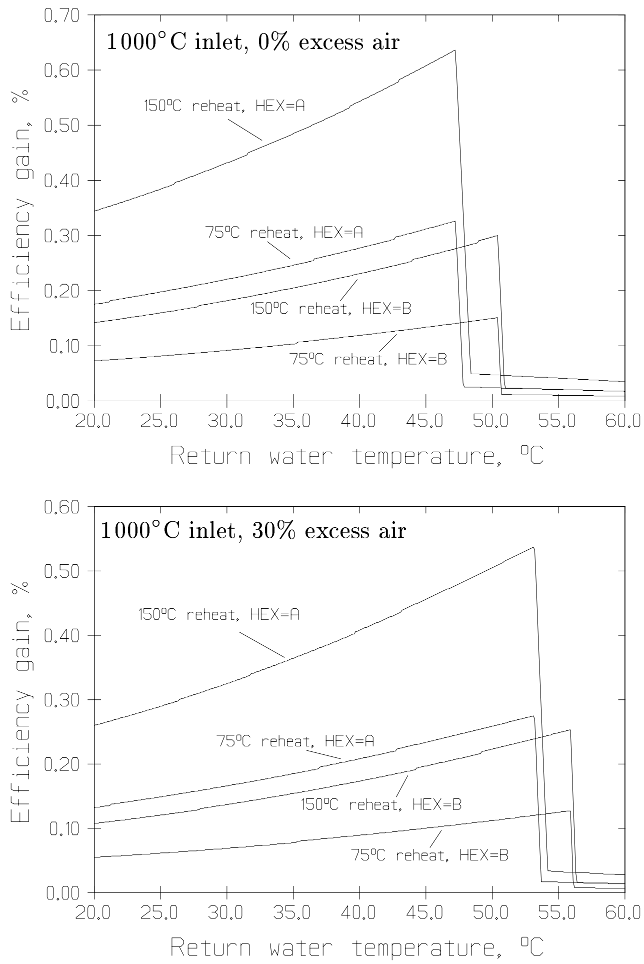

Figure 5.18: Efficiency gain due to changed flue gas temperature at the heat exchanger inlet. Baseline conditions are 1000°C inlet temperature, 0% (top graph) and 30% excess air. Reheating is 75°C and 150°C. Lines marked with HEX=A represent the heat exchanger with larger difference between flue gas temperature and return water temperature

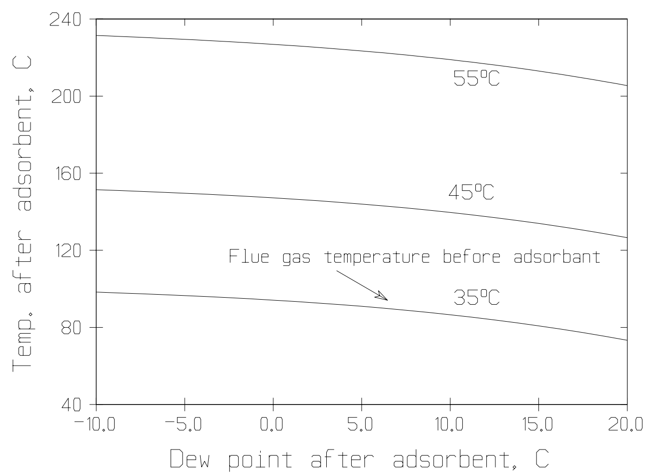

Figure 5.19: Flue gas temperatures before and after an adsorbent bed

6

Flue Gas Drying Tests

Tests were performed to investigate the characteristics of boilers with flue gas reheating, such as efficiency, heat losses and their origin, and the heat exchanger performance. Two boilers of type II, described in the previous chapter were designed and built. The results are earlier presented in [54, 55].

6.1 Test Set Up and Test Conditions

In all tests performed, the boilers were connected to a hydronic heating system emulator. The operation of this emulator is controlled by a PC and a data acquisition system. Return water temperature to the boiler is calculated and controlled by means of measured flow temperature and water flow. The heating system model used is the same as described on page 64. Input such as heating system output at full load and water content are given in order to facilitate the simulation of the dynamic behaviour of the heating system and the building.

The boiler is controlled by a boiler thermostat only. It is set manually for each test. Due to the small water content and heat capacity the operating cycles are very short. This is seen in the figures showing the flue gas temperatures in the boiler. No attempt was made to change this boiler characteristic.

Boiler performances were measured at four heat loads from 3.4 kW to 8.9 kW. These heat loads will cover most of the year except the warmest periods. The main purpose of the tests though, is to investigate reheating performance at different operating conditions, not to measure and calculate annual efficiency. The boilers were tested with the same thermostat and water flow settings for each test case whether reheating was used or not. The house simulated in the tests has a heat demand of approximately 12 kW at –14°C outdoor temperature. The heating system, a two-string hydronic system, has a capacity of 16 kW at 80°C flow temperature and 60°C return temperature at nominal flow. The water flow was set to 0.113 kg/s in test case A and set to 0.189 kg/s in test cases B, C and D.

Flue gas temperatures were measured along the heat exchanger using thermocouples type K. Water temperatures were measured at inlet and outlet using Pt100 sensors.

It should be borne in mind that the efficiency data are valid for experimental boilers, not of commercial standards. For example, the convective heat losses are much larger than those acceptable in a commercial boiler.

6.2 Reheating in a Boiler with a Cylindrical Burner

This investigation is described more in detail by the author in [55]. A boiler with a cylindrical burner surrounded by a finned tube heat exchanger for the space heating loop and a smooth tube for the reheating was built and tested. A schematic drawing of the boiler is shown in figure 6.1. The overall sizes were an outer diameter of 350 mm and a height of 600 mm (450 mm to the top of the heat exchanger).

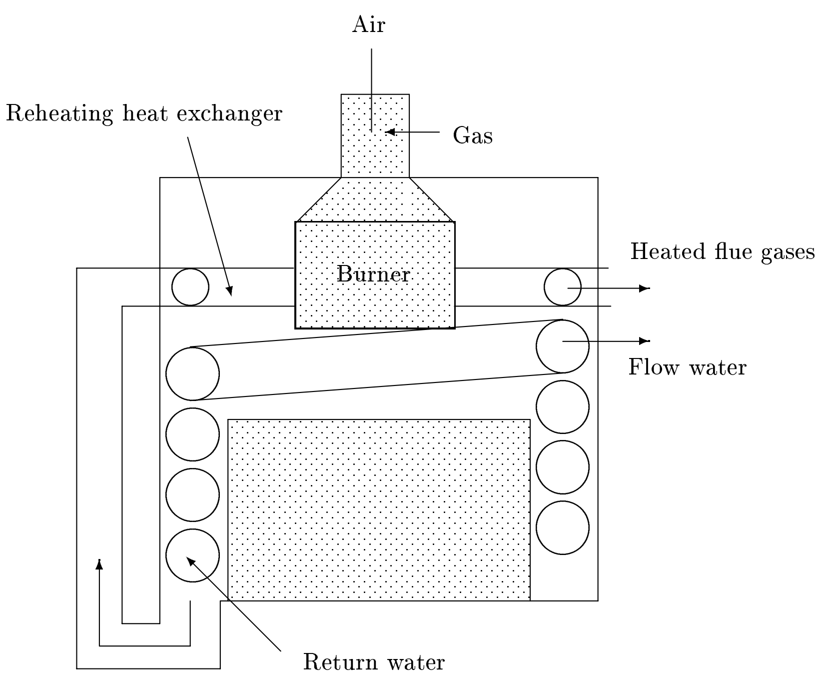

Figure 6.1: Experimental boiler design. Cylindrical burner and reheating

6.2.1 Burner

The burner in the tested boiler is a cylindrical, experimental Thermomax burner developed by Ruhrgas AG. Characteristic features are a fully premixed operation at approximately 25% excess air and very low NO_x emissions making it an interesting alternative for newly developed appliances. The stand-by loss is assumed to be low when this burner is used. These characteristics have all been observed in the boiler tests. The burner design is thoroughly described by Berg and Jannemann [6] and is here only briefly described. A drawing of the burner is shown in figure 6.2. Air and fuel are mixed at the burner inlet in the top part of the drawing. The mixture is combusted close to a perforated metal sheet acting as burner surface. The two rods beside the burner are used for flame ignition and flame sensing.

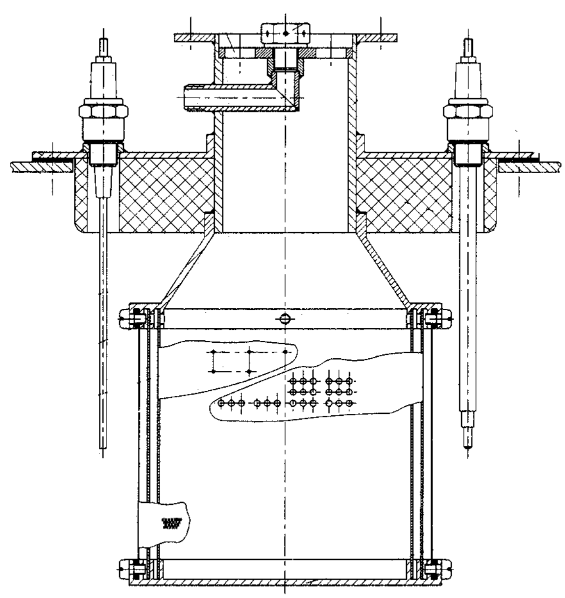

Figure 6.2: Thermomax cylindrical burner (Ruhrgas)

The burner has a nominal gas input of 20 kW. At the burner inlet, the combustion fan is located. During the efficiency tests, the burner had an input of 18 kW and operated with 20% excess air. In the experimental boiler, the burner can be vertically moved.

6.2.2 Heat Exchangers

The flue gas to water heat exchanger is a finned tube of 7.9 m length. Outer diameter of the tube is 20.8 mm and outer diameter of the fin is 45 mm. The fin thickness is 0.4 mm and the spacing corresponds to 11 fins per inch. The aluminium fins are mounted on a liner in copper (Essem Final from Outokumpu Copper). The water content of the boiler, water in the heat exchanger tube only, is approximately 1.8 litres.

The reheating heat exchanger is simple. A smooth copper tube forms a single row heat exchanger around the burner. The tube has an inner diameter of 16 mm and 1 mm wall thickness.

The heat exchanger position was not changed between the tests. Thus, using no reheating, a considerable empty space was present above the water side heat exchanger. Also, space enough for a larger reheating heat exchanger was available. This space is an explanation to the large heat losses mentioned later in connection with the efficiency measurements.

6.2.3 Boiler Performance with No Reheating

Boiler performance with no reheating is presented as measured heat exchanger performance and flue gas temperatures at steady-state and part-load operation. Boiler part-load efficiency at different loads and associated losses are also shown.

Heat Exchanger Performance

The flue gas steady-state temperature at the heat exchanger outlet was measured at different return water temperatures. The heat exchanger performance is shown as a function of the return water temperature in figure 6.3. The performance is expressed as the difference between measured flue gas and return water temperatures.

No changes in performance were found for different excess air ratios. The change in excess air also affects the burner radiation characteristics and this could lead to the conclusion that the radiation output does not have any significant influence on the heat transfer. However, the location of the space heating heat exchanger allowed only 3 rows to be visible for the burner surface heat radiation.

Boiler Efficiency

The efficiency was measured at the four different heat loads earlier mentioned. In table 6.1 the test results are summarised.

In table 6.1, $\dot{Q}_{load}$ is the heat load, T_{return} is the water return temperature, T_{fg} is the average flue gas temperature during burner operation, η_{theo} is the theoretical efficiency calculated from the average flue gas temperature

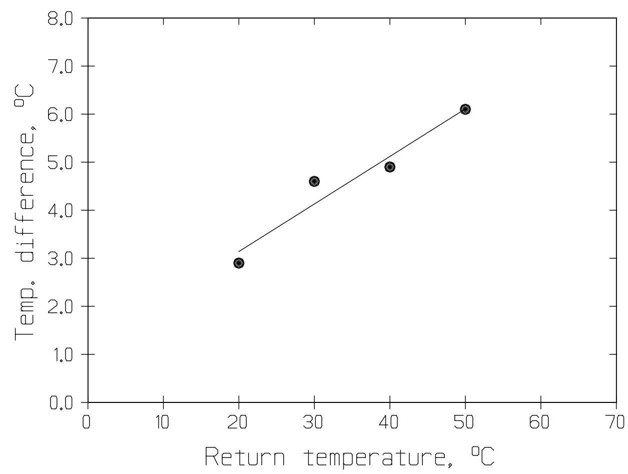

Figure 6.3: Measured temperature difference between return water and flue gases at the boiler outlet at steady-state operation. Boiler with cylindrical burner and with no reheating.

and excess air ratio, $\dot{Q}_{loss}$ is the heat loss and η_{meas} is the measured efficiency. It is clear that the heat loss is large compared to commercial boilers. The calculated heat loss $\dot{Q}_{loss}$ in test cases A and B suggest that the heat loss origin from parts not containing water. The loss is probably caused by some hot surface areas close to the burner which are not sufficiently insulated. Most of the heat loss is assumed to be convective/radiative since there is little, if any, air flow through the boiler during the stand-by period. The only air flow during this time is during the pre-purge period. The average heat loss $\dot{Q}_{loss}$ is 0.57 kW, which corresponds to 3.1% of the burner input. An efficiency measuring error of 1% equals 10% of the value of $\dot{Q}_{loss}$. This demonstrates the difficulty to determine the convective loss from heat balances with a high degree of accuracy. No evidence is given for influence of burner operating time or average boiler water temperature. The major part of $\dot{Q}_{loss}$ is therefore assumed to be convective loss from the boiler surface.

Table 6.1: Measured and calculated results for the boiler with cylindrical burner and with no reheating

Test case	A	B	C	D
$\dot{Q}_{load}$ (kW)	3.79	4.18	5.55	8.88
η_{meas} (%)	94.5	94.9	96.1	94.7
T_{return} (°C)	20	22	28	43
T_{fg} (°C)	22	24	36	51
η_{theo} (%)	109.6	109.3	106.8	101.1
$\dot{Q}_{loss}$ (kW)	0.57	0.60	0.67	0.44

Flue Gas Temperatures with No Reheating

In the boiler with no reheating, flue gas temperature was measured at four points: beside the burner and in front of the first row of the heat exchanger, in the middle of the heat exchanger, one row before the heat exchanger outlet and finally at the boiler outlet. The temperatures measured for the four heat loads previously described, are seen in figure 6.4.

The short burner operating and stand-by times are clearly visible. The notch, visible in some of the graphs marks the beginning of the fan operation during the pre-purge time. The temperature drops rapidly in the heat exchanger and it would probably give equal performance if it was smaller. At intermittent burner operation, the same temperature difference between return water and flue gases as in steady-state operation is not obtained. At steady-state operation the temperatures were measured to 960°C and 150°C at the first two points. These temperatures were not changed when the burner was moved vertically approximately 70 mm.

6.2.4 Boiler Performance with Reheating

The reheating obtained was found to be far too large with the simple reheating heat exchanger, and 300–450°C outlet temperature was measured at full load. The degree of reheating can be reduced if only a small amount of the flue gases are reheated. The heated gases are then mixed with cool flue gases from the condensing heat exchanger outlet. This solution is suitable, because from a manufacturing point of view, it does not seems feasible to break up the water side heat exchanger, in order to locate the reheating heat exchanger at a point where the temperature gain is appropriate.

Due to overheating in the boiler, which caused flue gas leakage, the tests were terminated after the efficiency tests where the entire flue gas flow passed the reheating heat exchanger. This problem was a result of the "flexible" boiler design, allowing for example an altered burner position. The flue gas leakage made the measurements unreliable. However, splitting

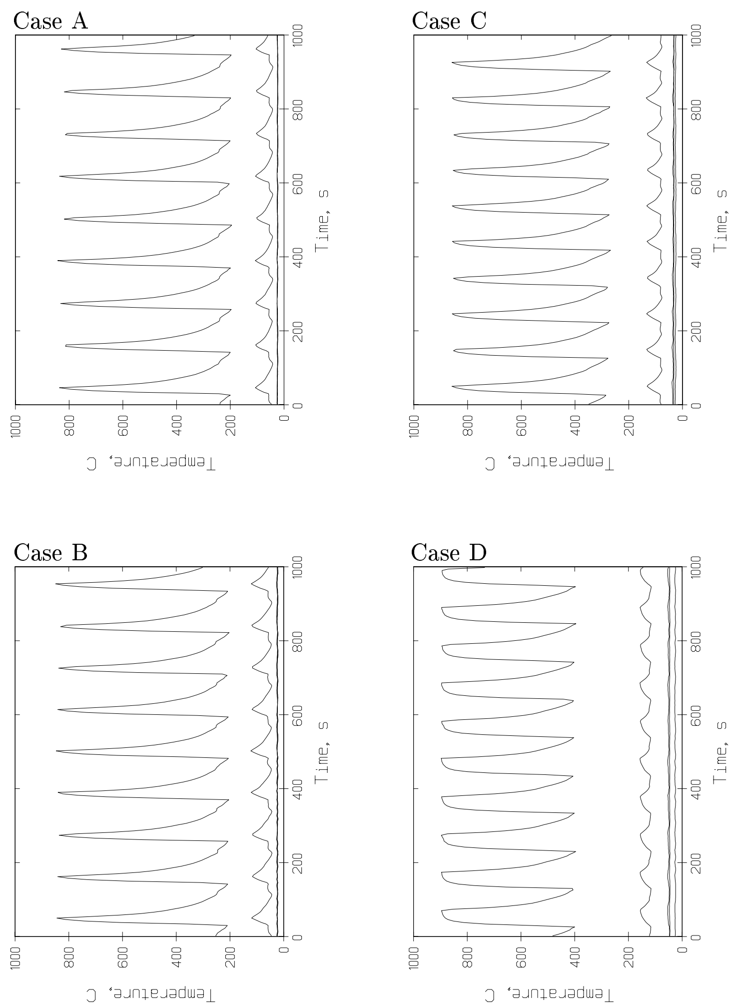

Figure 6.4: Flue gas temperatures in the boiler with cylindrical burner and no reheating

the flue gas flow was found to give a simple and stable reheating function. No efficiency measurements were conducted in this case due to the problems related to overheating.

Boiler Efficiency with Reheating

As mentioned earlier, thermostat and water flow settings were not changed between the tests. The test results are summarised in table 6.2 where $T_{out,av}$ denotes the average flue gas temperature after reheating, i.e. at the boiler outlet. The theoretical boiler efficiency η_{theo} is calculated from the flue gas temperature at the condensing heat exchanger outlet T_{fg}, the average temperature after reheating $T_{out,av}$, and the excess air ratio λ. Calculated values of the theoretical boiler efficiency in case of a different heat exchanger or burner performance are added to the table.

Table 6.2: Measured and calculated results for the boiler with cylindrical burner and reheating. All flue gases pass the reheating heat exchanger.

Test case	A	B	C	D
$\dot{Q}_{load}$ (kW)	3.40	3.73	4.95	8.16
η_{meas} (%)	70.5	76.5	73.6	78.7
T_{return} (°C)	20	21	28	43
T_{fg} (°C)	24	24	36	51
$T_{out,av}$ (°C)	251	263	324	340
η_{theo} (%)	99.6	99.1	93.9	86.9
$\dot{Q}_{loss}$ (kW)	0.99	0.84	1.00	0.85
η_{theo} (%) $T_{fg} + 5°C$	98.8	98.3	92.4	83.4
η_{theo} (%) $T_{fg} + 10°C$	97.8	97.3	90.4	83.1
η_{theo} (%) $\lambda + 0.1$	98.7	98.1	92.5	84.9
η_{theo} (%) $\lambda + 0.2$	97.7	97.1	91.0	82.8

The tests showed a large efficiency decrease when reheating was used and the measured efficiencies were far from acceptable, see table 6.2. The earlier mentioned convection loss probably represent the dominant part of the total losses. A comparison between tables 6.1 and 6.2 show an increased heat loss and the hot flue gas outlet of the reheating heat exchanger is the most probable reason for this, due to heat conduction from the boiler interior. The heat losses are equivalent to 4.5–5.5% of the burner input for the test cases shown. If the heat losses could be reduced to 0.200 kW, approximately 1% of the burner input, the efficiencies should increase to 86.9%, 89.6%, 84.9% and 85.0% for test cases A, B, C and D respectively. These values correspond to increased efficiencies of 11.3–16.4% compared to measured data.

Letting the entire flue gas flow pass the reheating heat exchanger gave

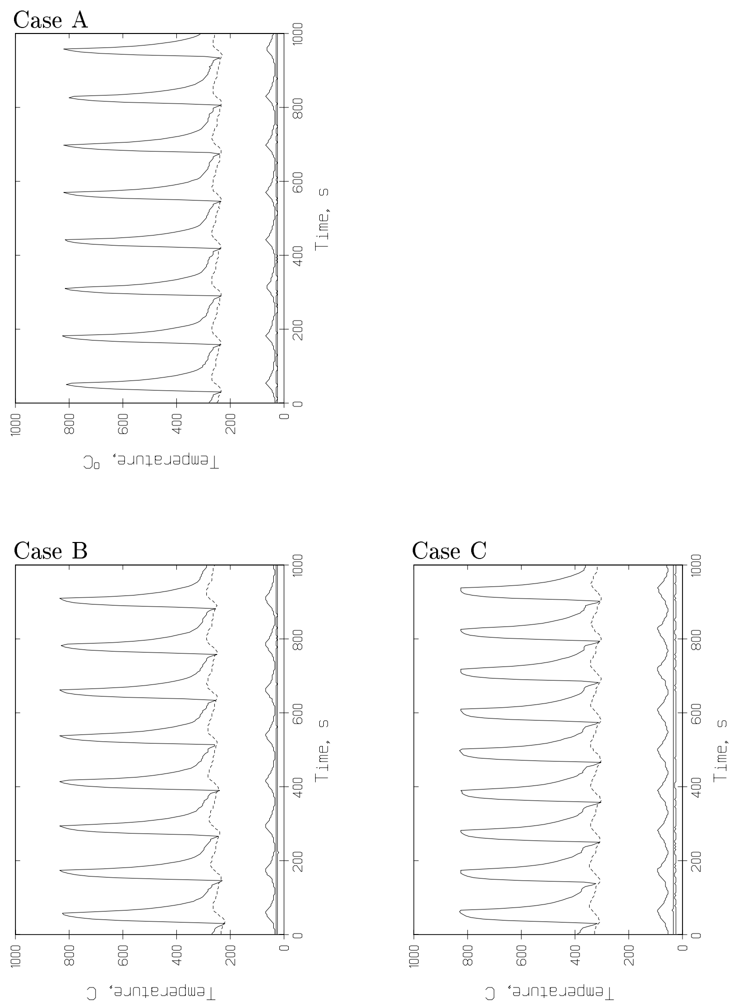

Figure 6.5: Flue gas temperatures in the boiler with cylindrical burner and reheating. The entire flue gas flow is passing through the reheating heat exchanger. Dotted lines show temperatures after the reheating.

too large a temperature rise. Even though the efficiency was not measured when the reheating was at an adequate level, the theoretical values can be used for an estimation of the maximum acceptable heat losses. The lowest flue gas temperatures, T_{fg}, are known from the tests. In table 6.3 calculated efficiencies for the different test cases are shown. The flue gases are heated 100°C and 150°C.

Table 6.3: Theoretical boiler efficiencies at 100 °C and 150 °C reheating. Values are based on data for the boiler with cylindrical burner. Heat losses are not included in the values.

Test case	T_{fg} (°C)	$\Delta T = 100°C$ η_{theo} (%)	$\Delta T = 150°C$ η_{theo} (%)
A	24	105.1	103.0
B	24	105.1	103.0
C	36	102.5	100.3
D	51	96.4	93.9

6.3 Reheating in a Boiler with a Flat Burner

The boiler used for reheating with a flat burner is almost identical to the boiler simulated in the previous chapter. It is designed for large flexibility, i.e. a large number of heat exchanger sizes and boiler heat capacities are possible. The study of flue gas reheating has, however, only been carried out on one design.

6.3.1 Burner

The flat burner is based on a metallic fibre burner sheet from the Belgian company Acotech. This involves a surface combustion and a higher degree of infra red heat emission compared to a conventional gas burner. The burner plate size is 305×185 mm, and with a load of approximately 350 kW/m^2 the gas input is 20 kW. It is possible to change the burner load between 300 and 1000 kW/m^2, which corresponds to 17–56 kW burner input, in radiant mode. For loads exceeding 1 000 kW/m^2, combustion occurs in a blue flame mode. A changed burner load affects the amount of heat radiated from the burner surface. In conclusion, this flat burner has approximately the same characteristics as the cylindrical Thermomax burner.

6.3.2 Heat Exchangers

Finned tubes of the same design were used in the boilers with cylindrical and flat burners. In the boiler with a flat burner the heat exchanger is configured as a number of tube rows. 7 rows in an in-line arrangement was used. The small water vessels connecting tube rows, and used in the boiler model, were not used in these tests. Instead, hoses were used to connect the tube rows.

6.3.3 Boiler Performance with No Reheating

This heat exchanger configuration shows a slightly larger difference between inlet water temperature and flue gas temperature at the boiler outlet than the boiler with a cylindrical burner and helically shaped heat exchanger. This temperature difference is shown in figure 6.6. The flue gas temperatures in the boiler with no reheating are shown in figure 6.7. This graph corresponds to the graphs in figure 6.4.

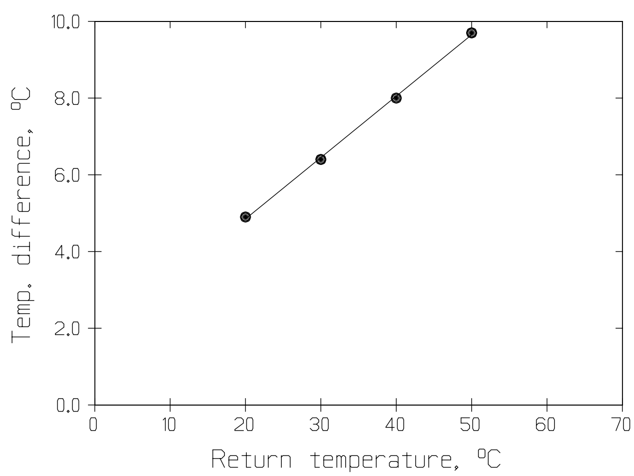

Figure 6.6: Measured temperature difference between return water and flue gases at the boiler outlet at steady-state operation and 7 tube rows in an in-line configuration. Boiler with flat burner and with no reheating.

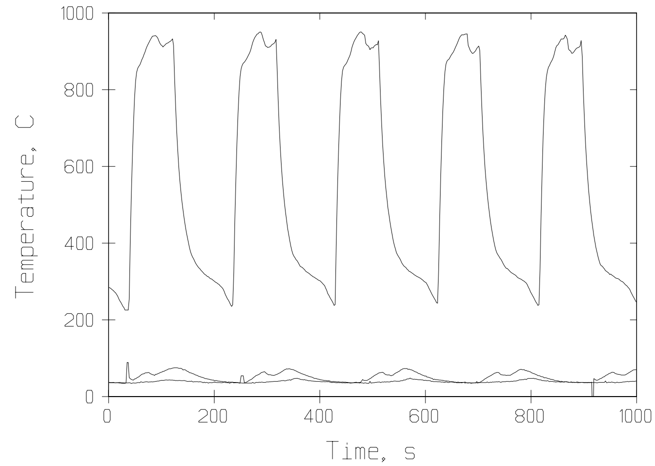

Figure 6.7: Flue gas temperatures in the boiler with flat burner and with no reheating. The heat load is 8.50 kW, test case B.

The results of three tests including measurements of efficiency and other data are shown in table 6.4.

Table 6.4: Measurement results for the boiler with a flat burner and with no reheating

Test case	A	B	C
$\dot{Q}_{load}$ (kW)	6.30	8.50	9.40
η_{meas} (%)	97.4	97.3	97.9
T_{return} (°C)	25	32	34
T_{fg} (°C)	33	38	41
η_{theo} (%)	107.4	106.1	105.1
$\dot{Q}_{loss}$ (kW)	0.63	0.75	0.67

6.3.4 Boiler Performance with Reheating

Unlike the boiler with cylindrical burner, this boiler design offers a “free” choice of location for the reheating heat exchanger. The reheating heat exchanger was located after the first water side tube row. The reheating heat exchanger consists of four finned tubes identical to the water side tubes. This means that the gas to water heat exchanger comprise 6 tube rows when reheating was added. No more changes were made to the boiler.

The temperatures measured in the boiler with reheating, 7.73 kW heat load, are shown in figure 6.8. The dotted line shows flue gas temperature at the boiler outlet, i.e. after the reheating. The temperature is nearly constant and corresponds to a temperature rise of approximately 100°C, which is a reheating level at the lower end suggested in the calculations of necessary reheating. Measured data are given in table 6.5. In conformity with the other boiler design, theoretical boiler efficiencies η_{theo} are added to the measured values. The heat loss in this boiler is not affected by the added heat exchanger for reheating. The explanation is twofold. Firstly, the lower degree of reheating gives lower material temperatures and secondly, the outlet from the reheating heat exchanger is more efficiently insulated than in the other boiler. If, as with the boiler equipped with a cylindrical burner, the heat loss is assumed to be 0.200 kW instead of the values calculated, the efficiencies become 98.9%, 97.9% and 96.7% respectively, i.e. an efficiency increase of 4.7–7.1%.

Table 6.5: Measurement results for the boiler with flat burner and reheating.

Test case	A	B	C
$\dot{Q}_{load}$ (kW)	5.87	7.01	7.73
η_{meas} (%)	91.8	91.1	92.0
T_{return} (°C)	29	35	40
T_{fg} (°C)	36	41	45
$T_{out,av}$ (°C)	120	122	130
η_{theo} (%)	102.9	101.4	99.6
$\dot{Q}_{loss}$ (kW)	0.65	0.72	0.59
η_{theo} (%) T_{fg} + 5°C	101.2	99.3	97.1
η_{theo} (%) T_{fg} + 10°C	99.2	96.8	93.9
η_{theo} (%) λ + 0.1	102.2	100.7	98.7
η_{theo} (%) λ + 0.2	101.6	99.9	97.8

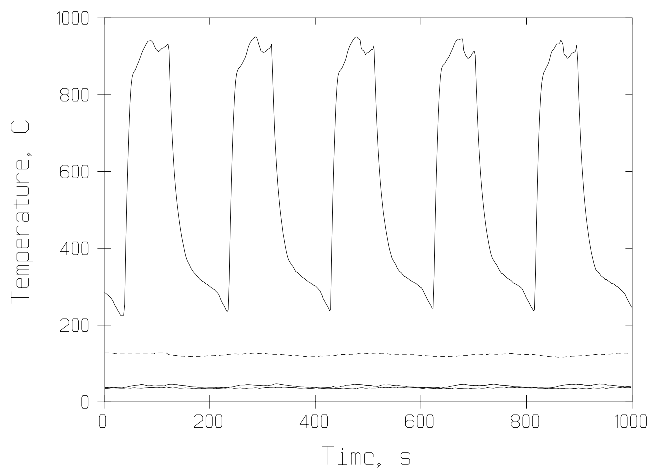

Figure 6.8: Flue gas temperatures in the boiler with flat burner and reheating. The dotted line shows the flue gas temperature after reheating. The heat load is 7.73 kW, test case C.

6.4 Conclusions About Flue Gas Drying

The boiler tests showed that a well operating reheating is possible without a complicated heat exchanger design. Different behaviour regarding the degree of reheating and boiler efficiency were observed for the two boilers. What are the advantages and disadvantages with these designs, and in what way is it possible to improve the performance compared to the measured efficiencies? These topics are discussed in this concluding section.

6.4.1 Overall Boiler Design

Which is the best boiler design if flue gas reheating is used? The test results are here used to form an opinion about a “good” boiler design.

The tests presented here are all performed on type II condensing boilers, i.e. boilers with an integrated gas to water heat exchanger. The items mentioned below show the main reasons to favour type II boilers.

- Location of heat exchanger
- Burner
- Draught during burner stand by, stand-by loss

As previously mentioned it is easier to design and locate a reheating heat exchanger in a type II boiler to meet requirements regarding reheating level. Residential type I boilers are usually equipped with atmospheric burners. These have a high excess air ratio and allow an air draught through the boiler during the burner stand-by period. The draught causes a cooling of the reheating heat exchanger which is not seen in the tested type II boilers with premix burners, see figures 6.5 and 6.8.

The reheating heat exchanger introduces a new source for heat loss compared to other condensing boilers. Heat from the burner region is easily transferred to the outlet and careful insulation seems necessary. The tests clearly show this. Heat loss during the pre-purge period has the same source, and the easiest way to reduce this loss is to obtain a low cycle frequency.

An increased boiler heat capacity reduces the cycling frequency. A concentration of the heat capacity to the water side rather than the gas side is probably the best way to accomplish low cycling frequency and reduce heat loss during the pre-purge period.

To obtain an annual efficiency of 90–95%, the tests show that the losses (assumed to be convective) should not exceed approximately 200–300 W. This could also be expressed as 1–1.5% of the burner input assuming a 20 kW burner.

Changes in heat exchanger performance of course also affect the boiler efficiency. Figure 6.9 shows deviation in boiler efficiency where the temperature difference between flue gas and return water, the excess air ratio and the reheating level are changed. The base case is 20% excess air and a flue gas temperature equal to the return temperature.

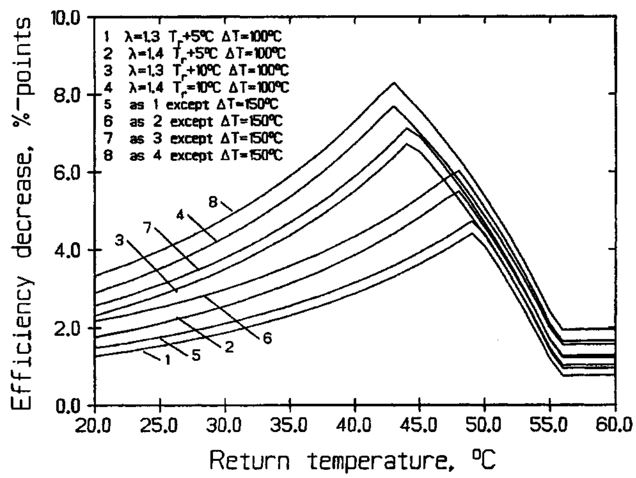

Figure 6.9: Loss of efficiency at excess air ratios exceeding 20% and flue gas temperatures higher than the return temperature, T$_{return}$ (T_r)

It is seen that the efficiency loss due to a higher excess air ratio and a less efficient heat exchanger has a maximum for a return temperature of 40–45°C. This corresponds to operating conditions occuring during a large part of the heating season. A smaller heat exchanger can be compensated for if the heat losses are further reduced.

From this discussion, an overall residential boiler design incorporating flue gas reheating should be as follows.

- Integrated heat exchanger and a fan assisted or premix burner firing at a low excess air ratio.
- A highly efficient heat exchanger, i.e. as small temperature difference as possible between flue gas and return water.
- Careful heat insulation.
- Operation at a low cycling frequency achieved by for example a reasonably high heat capacity.

7

Discussion and Conclusions

Two aspects of residential condensing gas boilers were chosen in this thesis. Firstly, the performance of condensing boilers was studied and boiler design parameters as well as the influence of the heat load and heating system temperatures were evaluated. The possibility to design condensing boilers without the need to use chimney liners was studied in the second part. Other topics regarding for example materials and manufacturing were not studied.

Condensing boilers are highly efficient space heating appliances. Since the first boilers commonly used in Europe in the late 1970s the design has changed considerably. Early boilers often involved non-condensing boiler technology with an added condensing heat exchanger while new boilers have integrated heat exchangers and other types of burners. Often, modern premix low-pollution burners are used thus making the modern residential condensing gas boiler the cleanest fossil fueled space heating appliance.

Predictions of the part-load efficiency have normally been based on two steady-state conditions which are weighted to fit the part-load studied. These methods are often accurate enough to predict the annual efficiency if the losses are separately and reasonably described. The accuracy can be within ±2–3% of measured values. However, models intended as a design tool need a description of the boiler geometry and, preferrably, a dynamic modelling approach to predict the performance in real operating conditions.

"Part 1"

A transient heat transfer analysis of boilers is necessary to evaluate the boiler characteristics in specific operating conditions. A detailed model can provide a tool for the development of simple yet highly efficient boilers.

In the thesis a residential gas boiler is modelled with three heat capacities, the flue gases, the heat exchanger material and the heating system water. Heat transfer correlations are obtained from literature. The model describes a boiler where heat is transferred from the flue gases to finned heat exchanger tubes and between water and material in vessels connecting the tube rows. The walls around the finned tubes are assumed to be adiabatic. A number of combinations of boiler designs, building and heating system were simulated in order to evaluate the efficiency.

This boiler design, with a finned tube heat exchanger and a premix burner, is a common design on the European market. However, some differences between the design in the model and commercial boilers exist. The main differences are the adiabatic walls and a constant heat exchanger cross section in the model. Commercial boilers have walls or manifolds containing water and acting as a part of the heat exchanger. This also means that the boiler parts which connect the tube rows are in contact with flue gases. Commercial boilers also often have a decreasing heat exchanger cross section in the flow direction.

A finned tube heat exchanger with different fin profiles is simulated in steady-state conditions. From these simulations a high thin fin profile was chosen for the part-load simulations.

A single family house was modelled to simulate heat loads representing a 15 000 kWh/year heat demand. Three different heating systems and three different heat loads were also used. The heat loads are representative for different periods of the heating season.

All simulations showed a part-load efficiency in the 97–107% range taking into account different heat exchanger sizes and tube arrangements as well as various boiler heat capacities. The convective loss was small, only equal to an efficiency loss of 0.2–0.3%. The part-load simulations showed that a larger thermostat hysteresis gives a slightly lower efficiency, $<1\%$, due to a higher average flue gas temperature. The boiler least sensitive to changes in heat load has a large heat exchanger, a low flue gas side heat transfer coefficient and a high thermostat hysteresis. Among the boiler designs simulated this difference was in a 1.5–4% range for boilers with a heat capacity of 1 500–2 000 J/kW K. A low heat capacity results in a higher boiler part-load efficiency as long as the pre-purge loss is not too large.

The efficiency difference between the three heat loads increases for high temperature heating systems. Consequently, higher heat capacity means a reduced boiler efficiency, but these boilers also show a smaller difference between the heat loads. Taking into account the heat exchanger size, the best boiler design is one where the heat flux per unit area is higher. Only a negligible efficiency loss occurs, but this is only valid if the heat exchanger material temperatures are close to the adjacent water temperature and the burner cycling frequency is not too high.

In no simulation the pre-purge loss, expressed as decreased efficiency, was larger than approximately 1%. However, at shorter burner operating times (in seconds) due to less boiler heat capacity the pre-purge loss is rapidly increasing.

The calculation of total heating cost, including gas and electricity, showed that the highest cost occurs at a low heat load due to the heat supplied by the circulation pump. This is more evident as the relation between gas and electricity prices is increased. The electricity consumption can be reduced either by using a pulse combustor and/or a circulation pump timer. Using a pulse combustor may save 0.5% of the heating costs when the electricity rate is twice the gas rate. The potential of using a circulation pump timer was not evaluated but is probably larger than a change of burner.

"Part 2"

"Dry" flue gases are necessary to avoid chimney liners when condensing boilers are used. Flue gas reheating by means of a heat exchanger and heat pipes as well as adsorbent drying were studied. Both theoretical aspects, mainly regarding the influence on boiler efficiency, and experimental investigations on two boilers were used to evaluate condensing boilers with dry flue gases.

Heat transfer in chimneys was calculated using a quasi-stationary approach. This gave the possibility to take into account different heat loads as well as boiler oversizing. The reheating necessary for condensate free operation was estimated to 100–150°C. The values are valid for uninsulated brick chimneys connected to 15–20 kW boilers. The excess air ratio in this calculations was 25%. If the flue gases are diluted, the necessary reheating could be reduced by 40–50°C. However, the dilution air increases the heat demand. It was shown that the gas consumption became larger if dilution air was used.

The two boilers built and tested with and without reheating showed no major technical problems associated with reheating in modern boiler designs. The boilers were tested at heat loads between 3.4 and 8.9 kW. The gas input to both boilers was 18 kW. In the first design, where a cylindrical burner was surrounded by a finned tube and the reheating heat exchanger was close to the burner, the reheating was too high, approximately 300–450°C. It is necessary to split the flue gas flow at the condensing heat exchanger outlet and only heat a part of the flow in order to get a proper reheating and an acceptable boiler efficiency.

The second design had a flat surface combustion burner firing downwards facing rows of finned tubes. In this design it was easier to locate the reheating heat exchanger at a place with a lower temperature than in the first boiler design, between the first and second tube row. This gave an almost perfect reheating, compared to calculated values of necessary reheating. Heat insulation was easier to apply to this experimental design and thus was the measured efficiencies higher than for the first design.

It was found from the experiments that the following characteristics and designs should be used in a condensing boiler with reheating. The heat exchanger should be integrated, i.e. not split up in a non-condensing and a condensing heat exchanger. The burner should either be a fan assisted or a premix burner firing at low excess air ratios. The heat exchanger should be as efficient as possible with a small difference between flue gas and return water temperature. A careful heat insulation is necessary, especially since the reheating heat exchanger is a new source for heat loss. Finally, the boiler ought to operate at a low cycling frequency achieved either by a high boiler heat capacity or by the control system.

A proper design of a boiler with reheating ought to give a part-load efficiency of approximately 100% on condition that a low temperature heating system is used.

Bibliography

[1] Ahmad, M.; Marley, S.J.; Chaudhary, A.P. and Nelson, R.H., *A Model of Biofueled Hydronic Heating Systems*, ASHRAE Trans., Vol. 97(2) 1991, pp. 197–203

[2] Aronov, M. and Sheridan, R., *Furnace Compact Heat Exchanger*, Preprints 1992 Int. Gas Research Conf., Orlando Florida, November 1992

[3] Aziz, A., *Periodic Heat Transfer in Annular Fins*, ASME J. Heat Transfer, **97** (1975), No. 2, pp. 302–303

[4] Ball, D.A. and White, E.L., *Condensing Heat-Exchanger Systems for Oil-Fired Residential/Commercial Furnaces and Boilers, Phase I and II*, October 1982, DE83–005996, BNL–51617

[5] Becker, F.E. and Searight, E.F., *Development of a Gas-Fired, Heat-Pipe, Warm-Air Heating Systems*, Proc. 1981 Int. Gas Research Conf., Los Angeles, September/October 1981, pp. 1513–1525

[6] Berg, H. and Jannemann, T., *Entwicklung eines schadstoffarmen Vormischbrenners für den Einsatz in Haushalts-Gasheizkesseln mit zylindrischer Brennkammer*, Gas Wärme International, **38** (1989), No. 1, pp. 28–34

[7] Bonne, U.; Janssen, J.E.; Nelson, L.W. and Torborg, R.H., *Control of overall thermal efficiency of combustion heating systems*, Proc. 16th Symp. (Int.) on Combustion, Massachusetts Institute of Technology, Cambridge, Mass., August 1976, pp. 37–52

[8] Bonne, U., *Furnace and Boiler System Efficiency and Operating Cost Versus Increased Cycling Frequency*, ASHRAE Trans., Vol. 91(1B) 1985, pp. 109–130

[9] Bootsma, D. and Meijnen, A.J., *Developments in Modulating Combustion Systems for Domestic Central Heating Boilers*, Preprints 1992 Int. Gas Research Conf., Orlando Florida, November 1992

[10] Chen, L-T., *Two-dimensional fin efficiency with combined heat and mass transfer between water-wetted surface and moving moist airstream*, Int. J. Heat Fluid Flow, **12** (1991), No. 1, March, pp. 71–76

[11] Chen, H-T. and Chen, K-C., *Transient Response of Crossflow Heat Exchangers With Finite Wall Capacitance*, ASME J. Heat Transfer, **114** (1992), No. 3, pp. 752–755

[12] Churchill, S.W. and Chu, H.S., *Correlating Equations for Laminar and Turbulent Free Convection from a Vertical Plate*, Int. J. Heat Mass Transfer, **18** (1975), No. 3, pp. 1323–1329

[13] Claus, G. and Stephan, W., *A General Computer Simulation Model for Furnaces and Boilers*, ASHRAE Trans., Vol. 91(1B) 1985, pp. 47–59

[14] Colburn, A.P. and Hougen, O.A., *Design of Cooler Condensers for Mixtures of Vapors with Noncondensing Gases*, Ind. Engng. Chem., **26** (1934), No. 11, November, pp. 1178–1182

[15] Coney, J.; Sheppard, C.G.W. and El-Shafei, E.A.M., *Fin Performance with Condensation from Humid Air, a Numerical Investigation*, Int. J. Heat Fluid Flow, **10** (1989), No. 3, September, pp. 223–231

[16] Creare Inc., *Fluent manual, ver. 2.94*, 1987

[17] de Wit, J. and Paulsen, O., *A Calculation Method for the Estimation of Annual Efficiency for Gas Fired Domestic Heating Systems*, 18th World Gas Conf., Berlin 1991

[18] Dittrich, A., *Zum Jahreswirkungsgrad von Ein- und Mehrkesselanlagen*, HLH, **23** (1972), No. 12, December, pp. 381–386

[19] Ernst, D.M.; Eastman, G.Y. and Thomas Jr., W.E., *Development of a High Efficiency Warm Air Furnace using Heat Pipes*, Proc. 1981 Int. Gas Research Conf., Los Angeles, September/October 1981, pp. 1371–1379

[20] Etheridge, D.W.; Lightbourne, J. and Pride, R.D., *Developments in Domestic Fan Powered Miniature Flues*, Preprints 1989 Int. Gas Research Conf., Tokyo, November 1989

[21] Field, A.A., *Reclaiming latent heat in flue gases*, Heating, Piping and Air Conditioning, October 1974, pp. 85–90

[22] Fischer, R.D. and Stickford, G.H., *Users Manual for CONDHX: A Simulation Model as a Design Tool for Finned-Tube Condensing Heat Exchangers*, Interim Report from GRI's Gas Appliance Technology Center, May 1988

[23] Gardner, K.A., *Efficiency of Extended Surface*, Trans. ASME, **67** (1945), pp. 621–631

[24] Information material from GRACE

[25] Personal communication, GRACE, Helsingborg, Sweden

[26] Gundtoft, S., *Extrapolation of Test Results by Detailed Modelling*, Report on: European Workshop Concerning Interaction between Heat Generators/Heating Systems and Buildings – Annual Efficiency for Domestic Boilers, Danish Technological Institute, Copenhagen, June 1991

[27] Hargreaves, K.J.A. and Patterson, M.C., *Advanced combustion systems for high efficiency domestic appliances*, Preprints 1986 Int. Gas Research Conf., Toronto, September 1986

[28] Hensen, J.L.M., *On the thermal interaction of building structure and heating and ventilation systems*, Diss., Eindhoven Institute of Technology, 1991

[29] Hensen, J.L.M., *Towards an integral approach of building and HVAC system*, Energy and Buildings, **19** (1993), pp. 297–302

[30] Hindin, B., *Bibliography on Design for Corrosion Resistance in Gas Appliances — with Emphasis on Condensing Heat Exchanger*, Gas Appliance Technology Center, January 1988, GRI-88/0010 548–552

[31] Huge, E.L., *Experimental Investigation of Effects of Equipment Size on Convection Heat Transfer and Flow Resistance in Cross Flow of Gases Over Tube Banks*, Trans. ASME, **59** (1937), October, pp. 573–581

[32] Idem, S.A., *An instantaneous condensing gas-fired water heater: modeling and performance*, Diss., Purdue University, 1986

[33] Idem, S.A.; Jacobi, A.M. and Goldschmidt, V.W., *Heat Transfer Characteristics of a Finned-Tube Heat Exchanger (with and without Condensation)*, ASME J. Heat Transfer, **112** (1990), No. 1, pp. 64–70

[34] Jakob, F.E.; Crisafulli, J.J.; Menkedick, J.R.; Fischer, R.D. and Philips, D.B., *Assessment of Technology for Improving the Efficiency of Residential Gas Furnaces and Boilers, Volume I*, GRI-94/0175.1, September 1994

[35] Jakob, F.E.; Crisafulli, J.J.; Menkedick, J.R.; Fischer, R.D. and Philips, D.B., *Assessment of Technology for Improving the Efficiency of Residential Gas Furnaces and Boilers, Volume II: Appendices*, GRI-94/0175.2, September 1994

[36] Jannemann, T., *Kompendium Gas-Brennwerttechnik*, 2nd ed., Vulkan-Verlag, Essen 1996, ISBN 3-8027-2540-9

[37] Kern, D.Q. and Kraus, A.D., *Extended Surface Heat Transfer*, McGraw-Hill, 1972

[38] Kirk, W.B., *Current Activity in Appliance Design*, Proc. 3rd Conf. on Natural Gas Research and Technology, Dallas, March 1974

[39] Koot, M.; Schweitzer, J.; de Wit, J. and Paulsen, O., *Annual Efficiency Calculation, A Comparison Between Various Methods*, IGU/E4-94, 19th World Gas Conf., Milan, June 1994

[40] Koot, M.; Koschowitz, M. and Näslund, M., *Annual Efficiency Calculation Method for Domestic Boilers, Technical Report Work Package 6: Start/Stop Losses Measurement Method. Evaluation of possible methods to be used*, SAVE Project XVII/4.103/93-008, June 1995

[41] Krighaar, M.; de Wit, J. and Paulsen, O., *Performance Characteristics of Water-Cooled Condensing Heat Exchangers under varying Operations Conditions*, Proc. 2nd European Conf. on Industrial Furnaces and Boilers, Vol. 1, Algarve Portugal, 1991

[42] KW Energiprodukter, *Utvärdering av anläggningarna med avgaskondensorer*, Pamphlet from KW Energiprodukter, Stockholm, April 1991

[43] Laret, L.J., *Simplified Performance Models for Cycling Operation of Boilers*, ASHRAE Trans., Vol. 97(2) 1991, pp. 212–218

[44] Lebrun, J.J.; Hannay, J.; Dols, J.M. and Morant, M.A., *Research of a Good Boiler Model for HVAC Energy Simulation*, ASHRAE Trans., Vol. 91(1B) 1985, pp. 60–86

[45] Lux Jr, J.J.; Razgaitis, R.G.; Ball, D.A. and Locklin, D.W., *Development of an Analytical Design Technique for Condensing Flue-Gas Heat Exchangers*, 1983 Int. Gas Research Conf., London, June 1983

[46] McGlothin, S.D., *High Efficiency Hydronic Heating Unit. Final Report November 83–January 87*, NTIS PB87-176350, GRI-86/0291, January 1987

[47] McQuiston, F.C., *Fin Efficiency with Combined Heat and Mass Transfer*, ASHRAE Trans., Vol. 81(1) 1973, pp. 350–355

[48] McQuiston, F.C., *Correlation of Heat, Mass and Momentum Transport Coefficients for Plate-Fin-Tube Heat Transfer Surfaces with Staggered Tubes*, ASHRAE Trans., Vol. 84 1978, pp. 294–309

[49] Nevrala, D.J.; Curran, A.H. and Davies, K.J., *Warm Air Heating with Mechanical Ventilation and Heat Recovery*, Preprints 1989 Int. Gas Research Conf., Tokyo, November 1989

[50] Newcombe, J. and Dixon, J.L., *Heat Transfer Modelling of Residential Space Heating Units*, Preprints 1989 Int. Gas Research Conf., Tokyo, November 1989

[51] Nielsen, J.K. and Spiegelhauer, B., *Individuelle naturgasfyrede varmesystemer år 2000*, Danish Gas Technology Center and Danish Technological Institute, November 1990, ISBN 87-983073-0-4

[52] Näslund, M., *A Condensing Boiler with Reheated Flue Gases*, Proc. 1987 Int. Symp. on Condensing Heat Exchangers, 14–16 April 1987, Columbus, Ohio, GRI–87/0091.2, BNL 52068, pp. 305–316

[53] Näslund, M., *Avgasåtervärmning i små kondenserande gaspannor*, LUTMDN/(TMVK-7007)/1-106/(1991), May 1991

[54] Näslund, M., *Condensing Boilers with Dry Flue Gases*, 1992 Int. Gas Research Conf., Orlando Florida, November 1992

[55] Näslund, M., *Experimental Investigation of a Condensing Boiler with a Thermomax Burner and Flue Gas Reheating*, March 1993, ISRN LUTMDN/TMVK-3149-SE

[56] Näslund, M., *A Calculation Method for the Prediction of Part-Load Efficiency of Domestic Gas Boilers*, Swedish Gas Association Annual Meeting, September 1993

[57] Näslund, M., *Utveckling av en värmeöverföringsmodell för skorstenar vid gaseldning*, Värmeforsk rapport 542, August 1995

[58] Paulsen, O. and Gundtoft, S., *Dynamisk afprøvning af små varmecentraler*, Teknologisk Institut, Tåstrup, Denmark, 1985

[59] Pelloux-Prayer, D., *Condensing Boilers in France: Computational Methods for new Appliances and Field Experience*, Proc. 1987 Int. Symp. on Condensing Heat Exchangers, 14–16 April 1987, Columbus, Ohio, GRI–87/0091.2, BNL 52068, pp. 391–410

[60] Pfeiffer, P., *Berechnung des stationären und instationären Betriebes von Gasheizkesseln*, gwf–Gas/Erdgas, **135** (1994), No. 2, pp. 65–79

[61] Pickup, G.A. and Miles, A.J., *The performance of domestic wet heating systems in contemporary and future housing*, The Institution of Gas Engineers, Communication 1041, November 1977

[62] Pierson, O.L., *Experimental Investigation of the Influence of Tube Arrangement on Convection Heat Transfer and Flow Resistance in Cross Flow of Gases over Tube Banks*, Trans. ASME, **59** (1937), October, pp. 563–572

[63] Pitschak, B.; Feldpausch-Jägers, S. and Kremer, H., *Matematische Modellierung der instationären Temperaturverteilung an einschaligen Hausschornsteinen*, Gas Wärme International, **42** (1993), No. 6, June, pp. 280–287

[64] Plate, J. and Tenhumberg, J., *Theoretische und experimentelle Ermittlung des Nutzungsgrades von Wärmeerzeugern – Ein Vergleich*, HLH, **35** (1984), No. 3, March, pp. 95–99

[65] Plate, J. and Tenhumberg, J., *Auswirkungen niedriger Abgasverluste auf den Kamin*, Gas Wärme International, **34** (1985), No. 11, November, pp. 459–464

[66] Rado, L., *Die „Totale Energienutzung“ – 100% Wirkungsgrad? – Die Brennwertnutzung bei gasgefeuerten Wärmeerzeugern*, Gas Wärme International, **25** (1976), No. 7/8, pp. 378–382

[67] Ransmark, S-E., *Kondenserande värmepanna – tekniska och ekonomiska aspekter på ett effektivt utnyttjande av naturgas*, LUTMDN/(TMVK-3123)/1-92/(1984)

[68] Rawe, R. and Schulz, K., *Strahlungs- und Bereitschaftsverluste von Gasgeräten – neue Forschungsergebnisse*, gwf–Gas/Erdgas, **131** (1990) No. 10/11, pp. 507–514

[69] Rosa, L. and Tosato, R., *Flue Gas Conditioning in Gas-Fired Condensing Boilers to avoid Water Vapor Condensing in Flue Ducts*, Proc. 19th Intersoc. Energy Conv. Eng. Conf., San Fransisco, USA, 1984

[70] Rosemann, H., *Berechnung von zulässigen Abgaszuständen einer Gasfeuerung mit Wärmerückgewinnung unter Berücksichtung der Kondensationsbedingungen am Kamin* (unpublished manuscript), Joh. Vaillant GmbH, Remscheid, Germany

[71] Rutz, A.L.; Paul, D.D.; Talbert, S.G.; Crisafulli, J.J.; Whitacre, G.R. and Fischer, R.D., *Users Manual for VENT-II (version 3.0) with Diskette: A Dynamic Microcomputer Program for Analyzing Gas Venting Systems*, November 1988, GRI-88/0304

[72] Schweitzer, J., *Annual efficiency calculation method for domestic boilers*, European Union SAVE program Contract No. XVII/4.1031/93-008, Danish Gas Technology Center, 1996

[73] Searle, M. and Allen, C.G., *Development and Evaluation of a High Efficiency Boiler*, Preprints 1986 Int. Gas Research Conf., Toronto, September 1986

[74] Searle, M.; Pelloux-Prayer, D. and Stickford, G., *Factors Influencing the Design of Condensing Appliances "A View from Both Sides of the Atlantic"*, Preprints 1989 Int. Gas Research Conf., Tokyo, November 1989

[75] Spiga, G. and Spiga, M., *Two-Dimensional Transient Solutions for Crossflow Heat Exchangers with neither Gas Mixed*, ASME J. Heat Transfer, **109** (1987), No. 2, pp. 281–286

[76] Spiga, M. and Spiga, G., *Transient Temperature Fields in Crossflow Heat Exchangers with Finite Wall Capacitance*, ASME J. Heat Transfer, **110** (1988), No. 1, pp. 49–53

[77] Stasiulevičius, J. and Skrinska, A., *Heat Transfer of Finned Tube Bundles in Crossflow*, Hemisphere Publishing Company, 1988, ISBN 0-89116-360-3

[78] Statens Provningsanstalt, *Bestämning av årsmedelverkningsgrad och varmvattenkapacitet för vedeldade ackumulatorsystem*, SP Metod 1415, July 1994

[79] Stevens, R.L. and Morgan, G.C., *Materials for High Efficiency Appliances*, Preprints 1986 Int. Gas Research Conf., Toronto, September 1986

[80] Tang, D., *Modelling of heating and air-conditioning systems*, Diss., University of Strathclyde, Glasgow, 1985

[81] van Rij, M. and Overman, P., *Efficiency of CH Boilers under Laboratory and Practical Conditions*, Preprints 1986 Int. Gas Research Conf., Toronto, September 1986

[82] *VDI-Wärmeatlas – Berechnungsblätter für den Wärmeübergang*, 4th ed., VDI-Verlag, Düsseldorf 1984

[83] Viessmann Werke, Pamphlet from Viessmann boiler company in Germany about the Viessmann Mirola, 1992

[84] Winberg, J., *On hot Water Storage in District Heating Subscriber Stations — System Measurements*, LUTMDN/(TMVK-7009)/1-76/(1992)

[85] Yau, K.K. and Rose, J.W., *Prediction of the Performance of Domestic 'Condensing Boilers'*, Gas Engineering and Management, **33** (1993), July/August, pp. 198–203

[86] Žukauskas, A., *High-Performance Single-Phase Heat Exchangers*, Hemisphere Publishing Company, 1989, ISBN 0-89116-715-3